GENERATION OF TOLEROGENIC HUMAN DC THROUGH RAPAMYCIN CONDITIONING AND GENETIC MODIFICATION WITH HLA-G

A thesis submitted in partial fulfillment of the
PhD degree

in

The Department of Medicine
Faculty of Health Sciences
The University of Adelaide

by

Boris Fedoric

June 2009

CHAPTER 1
LITERATURE REVIEW

1.1 Organ transplantation – Australian and USA statistics

Organ transplantation is the most beneficial treatment for end stage organ failure. Patients who have received an organ transplant have higher survival rates and better quality of life compared to patients undergoing dialysis (1-3). Data collected from hospitals throughout Australia in 2007 indicated that there were 1,264 patients in need of a solid organ transplant with only 615 transplants performed annually. Compared to Australia, records from USA in 2008 indicated that there were approximately 100,000 patients waiting for an organ transplant, with only 25,000 transplants performed in that year (1, 4). The availability of organs for transplant still remains the major limiting factor contributing to the large number of patients on the waiting list (1, 4). Importantly, 20% of patients requiring an organ transplant in Australia were in need of a second transplant as a result of failure of the initial organ transplantation (1). Therefore there is an urgent need to improve the success of ongoing post operative treatment of transplanted patients. In summary, organ transplantation provides the treatment of choice for end-stage organ failure. Nevertheless limitations such as the availability of the organs for transplant and immunological and non-immunological factors limit its success.

1.2 Immunosuppressive Agents and Tolerance Induction

Alloimmune responses play a major role in allograft loss although there are non-immunological factors (i.e. ischemia reperfusion injury, drug-specific toxicity and hypertension) which also contribute to allograft rejection (5). Allograft rejection occurs when the recipient's T cells recognise donor Human Leukocyte Antigens (HLA) expressed by the allograft (6, 7). These HLA, also termed Major Histocompatability Complex Antigens (MHC), are highly polymorphic glycoproteins which are divided into two classes,

MHC class I and class II. It is now widely accepted that MHC class I molecules are expressed rather ubiquitously on the surface of most nucleated cells, while MHC class II molecules are restricted to Antigen Presenting Cells (APC) such as dendritic cells (DC). The major role of DC in the cell mediated immunity is to process and present foreign antigens to the naïve and memory $CD4^+$ and $CD8^+$ T cells, and thereby induce antigen specific T cell mediated immune responses (8). This immunological interplay between DC and T cells, which protects an individual from pathogen invasion, is the same response that initiates anti-donor immunity during allograft rejection.

In the 1970's, immunosuppressive drugs (**summarised in Table 1.1**) were introduced to prevent acute allograft rejection by suppressing the recipient's immune system. The first successful transplant, which resulted in long term allograft survival, was performed between identical twins in the absence of any immunosuppression (9, 10). However, the introduction of immunosuppressive agents permitted prolonged allograft survival in the allogeneic organ recipient population. Current statistics show that immunosuppressive agents can effectively inhibit acute allograft rejection and provide greater than 77% allograft survival for the first year of all of the solid organs commonly transplanted (7). However these immunosuppressive agents, administered systemically, act indiscriminately on homeostatic immune response thus increasing the occurrence of opportunistic infections in transplant patients after long-term use (11-13). In addition, these agents are toxic to organs and they increase the occurrence of malignancies (14, 15). As a result of the detrimental side effects and lack of immune selectivity, immunosuppressive drugs do not prevent the development of chronic rejection and thus long term allograft survival has not improved greatly over the years (7, 14).

Currently, transplantation clinicians are trialling various treatment regimens which involve withdrawal of immunosuppressive agents in order to induce transplant tolerance (7, 14, 16). Transplant tolerance is considered to be the “holy grail of transplantation” and it is defined as a state in which there is absence of immunological destruction of the donor organ devoid of any immunosuppressive treatment (16). There are indeed rare groups of patients who have developed clinical tolerance and these include: patients receiving bone marrow and kidney transplants, patients that received lymphoid radiation and some non-compliant patients who stopped taking immunosuppression (16, 17). In the latter situation, an individual received HLA-identical kidney transplant from her sister in 1968 which was maintained for 5 years with Azathioprine and Prednisone (18). However, the recipient ceased taking immunosuppression and to the great surprise of clinicians, the allograft maintained excellent function for 32 years. When the recipient and her family were subjected to immunological testing in 2004, it was noted that this patient was microchimeric with her sister for T cells and peripheral DC (19). The patient was however mismatched at the minor Histocompatability locus HA-1, but contained CD8 suppressor T cells which were able to suppress immune responses to those HA-1 disparate antigens (19). In another example, clinical transplantation tolerance was successfully induced in a patient with renal failure who also suffered from multiple myeloma (20, 21). The patient was pre-conditioned with cyclophosphamide, antithymocyte globulin, and thymic irradiation prior to the simultaneous bone marrow and kidney transplant (22). Cyclosporine A was administered as a sole immunosuppressant for 73 days in order to prevent episodes of acute rejection. At day 73, post-transplant cyclosporine A was withdrawn. The patient was examined and the results revealed stable graft function and absence of graft-versus host disease at day 170 post-transplant. It was further shown that the patient developed mixed

lymphohematopoietic chimerism and had functional anti-tumour immune response (22). Following this initial report, 5 other patients have been transplanted in the same hospital and they were reported to have also developed tolerance and mixed chimerism (20, 21). However, longitudinal studies are essential in order to identify the benefits of such tolerance induction therapies.

At present, no link has been identified between the use of immunosuppressive agents and the induction of transplantation tolerance, despite the success in inducing transplantation tolerance in rodent animal models (16). Nevertheless, there are several reagents currently undergoing testing for their use as either additive to current immunosuppressive regimens or as sole tolerance inducing molecules. These agents can either block T cell activation (Belatacept), deplete T cells (Campath-1H) or block costimulatory molecule interactions between DC and T cells (7, 23, 24). Although these agents primarily target immune cells and thus exert more selective immunosuppression, they are not allo-antigen specific. These agents, like immunosuppressive drugs, could also impair the function of other immune cells, which are for example selected to fight pathogen. Therefore current research in the field of transplantation immunology has focussed on generating allospecific tolerance inducing therapeutics with minimal side effects, which would be targeting major mediators of alloimmune response, namely T cells and DC (16). One prospective tolerance inducing therapy may involve infusion of *in vitro* generated tolerogenic DC into the transplant recipient (25, 26). Observations made in the non-compliant tolerant patient mentioned previously who developed DC microchimerism has highlighted the possible involvement of DC in tolerance induction in humans (19). The next section will therefore highlight the immunological features of DC which may enable them to be used as a potential cell based tolerogenic therapeutic.

1.3 Dendritic cell immunotherapy

As reviewed in the subsequent chapter (**1.4.2**), DC can either induce or suppress immune responses depending on their maturation state (27-29). The unique characteristic of DC has attracted transplant immunologists to use DC as an experimental tool in order to develop antigen-specific cell-based tolerogenic therapy. To date, biologic, pharmacological and genetic approaches have been used to modify the stimulatory capacity of DC by enhancing their tolerogenic properties (30). Although these approaches have yielded promising results both *in vitro* and in rodent animal models, there is a lack of translational studies evaluating tolerogenic DC in large animal models or human clinical trials (**see 1.9.1 and 1.9.2**) (30).

The first clinical trial using tolerogenic DC commenced at the University of Pittsburgh (USA) and is currently recruiting patients (www.clinicaltrials.gov). In this Phase I safety trial adults afflicted with insulin-requiring type-1 diabetes will be given autologous, *ex vivo* monocyte-derived DC treated with antisense phosphorothioate-modified oligonucleotides targeting CD40, CD80 and CD86 positive costimulatory molecules. These maturation arrested DC exhibited *in vivo* tolerogenic properties by delaying the incidence of diabetes when injected into the NOD mice (31). The tolerogenic DC significantly increased the numbers of $CD4^+$ $CD25^+$ T regulatory cells (**see 1.5.3**) which was believed to, in part, contribute to the delay of the onset of diabetes (31). It is therefore hypothesised that, in the human setting, these tolerogenic DC would reduce the immunological attack of β-cells by generating regulatory T cells. It has also been noted in the review by Thomson and Robbins that another two clinical trials will be initiated shortly using tolerogenic DC (26). The first Phase I trial will be conducted through the University of Queensland (Australia) where autologous modified monocyte-derived DC will be pulsed

with citrullinated peptide antigens and assessed for their ability to alleviate rheumatoid arthritis (RA) progression. The second Phase I trial will be initiated at the University of Newcastle (England) where the effect of tolerogenic DC, generated using Vitamin $D_{3,}$ will be studied for a potential treatment for RA.

Besides using DC as tolerogenic therapy, DC are also being used to stimulate specific immune responses in cancer patients. Several clinical phase I, II and III trials have been conducted investigating the safety and efficacy of DC as anti-tumour immunotherapy and showed notable success (32-34). For example, placebo-controlled phase III study of Sipuleucel-T (autologous *ex vivo* pulsed DC with GM-CSF-conjugated prostatic-acid phosphatise) demonstrated that there was an increase in median survival rate of 5 months for Sipuleucel-T versus the control group (34). In addition, there was an 8-fold increase in T cell stimulation in Sipuleucel-T group compared to the control.

Although Phase I clinical studies have been initiated investigating the tolerogenic potential of DC-based therapy in rheumatoid arthritis and diabetes, there is still a need to generate DC with tolerogenic properties to be used in transplant patients. Generating efficient tolerogenic DC will be the major focus of the current thesis and in order to do so it is important to understand the immunobiology of DC during alloimmune response.

Drug Name	Biological Target	Side Effects	References
Rapamycin	Blocks IL-2 activation and phosphorylation of 70 S6 kinase, thus inhibiting T cell progression from the G to S phase of cell cycle	Interstitial pneumonitis Alveolar hemorrhage Glomeluropathy	(35-39)
Cyclosporine A	Blocks IL-2 production by inhibiting calcineurin	Renal damage Hypertension Vascular arteriosclerosis	(40, 41)
Steroids	General anti-inflammatory agent APC and cytokines	Cushingoid Syndrome, Cataracts, Hypertension, Bone necrosis, Hyperglycemia, Hyperlipidemia, Growth retardation	(42)
Tacrolimus	Binds to FK binding proteins resulting in calcineurin inhibition	Renal damage Hypertension Vascular arteriosclerosis	(41, 43)
Mycophenolate Mofetil (MMF)	Inhibits purine synthesis and the type II isomer of inosine monophosphate dehydrogenase thereby inhibiting activated lymphocytes	Minimal side-effects but must be used as adjunctive therapy	(44, 45)
Azathioprine	Prevents mitosis of fast-dividing cells. De novo purine biosynthesis.	Leukopenia Thrombocytopenia Megaloblastic anemia	(46, 47)

Table 1.1. Currently used immunosuppressive agents, their cellular targets and specific side-effects
The above immunosuppressive agents are either used alone or in combination to inhibit allograft rejection. Despite successfully inhibiting acute allograft rejection, these agents failed to inhibit chronic rejection. These agents are largely non-specific and have detrimental side-effects (listed above) of which many can directly contribute to chronic rejection

1.4 Immunobiology of DC

1.4.1 DC origin and differentiation

Human myeloid DC originate from the bone marrow $CD34^+$ myeloid haematopoietic stem cells, which can differentiate into the two lineages $CD14^+CD11c^+CD1^-$ and $CD14^-CD11c^+CD1^+$. $CD14^+CD11c^+CD1^-$ (or monocytes) precursors further differentiate into 1) immature DC (iDC) in response to granulocyte/macrophage colony-stimulating-factor (GM-CSF) and Interleukin (IL)-4 and 2) macrophages in response to macrophage colony stimulating factor (M-CSF) (27, 28, 48). In contrast, $CD14^-CD11c^+CD1^+$ progenitor can differentiate into 1) Langerhans cells in response to GM-CSF, IL-4 and transforming growth factor beta (TGF-β), or 2) into macrophages in response to M-CSF (27, 28, 48).

In humans, circulating numbers of DC are only 0.01-0.7 % of total PBMC (49). For this reason, DC are obtained by culturing monocytes in the presence of GM-CSF and IL-4. This enables the generation of sufficient numbers of DC for *in vitro* and *in vivo* experiments. In addition, culturing DC from monocytes *in vitro* provides a model to study the ability of pharmacological or genetic manipulation of DC to interfere with the differentiation process. Indeed, the seminal work of Randolph and co-workers has shown that monocytes do undergo differentiation into DC *in vivo* and therefore, this *in vitro* model is a representation of the *in vivo* process (50, 51).

1.4.2 Differential function of immature DC versus mature DC

Following the *in vivo* differentiation from monocytes, iDC migrate into the blood and then into the lymphoid tissues, where under steady state, iDC phagocytose "self-antigens" from apoptotic cell and present them to the T cells (27, 28, 48). The iDC are characteristic for their high phagocytic and endocytic abilities, low expression of positive costimulatory molecules CD40, CD80, CD86 and low expression of MHC II molecules (27, 28, 48). It has been established that in the absence of inflammatory mediators iDC sample self-antigens and present them to the T cells, a mechanism by which DC mediate self-tolerance (29, 52). As a result of bacterial infection or tissue damage during transplantation, inflammatory mediators are released (i.e. TNF-α and LPS) which induce maturation of iDC. Mature DC (mDC) have reduced phagocytic and endocytic ability but have increased antigen processing and presentation capacity (i.e. high MHC II expression). Mature DC have also high expression of CD40, CD80 and CD86 molecules, together with adhesion molecules (CD54 and CD58) and CCR7 chemokine receptor (27, 28, 48). The phenotype of mDC enables them to activate both naïve and memory CD4 and CD8 T cells, thus mounting a strong antigen specific immune response which can eliminate pathogen or rejects allograft.

The tolerogenic property of iDC has been demonstrated in humans, where following the single injection of iDC pulsed with influenza matrix peptide (MP) and keyhole limpet hemocyanin (KLH) inhibited $CD8^+$ effector T cell function specific for MP (53). In addition, it was demonstrated that 7 days post iDC injection, these $CD8^+$ T cells could suppress other MP-effector T cells, suggesting that injection of iDC induced suppressor/regulatory $CD8^+$ T cells (54). Conversely, injection of 9 healthy subjects with mDC pulsed with MP, KLH and tetanus toxoid (TT) resulted in priming of $CD4^+$ T cells in

all 9 subjects against KLH and in 5-6 subjects against TT (55). Injection of mDC with MP resulted in several fold increase in Interferon (IFN) gamma (IFNγ) producing $CD8^+$ T cells in all 6 subjects expressing particular HLA allele (55). Therefore, these findings strongly support that the lack of DC maturation is linked to its immunomodulatory properties. However, understanding how the DC are involved in different aspects of alloimmune response is necessary, as it will enable us to appropriately modify DC in order to target major alloimmune response pathways. Thus, this review will closely examine the role of DC in both T cell activation and suppression.

1.4.3 T-Cell Activation

Complete activation of T cells requires three separate but complementary signals (**Figure 1.1**) (56). The first requirement for T cell activation is for DC to present antigens in association with Major Histocompatability Complex (MHC) molecules to T cells. Recognition of these MHC/Antigen complexes by the T cell receptor (TCR) provides the first signal (**signal 1**), however this alone is not sufficient for T cell activation. The second signal (**signal 2**) is provided by interactions between costimulatory molecules on the DC and the T cells including the CD28, CD40, ICOS, ICAM1, LFA3 and OX40 costimulatory molecules. Costimulatory molecule interactions can reduce the number of engaged TCR required by more than 80% (57), thereby reducing the threshold required for T cell activation. The cross-linking interactions between CD28 and CD80/CD86 costimulatory molecules provide one of the most important costimulatory pathways. Notably, TCR engagement in the absence of sufficient costimulation leads to T cell anergy, which is defined as a state in which the T cell is viable but fails to display functional responses such as proliferation or production of Interleukin 2 (IL-2) in response to its specific antigen

(58, 59). Finally, signalling through costimulatory molecules induces IL-12 production by DC and IL-2 production by T cells (**signal 3**) (60, 61). These cytokines further augment T cell activation and DC maturation leading to the fully-fledged immune response.

Consolidated interaction between the DC and T cell is required to facilitate TCR engagement and costimulation, leading to full T cell activation (62, 63). This requirement is facilitated by the formation of an immunological synapse.

1.4.4 The Immunological Synapse

The immunological synapse is a term used to describe the complex and highly structured interface between APC and T cells, which facilitates prolonged molecular interactions and association of the necessary signalling molecules to an intimate core (64-66). The physical organisation of the immunological synapse is characterised by a ring of adhesion molecules, including CD2, CD48, LFA-1 and ICAM-1 molecules which form the peripheral supramolecular activation cluster (p-SMAC) around a central cluster of TCR–peptide–MHC molecules (c-SMAC) (66, 67). The importance of the immunological synapse was demonstrated by interfering with key molecules including ICAM-1, LFA-1, CD48 and CD2, where disruption of any prevented T cell activation (68-70). Furthermore, CD80 and CD86 are also located within the immunological synapse where they facilitate T cell activation, however these molecules were also shown to have regulatory properties during alloimmune response.

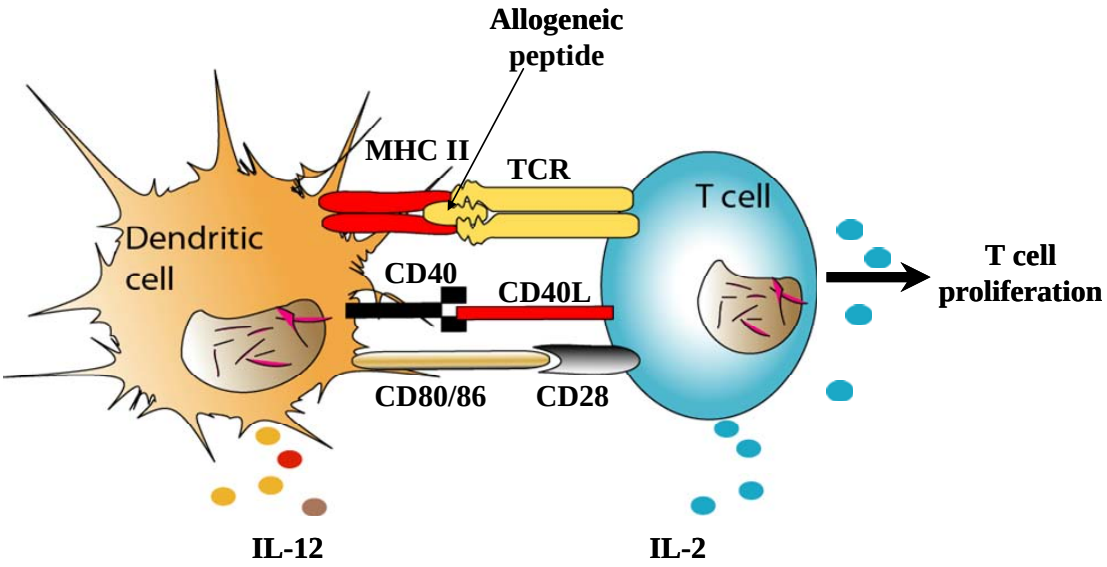

Figure 1.1. Outline of DC and T cell interactions. Upon successful organ transplant two pathways of allorecognition take place, direct and indirect. In case of direct alloantigen presentation naïve autologous (to recipient) T cells recognise donor MHC II/peptide complexes from allogeneic DC. During indirect allorecognition pathway autologous naïve T cells recognise processed alloantigens on the surface of autologous DC. The engagement of MHC II/TCR molecules is termed **signal 1**. Following signal 1, upregulation of CD40 and then CD80/86 occurs in DC to induce activation signals on T cells (**signal 2**). Although not depicted, other molecules such as OX40, LFA3 and ICAM1 are also involved in the signal 2. Both signal 1 and 2 lead to the production of IL-12 and IL-2 from DC and T cells respectively (**signal 3**). Now T cells can undergo active proliferation and education to develop into T effector cells and destroy allograft.

1.4.5 CD80 and CD86 in allo-activation and tolerance

Although CD80 and CD86 share a similar secondary structure, CD86 is expressed on the cell surface as a monomer (71, 72) while CD80 was shown to be expressed as homodimer (73). However, both CD80 and CD86 can bind to CD28 and CTLA-4 (74). A major difference between CD80 and CD86 molecules is in their dissimilar kinetics of expression. While CD80 is absent on resting APC and has delayed expression kinetics, CD86 is expressed on APC at low levels and is rapidly up-regulated upon activation (74). Activation of DC with CD40/CD40L leads to upregulation of CD80 and CD86 molecules (75, 76) and their expression was shown to play an important role in the homeostasis of regulatory T (T_{reg}) cells. CD80/86 interactions with CD28 on T_{reg} cells were also shown to be important for sustaining T_{reg} cell viability (77, 78).

Interestingly, CD80/86 molecules were originally thought to promote activating signals, however cross-linking of CD80/86 expressed on DC with membrane bound CTLA4 (including from T_{reg} cells) was shown to induce IFN-γ production. IFN-γ then in turn induced DC production of indoleamine 2,3-dioxygenase (IDO), an enzyme that can degrade tryptophan, which inhibited T cell proliferation (79-81). Therefore, CD80/86 represents pivotal costimulatory molecules involved in DC/T cell interactions, which under appropriate conditions can either induce or inhibit T cell responses.

Besides membrane bound immunomodulatory molecules, cytokine production has also been demonstrated to play an important role in skewing alloimmune responses towards either tolerance or rejection.

1.4.6 Th1/Th2 Paradigm in Transplantation

$CD4^+$ T helper (Th) cells can be divided into two distinct functional subsets (Th1 and Th2) each able to produce their own set of cytokines and direct T cell differentiation (82). Th1 cells specifically produce IL-2 and IFN-γ and are associated with cell-mediated immunity. Th2 cells specifically produce IL-4 and IL-10 and initiate the humoral response.

In general, Th1 polarised response has been implicated in the rejection of transplants while Th2 skewed response is believed to promote tolerance in transplantation models (83). This is supported by the expression of the Th2 cytokines IL-4 and IL-10 in grafts of tolerant animals; while rejected grafts were found to have high levels of the Th1 cytokine IFN-γ (84). It has been also shown that DC could be playing a role in skewing the immune responses. For example, mouse liver DC and rat airway-derived DC were able to selectively activate Th2 cells, while in humans, G-CSF mobilisation of peripheral blood stem cells generated DC that promoted deviation of CD4+ T cells into Th2 cells (85-87). Another DC subset called plasmacytoid DC (pDC), which reside in the T cell area in secondary lymphoid tissues and in blood, can produce high amounts of IFN-α and selectively induce Th2 polarised response (88-90). Although pDC have been shown to prolong survival of fully MHC-mismatched allograft in murine models (91, 92), this DC subset will not be studied in the current project. Paradoxically, studies using rat liver transplant model have challenged the above Th1/Th2 paradigm by showing the lack of Th1 (IFN-y/IL-2) to Th2 (IL-4/IL-10) skewing in tolerant animals, and vice versa (93).

Additional T helper cell subset which has recently been described in mouse was shown to exclusevly produce IL-17 cytokine and therefore this subset was termed Th17

cells. While there is no direct evidence for the existence of exclusive Th17 subset ih humans there are reports of IL-17 secreting T helper cells (94-96). T helper cells can be skewed towards Th17 cells in theresence of Transforming growth factor betta (TGF-β) (97). Althought the role of Th17 cells in transplantation is still not clear, it has been reported that human renal allografs with borderline allograft rejection have elevated IL-17 mRNA expression (98).

Therefore, in the absence of any modification some DC subsets (i.e. pDC) can generate T cells expressing certain types of cytokine and consequently prolong allograft survival. Subsequently, it may be anticipated that manipulation of myeloid DC could generate tolerogenic DC capable of inducing tolerogenic cytokine production and in turn promote long-term allograft acceptance.

1.5 Mechanisms involved in allogeneic T cell Hyporesponsiveness

As the T cells are the main effector cell population involved in allograft rejection, a significant amount of research has been conducted to understand the mechanisms by which T cells can induce immunity or tolerance. T cell immune response, as described in section **1.5.3**, involves recognition of antigen in the presence of costimulatory molecules and results in the clonal expansion of the reactive T cells. However, there are a number of mechanisms which can induce T cell tolerance and hence control autoreactive T cell activation. These mechanisms include T cell anergy, apoptosis, activation induced cell death (AICD) and the generation of regulatory T cells. In some situations non-manipulated DC have been shown to induce T cell anergy (99), T cell apoptosis (100) and facilitate generation of Treg cells (101). It is therefore a desired outcome for either

pharmacologically or genetically manipulated DC to have the capacity to promote the tolerogenic mechanisms in T cells which could potentially lead to transplantation tolerance.

1.5.1 T cell Anergy

T cell anergy is a tolerance mechanism where the T cell becomes functionally inactivated following an antigen encounter (102). Anergy was first observed in T cells encountering antigen presentation in the absence of necessary costimulation. In the experimental situation, a competitive inhibition of CD28 signalling by blocking CD80/86 with CTLA4-Ig upon TCR engagement, resulted in the inability of T cell clones to proliferate or produce IL-2 upon antigenic rechallenge (103). Therefore the CD28 costimulatory pathway is important for the induction of anergy. Generally, T cell anergy can be overcome by the inhibition of anergy promoting factors such as E3 ubiquitin ligase GRAIL (104) or as a result of production of growth factors such as IL-2 (105). Indeed, the mechanism by which CD28 pathway prevents T cell anergy appears to be the induction of IL-2 secretion by T cells, as anergy induced by the blockade of CD28 costimulation in the experimental setting was overcome by the addition of the exogenous IL-2 (106, 107), although in some circumstances TCR activation was also required (108). Furthermore, signalling through CTLA-4 on the other hand can induce 'division arrest' anergy which is a state in which the T cell proliferation could not be restored by the addition of exogenous IL-2 (106).

1.5.2 Apoptosis and Activation Induced Cell Death (AICD)

In a multicellular organism there is a constant turnover of cells in order to maintain cellular homeostasis (109). The process in place is known as programmed cell death or

apoptosis. Apoptosis is characterised by shrinkage of the cell, collapse of the nucleus and phagocytosis by macrophages prior to cell lysis, to minimise inflammatory responses (110). Signalling through CD28 pathway facilitates the expression of anti-apoptotic proteins, including Bcl-XL, which promote cell survival (111). Blockade of CD80/86 with CTLA4-Ig promotes T cell apoptosis and has been shown to be FasL independent (112).

Activation induced cell death (AICD) is another form of apoptosis which occurs as a result of activation via the TCR. AICD plays a vital role in both central and peripheral tolerance preventing the induction of autoimmune disease and is mediated by the expression and engagement of Fas/FasL molecules or TNF activity (113).

1.5.3 Generation of regulatory T cells (T_{REG})

Although the concept of regulatory or suppressor T cells was introduced some 30 years ago (114), it was not until 20 years later that the specific cell-surface markers enabled the characterisation of the $CD4^+$ $CD25^+$ phenotype of these cells (115). The importance of T_{REG} was recognised by many researchers around the world and this became evident by at least 500 publication each year reporting about regulatory T cells (116).

Several types of T_{REG} cells have been discovered in humans and mice. The most widely studied are the naturally occurring thymus-derived T_{REG} cells in addition to "induced" Tr1 and Th3 cells in periphery. T_{REG} cells function to prevent potentially detrimental immune responses raised against self and non-self antigens and play a vital role in maintaining autoimmune homeostasis (115). The phenotypical characteristic of thymus generated T_{REG} cells are the expression of CD4, constitutive expression of CD25 (the α-chain of the IL-2 receptor) (115), expression of the transcription factor FoxP3 (forkhead box P3) (117) and lastly, constitutive CTLA-4 cell-surface expression (118).

Functionally, $CD4^+CD25^+$ T_{REG} were shown to exert their function in a contact dependent manner. Moreover, the T_{REG} were shown to induce 'infectious tolerance' by converting naïve T cells into suppressive cells (119-121). These converted suppressive T cells in turn mediated their inhibitory actions by IL-10 (122) or TGF-β (123) production.

In contrast Tr1 and Th3 regulatory T cells do not express the CD25 marker nor FoxP3 but they do maintain significant expression of IL-10 and TGF-β respectively, to which their inhibitory function is attributed (124-126).

1.6 DC in transplantation

The role of DC in allograft rejection was first demonstrated in experiments conducted by Lechler and Batchelor, in which the injection of $1x10^4 – 5x10^5$ of donor DC restored immunogenicity to retransplanted renal allograft (127). On other hand, the involvement of T cells in allograft rejection was demonstrated by the work of Bolton *et al* (128). They showed that adoptive transfer of $CD4^+$ T cells into the athymic nude rat resulted in rapid kidney allograft rejection (128).

As reviewed in **1.4.2**, depending on the maturation status DC can either activate or inhibit specific T cell responses. Due to the lack of positive costimulatory molecules and MHC II, iDC are generally considered to have poor immunogenicity (29). Seminal experiments by Thomson's group in 1996 clearly demonstrated the immunomodulatory potential of iDC in the transplantation setting. The authors injected liver-derived iDC, which lacked MHC II, CD80 and CD86, intra-venously into the diabetic mouse 7 days prior to the pancreatic islet transplantation. These iDC prolonged mean allograft survival from 15 (control) to 30.3 days (iDC), in the absence of any immunosupression (129). In another study, systemic injection of MHC II^+ $CD80^{dim}CD86^{dim}$ bone-marrow derived iDC from B10

mice into the CH3 mice 7 days before the cardiac transplant, resulted in the prolonged median allograft survival time from 9.5 (control) to 22 days (iDC) without any immunosupression given (130). Interestingly, in both experimental models allografts were eventually rejected because these "tolerogenic iDC" were found to mature *in vivo* and induce alloimmune response against the allografts. These initial reports where iDC were shown to prolong allograft survival seeded the idea for manipulating DC to promote their immunosuppressive functions, for their potential use in cell-based immunotherapy.

Another two important aspects of alloimmune responses involving DC and T cells, such as sites of alloimmune response and forms of alloantigen presentation, need to be understood. These may become affected following DC manipulation or they may provide a better perspective on how to interfere with DC immunobiology more efficiently and facilitate the development of tolerogenic DC.

1.6.1 Sites of alloantigen presentation by DC

Final surgical procedure in the organ transplantation involves removal of a clamp which allows the recipient's blood to flow through the allograft. The donor DC which are resident in the allograft can migrate from the allograft and enter the blood circulation. Indeed, it was shown that following a cardiac transplantation murine DC from the allograft were able to migrate to the recipient's spleen and associate with resident $CD4^+$ T cells (131). In addition, donor leukocytes with DC morphology were found to migrate into the recipient's spleen and draining lymph nodes following vascularised hindlimb transplants in mice (132). These findings suggest that the recipient draining lymph nodes and spleen may be the place of initiation of an alloimmune response following the transplantation. However recent findings have demonstrated that cardiac allograft endothelium but not graft-derived

APC were able to activate $CD8^+$ T cells which led to the acute allograft rejection (133), suggesting that initiation of alloimmune response is also possible in allograft itself. Therefore it is important to manipulate DC to exert potent immunosuppressive function but at the same time not to alter the DC trafficking away from the sites of allorecognition.

1.6.2 Forms of alloantigen presentation by DC

It is generally accepted that allograft rejection can occur through either a direct or indirect interaction between DC and T cell. Direct allorecognition pathway occurs when donor DC migrate from the allograft into the recipient's secondary lymphoid organs and present their MHC molecules directly to the recipient T cells (6, 134, 135). Indirect allorecognition pathway occurs when recipient DC phagocytose allopeptides from apoptotic donor DC and present them to the T cells in the secondary lymphoid organs (6, 134, 135). Both of these allorecognition pathways can lead to a strong alloimmune response. The direct pathway of allorecognition is believed to be the primary cause of acute rejection (136). Transplanted organs have been shown to contain "passenger leukocytes" which migrate from the organs to the lymphoid tissue of the organ recipient within two days of transplantation (131, 137). This efficiently exposes donor DC to the recipient's immune system, facilitating direct allorecognition. There are 100-fold more T cells capable of participating in the direct allorecognition pathway than the indirect pathway (136), making the direct pathway an important target in the prevention of allograft rejection. More recent research using immunospot techniques has demonstrated that during acute murine skin allograft rejection, 90% of the T cell repertoire was directed against intact MHC molecules while only 10% was indirectly presented by host APC (135). However, it has also been demonstrated that the indirect pathway can contribute to chronic rejection

(reviewed in (138)). Noorchashm's group has demonstrated using the cardiac transplant model with targeted deficiency of MHC II-mediated antigen presentation that in the absence of T cell activation through indirect pathway there was a significant prolongation of allograft survival and abrogation of IgG alloantibody production (139). Also in patients with established chronic rejection, it was demonstrated that there was an increase in $CD4^+$ T cells with indirect alloimmune specificity (140, 141). Therefore the data suggests that both direct and indirect pathways of allorecognition play an important role in transplant rejection and therefore they both should be targeted using novel therapies in order to prevent the development of chronic rejection and potentiate the development of transplant tolerance (6).

Furthermore, a third mode of allorecognition pathway termed "semi-direct allorecognition pathway" has been proposed by Lechler's group (6). During this mode of antigen presentation, the recipient's DC were shown to acquire intact MHC I and II molecules from donor DC and in turn prime naïve $CD4^+$ and $CD8^+$ T cells (142, 143). In addition, both $CD4^+$ and $CD8^+$ T cells were also shown to acquire intact MHC II molecules from allogeneic DC (144). Besides MHC II, positive costimulatory molecules CD80 and CD86 were also transferred to T cells. When these T cells were used as APC they were able to induce both autologous and allogeneic T cell proliferation (144). This phenomenon of transfer of intact MHC molecules between immune cells was first noted some 25 years ago in murine thymocytes using immunoelectron microscopy (6). More recently this membrane exchange process has been termed "trogocytosis" and the authors showed (using PKH26 or PKH67 fluorescent lipid dye to stain cell membranes prior to cell co-culture) that the transfer of molecules was associated with membrane transfer between the two immune cells (145).

1.6.3 Involvement of trogocytosis in immune response

As reviewed in section **1.4**, T cell activation by DC requires complex cellular events to occur. It is widely acknowledged that T cells recognise antigens presented by DC and become activated via positive costimulatory molecules. However, reports have been demonstrated that T cells can also present antigens and activate other T cells. The ability to acquire MHC II and costimulatory molecules through trogocytosis was shown to be the primary mechanism responsible for this T cell function. Trogocytosis is a bi-directional process which occurs via: cell-cell contact (ie. association/disassociation), exosome uptake by T cells, nanotube mediated transfer of molecules and also through internalisation/recycling (146). Trogocytosis is thought to have evolved as an energy saving mechanism through which T cells gain immunological diversity by acquiring molecules synthesised by other cells (147). Membrane transfer between cells is a rapid process which has been shown to occur in minutes within the immunological synapse (145, 147). Hudrisier and colleagues proved the involvement of the immunological synapse in experiments named “redirected trogocytosis”. The authors used plasmacytoma cell line overexpressing FcR which bound specific mAb (via Fc portion) directed to molecules known to reside within the immunological synapse (145). These mAb specifically targeted TCR, CD3, CD4, CD8, CD28 and MHC II molecules. The cell membrane of plasmacytoma cells was also labelled with fluorescent membrane dye (PKH26) to allow for visualisation of membrane transfer. The authors then cultured these plasmacytoma cells with $CD4^+$ and $CD8^+$ T cells for 4h at what point T cells were harvested and analysed for PKH26 expression. The results demonstrated that all of the mAb were indeed able to trigger trogocytosis (as determined by the PKH26 acquisition by T cells) providing the evidence

that the immunological synapse is involved in trogocytosis. Furthermore, mAb directed to molecules outside the synapse (CD18 and CD71) did not trigger trogocytosis (145). Active intracellular signalling and actin polymerisation were shown to be required for sufficient trogocytosis (148). Nevertheless Bourbie-Vaudaine *et al*. 2006 demonstrated that Neuropilin-1 could be transferred from DC to T cells independently of T cell activation, however the transfer was enhanced when the T cells were activated (149). Moreover, trogocytosis has different requirements in different cell types. For example, activation was shown to be important for T cell trogocytosis while in B cells, trogocytosis occurred even at 4°C (inhibition of active processes in the cell) (148). Several cell types can undergo trogocytosis, CD4 and CD8 T cells (145, 150, 151), B cells (145), NK cells (152, 153), DC (142, 143) and monocytes (154). Recently, trogocytosis was shown to occur *in vivo* where murine double negative (DN) T_{REG} cells acquired MHC alloantigens from donor APC following the TCR engagement with MHC molecules on APC (155). Functionally, DN T_{REG} that acquired MHC antigens killed antigen specific syngenic $CD8^+$ T cells *in vitro* (155). Although Riond *et al*. 2007 were the first to demonstrate *in vivo* trogocytosis between DC and CD8+ T cells (151), the data by Ford McIntyre *et al* 2008 highlighted for the first time the physiological consequence of *in vivo* trogocytosis and provided a novel insight into the potential use of the trogocytosis approach for treatment of allograft rejection. Another recent study has also highlighted the existence of trogocytosis *in vivo*. In this study, DC acquired MHC-I/peptide complexes from tumour cells and stimulated adoptive T cell responses to the acquired tumour antigens, resulting in increased efficacy of T cell immune responses to tumours. The latter could be blocked by directly inhibiting DC trogocytosis, suggesting an active/important part of the trogocytosis mechanism during immune response (156).

In summary, there is strong evidence both *in vitro* and *in vivo* that suggests DC can proficiently transfer their membrane associated immune molecules to T cells as well as other DC. Through trogocytosis, T cells can acquire novel immune properties (ie. strong APC activity) while DC can acquire a diverse repertoire of foreign MHC/peptide complexes enabling DC to interact with T cells which otherwise would not have recognised DC if they had not acquired these novel antigenic complexes. Therefore, it is possible that the manipulation of DC such that they express molecules which give them tolerogenic properties may not be exclusive to only manipulated DC but may also be conferred to T cells and other DC through trogocytosis. The T cells or DC that acquired tolerogenic molecules via trogocytosis mechanism could then amplify the tolerogenic responses by interacting with other immune cells, resembling a form of infectious tolerance (119).

1.7 Inhibitory molecules in transplantation

It is well established that the absence of positive costimulatory molecules during APC and T cell interaction can lead to the development of tolerogenic mechanisms such as induction of T cell anergy and generation of Treg (**reviewed in 1.5**). In contrast, some proteins expressed on the APC induced T cell hyporesponsiveness and generated T_{REG} during interaction with T cells, even in the presence of normal levels of positive costimulatory molecules. In particular, molecules such as ILT3, ILT4 and HLA-G have potent suppressive functions on range of cell types and as such were chosen in this study to be used either for genetic manipulation of DC (i.e. HLA-G) or to be analysed for their involvement in function of RAPA-manipulated DC (i.e. ILT3 and ILT4).

1.7.1 Immunoglobulin-like transcript (ILT) 2, ILT3 and ILT4 structure, distribution and ligands

ILT2, ILT3 and ILT4 molecules are members of the Immunoglobulin (Ig) gene superfamily (157-159). ILT2 and ILT4 comprise of four extracellular immunoglobulin domains, while ILT3 was shown to contain only two (159). ILT3 ligand is currently unknown (157-159) whereas ILT2 and ILT4 bind human MHC class I molecules HLA-A, –B and –G but not HLA-C (160, 161). ILT2 and ILT4 were shown to have the strongest binding affinity to HLA-G in comparison to other HLA molecules (161). Since HLA-G was shown to have immunosuppressive functions relevant to transplantation (162) it could be speculated that cells expressing ILT2 and ILT4 could preferentially respond to suppressive HLA-G molecule (over classical stimulatory HLA molecules) during alloimmune response. Overexpression of HLA-G in DC may lead to competition of HLA-G with other MHC I molecules expressed on DC for binding to alloreactive T cell, a property that may promote tolerogenic alloresponses. One of the HLA-G ligands, ILT2, was shown to be expressed on $CD3^+$ T cells, $CD19^+$ B cells, $CD1a^+$ DC and $CD56^+$ NK cells (163). ILT3 expression was restricted to $CD1a^+$ DC, $CD14^+$ monocytes and in a small percentage of $CD16^+$ macrophages/NK cells (157), while second HLA-G ligand, ILT4, was expressed primarily on monocytes, macrophages and DC (158).

1.7.2 Outcome of Immunoglobulin-like transcript (ILT) 2, ILT3 and ILT4 signalling

Corresponding ligand interactions initiate a cascade of intracellular signalling which are specific to Immunotyrosine based inhibitory motifs (ITIM's) and subsequently carried out by SHP-1 phosphatase (157, 158) (**Figure 1.2**). SHP-1 can de-phosphorylate signalling

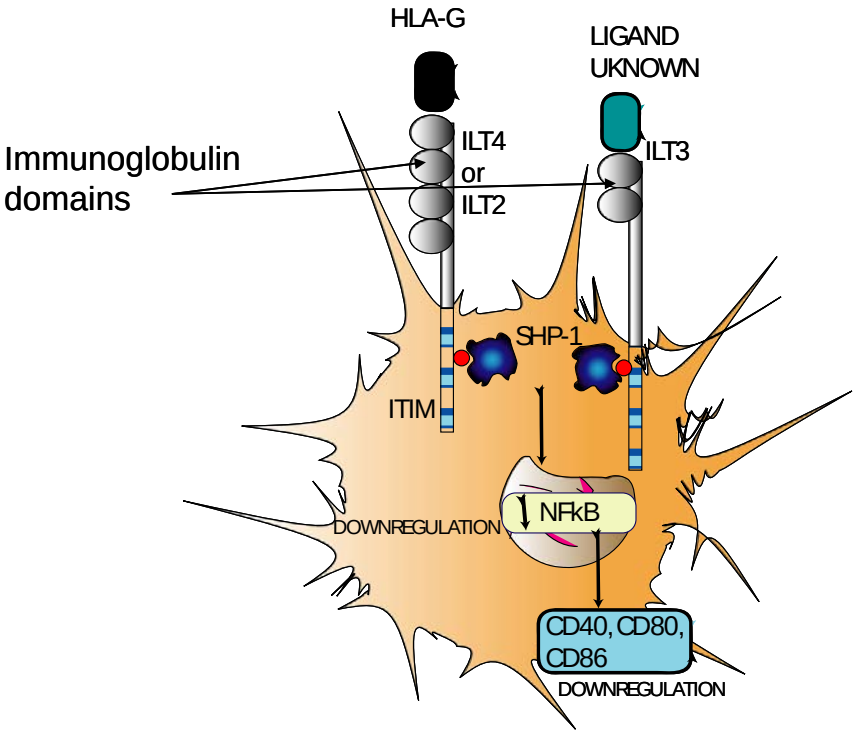

Figure 1.2. Structure and signalling of ILT2, ILT3 and ILT4 in DC. ILT2 and ILT4 molecules express four extracellular Immunoglobulin domains while ILT3 contains only two. ILT2, ILT3 and ILT4 contain cytoplasmic ITIM domains represented in light blue. Following ligand interaction ILT2, ILT3 and ILT4 molecules recruit SHP-1 phosphatase which modulates intracellular signalling events causing NFκB dependent downregulation of positive costimulatory molecules CD40, CD80 and CD86. Red circle indicates phosphorylation site recognised by SHP-1.

proteins thereby causing calcium-dependent downregulation of the NF-κB transcription factor (157, 158, 164). The latter was shown to be important for the expression of positive costimulatory molecules on the surface of DC (165). Direct evidence demonstrated that signalling through the ILT3 and ILT4 on DC downregulated CD80 and CD86 which led to impaired T cell activation (164, 166). Although there is lack of direct evidence regarding ILT2 signalling on DC, it could be speculated based on the similarities of ILT2 to ILT3 and ILT4 molecular structures that the interaction of ILT2 with its ligand would also lead to inhibition of positive costimulatory molecules.

1.7.3 Role of (ILT) 2, ILT3 and ILT4 in alloimmune response

High expression of ILT3 and ILT4 on human DC was recently shown to be induced via allogeneic T suppressor cells (Ts) or treatment with IL-10 in combination with INF-α (164, 167). When assessed in MLR, these DC were shown to inhibit allogeneic T cell proliferation in an ILT3 and ILT4 specific manner, since blocking of ILT3 and ILT4 interactions with specific mAb reversed the T cell inhibition (164, 167). Further studies showed that expression of high ILT3 and ILT4 inhibitory receptors on these tolerogenic DC played an important role in the induction of $CD4^{+}CD25^{+}$ T_{REG} cells *in vitro* (164, 167). In turn, these T_{REG} were subsequently able to induce DC tolerance *in vitro* (167). Therefore, the bidirectional interaction of the above tolerogenic DC and T cells perpetuates a cascade of events, which downregulate T cell activation and generate T cells with regulatory properties (168, 169). Clinical studies revealed that Ts and Treg cells in patients with long term heart allograft survival upregulated ILT3 and ILT4 expression on the cadaveric donor monocytes isolated from the cryopreserved tissue samples; however no such observations were made in patients who have experienced episodes of acute rejection (164, 167). The

correlation was observed between the ability of Ts cells and Treg to induce ILT3 and ILT4 expression and long term heart allograft survival (164, 167). This finding also highlighted a clinical relevance of these two inhibitory receptors in delaying transplant rejection. Besides ILT3 and ILT4, ILT2 was also shown to have immunosuppressive properties relevant to organ transplantation. Liang *et al*. 2006 have generated transgenic mice expressing human ILT2 on T cells, B cells, NK and NKT cells (170). Ligation of H-2D^{b} (a murine MHC I molecule cross-reactive with human ILT2) in these animals resulted in impairment in T cell activation, negative regulation in TCR signalling and inhibition of alloimmune response (170). Furthermore, signalling through ILT2 following the HLA-G ligation has been shown to amplify the murine CD11b^{+} Gr1^{+} Myeloid monocyte/macrophage suppressor cells in the above transgenic animals (171). Adoptive transfer of these suppressor cells into the NOD/SCID mice prolonged skin allograft survival, thus stressing the importance of HLA-G/ILT2 interactions in allograft acceptance (171). To date, HLA-G expression was correlated to several disease states, successful pregnancies as well as better transplantation outcome, thus implicating that HLA-G has complex immunobiology (172-174), which will be reviewed in the following chapter.

1.7.4 Immunobiology and function of HLA-G

1.7.4.1 Gene structure of human HLA-G

Sequence analysis of HLA-G primary transcript revealed 83% to 90% homology to other class I genes (i.e. HLA-A2 and HLA-Bw58) (175). Similar to other MHC I genes, 8 exons in HLA-G gene encode the following: exon 1 encodes signal peptide, exons 2, 3 and 4 encode α1, α2 and α3 domains respectively, the transmembrane domain is encoded by exon 5, while exons 6 and 7 encode intracellular domains (175). Alternative splicing of

this primary transcript yields 7 different proteins (**Figure 1.3**) where 4 of the proteins are membrane bound (HLA-G1 – G4) and the remaining 3 are secreted (HLA-G5 – G7) (176-179). Apart from the shorter cytoplasmic tail consisting of only 6 amino acids due to the in-frame termination codon in exon 6, the full-length isoform of HLA-G (termed HLA-G1) is similar to other class I genes (175, 180). This short cytoplasmic tail was shown to influence slow transport of HLA-G to the cell surface and to prolong HLA-G turnover (181, 182). Alternative splicing of the primary transcript also gives rise to HLA-G2 isoform which lacks exon 3 and undergoes homodimerisation to form MHC II-like structure (177, 183). As a result of splicing, both HLA-G1 and HLA-G2 can have inclusion of intron 4 sequence in between exon 4 and transmembrane domain exons. Intron 4 contains a premature stop codon which results in two soluble HLA-G isoforms, termed HLA-G5 (soluble form of HLA-G1) and HLA-G6 (soluble form of HLA-G2), being produced (176, 184). Another splice variant called HLA-G3 results from the removal of both exon 3 and 4 (177), while HLA-G4 lacks exon 4. In addition, the HLA-G7 transcript only contains exon 2 and part of intron 2 and it is believed that its translation product is a small soluble protein (reviewed in (185)). Another interesting feature of the HLA-G gene is that the transcription factor binding sites in the HLA-G promoter, which are functionally active in the promoters of classical MHC I molecules, are either disrupted or non-functional (186-189). In addition to the above, HLA-G transcription control was found to be blocked by DNA methylation and histone acetylation (190, 191). These unique properties of HLA-G promoter region and strong epigenetic control mechanisms make the induction of HLA-G difficult and restricted to certain cell types and pathological condition (192).

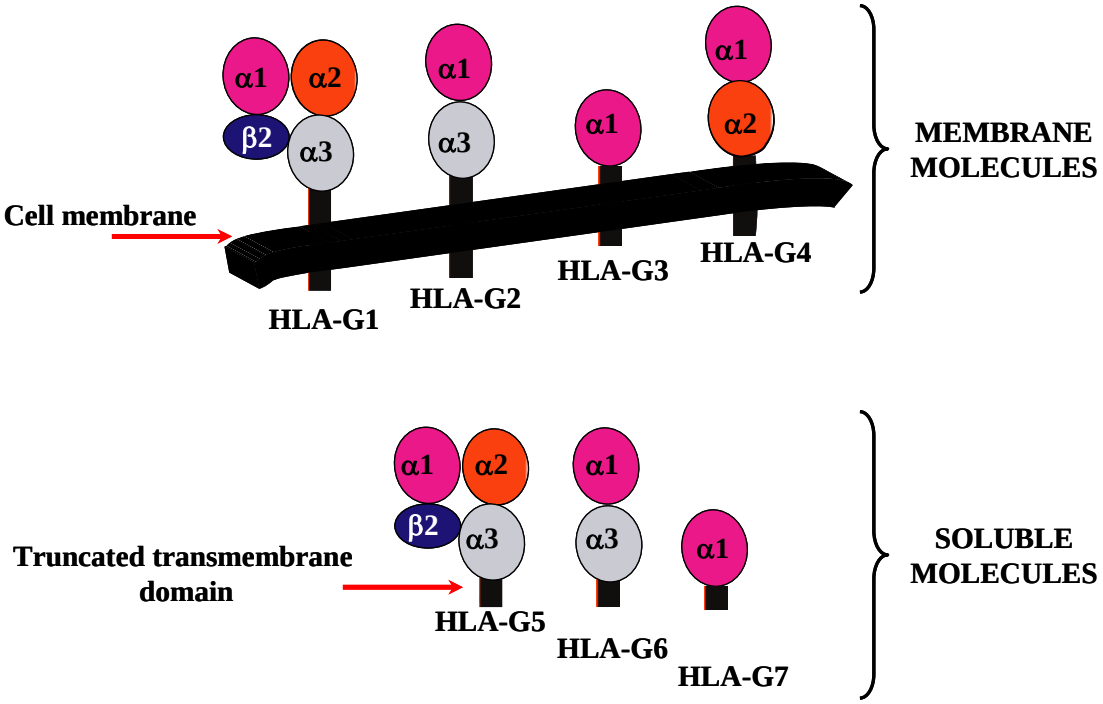

Figure 1.3. Structure of HLA-G isoforms. Processing of primary HLA-G transcript yields full-length HLA-G1 protein containing α1, α2, and α3 domains complexed with β2-microglobulin. HLA-G1 is a membrane bound molecule as it contains the transmembrane coding region. Differential splicing of the primary transcript generates seven different HLA-G isoforms of which three lack transmembrane domains, making them soluble proteins.

1.7.4.2 Protein structure of human HLA-G

A recent study by Clements *et al*. reported for the first time the crystal structure of monomeric HLA-G complexed with natural endogenous peptide ligand derived from histone H2A (193). The authors showed that HLA-G structure closely resembled that of other MHC I molecules, where the heavy chain comprised of 3 domains (α1, α2 and α3) which were non-covalently associated with beta-2 microglobulin (β2M) (193). In the same study it was reported that α3 domain, which was previously suggested to be important for selective and high affinity binding to the Immunoglobulin-like transcript (ILT) 2, (ILT2), and ILT4 (161), had increased hydrophobicity which may explain the high affinity and selectivity of the HLA-G binding to the ILT2 and ILT4 (193). Another unique property of HLA-G molecule is the presence of free Cys42 and Cys147 residues (175, 193), which play an important role in disulfide mediated dimerisation and trimerisation of HLA-G molecule, respectively (194-198). Indeed the recent study determined the crystal structure of the wild-type dimer of HLA-G1 which was connected by the intermolecular Cys42-Cys42 disulfide bond (198). This dimer structure had an oblique configuration in order to expose ILT and CD8 binding sites upwards, thus making them easily accessible for receptors. Affinity binding studies reported that HLA-G dimer had a higher overall affinity for its receptors ILT2 and ILT4 than its monomeric form (198). Mutation of Cys42 to Ser42 completely abrogated disulfide bond formation in transfected LCL 721.211 cells and hence dimer formation (197). The latter finding was supported by another group which showed that mutation of Cys147 to Ser147 prevented homeotrimerisation of the HLA-G in transfected LCL 721.211 cell lines (194, 195). It was also demonstrated that these mutations did not affect overall HLA-G surface expression (196, 197), however they did

reduce binding of HLA-G to the ILT2 receptor (194-196). LCL 721.211 cells transfected with genomic HLA-G (.211-HLA-G) were previously shown to be protected against ILT2 specific NK cells mediated lysis (199). The latter was supported in the report by Gonen-Gross *et al*., with an additional finding showing that both Cys42 and Cys147 mutations in HLA-G molecule led to an increase in NK mediated lysis (195). Besides HLA-G dimerisation, the association of HLA-G with β2M was shown to be important for ILT2 binding (194). After the removal of the β2M from the surface of .211-HLA-G with mild acid treatment there was complete reduction in ILT2 binding. In addition, removal of the HLA-G free heavy chain with papain treatment increased ILT2 binding, suggesting that free heavy chains may interact with the HLA-G/β2M molecule and provide only weak binding affinity towards the ILT2. This was confirmed by the functional studies showing that .211-HLA-G inhibited NK mediated lysis, however this inhibition was abolished following the acid and papain treatment of .211-HLA-G cells (194).

Apart from the dimerisation of HLA-G on the cell surface of transfected LCL 721.211 cell lines, untransfected Jeg-3 cells also contain HLA-G dimers on their surface. This suggested that HLA-G dimerisation is a naturally occurring process and not an artefact of transfection (194, 195, 200). In addition, human embryonic kidney cells (HEK 293) were shown to secrete HLA-G dimers in the culture, thus supporting the existence of HLA-G dimerisation in primary cells (183). Interestingly, soluble HLA-G molecules were shown to be released from the cell surface, unlike other MHC I molecules, through a mechanism which is most likely metalloproteinase-dependent (201). This data emphasised that attention is required to ensure that cloned HLA-G contains Cys42 and Cys147 residues, as these are necessary for HLA-G function.

1.7.4.3 Expression of HLA-G on Dendritic cells

Interestingly, monocyte derived DC failed to express detectable cell surface HLA-G1 (202). However, mRNA and secreted HLA-G were detectable, suggesting the role of post-transcriptional and post-translational modifications in controlling HLA-G expression (203). It may also be possible that lack of β2M expression is limiting HLA-G expression. This was supported through experiments where transfection of β2M into the β2M deficient Fon^- cell line led to a significant increase in the expression of classical HLA-A, B, C and non-classical HLA-G molecules (204). Conversely, HLA-G1 expression in HLA-G1 transfected Fon^- cells was weak, which was in concordance with β2M deficiency (204).

On the other hand, cell surface expression of HLA-G1 on DC was induced by the addition of tryptophan (Trp), and its metabolites kynurenine and 3-hydroxyanthranilic acid, during DC differentiation from monocytes via post-translational mechanism (205). Kynurenine increased HLA-G surface expression regardless of the maturation stimuli used, while 3-hydroxyanthranilic acid showed minimal cell surface HLA-G induction. Furthermore, maturation with a IFNγ/LPS cocktail in the presence of kynurenine increased HLA-G5 secretion (205). Interestingly, *in vitro* treatment of monocyte derived DC with IL-10, TGF-β, IFN-γ/IL-2/GM-CSF and LPS did not induce soluble HLA-G expression (203). In contrast to the DC from healthy individuals, surface expression of HLA-G was detected in DC from tumoral biopsies of lung carcinomas, pulmonary disease (206-208) and primary cutaneous lymphomas (209). It was suggested that the expression of HLA-G in these pathological states could divert normal immune response and compromise recovery.

1.7.4.4 HLA-G receptor interactions

Besides ILT2 and ILT4 receptors (section **1.7.2**) the HLA-G molecule was identified also to interact with KIR2DL4 and CD8 α/α.

1.7.4.4.1 KIR2DL4 receptor

The KIR2DL4 inhibitory receptor which, like the ILT2 and ILT4, contains ITIM motifs and associates with SHP tyrosine phosphatise, was shown to bind HLA-G (197, 210-212). KIR2DL4 is expressed on NK cells ($CD56^+$ population) as well as T cells ($CD3^+$ population). It was also demonstrated that the interaction of HLA-G on .211-HLA-G cells with KIR2DL4 on NK cells, inhibited specific NK cell mediated lysis of .211-HLA-G targets (210). It could be hypothesised that overexpression of HLA-G on DC could target both innate and adoptive immunity by interacting with T cells, B cells (through ILT2 and ILT4) and also NK cells (via KIR2DL4 and ILT2).

1.7.4.4.2 CD8α/α receptor

HLA-G can also directly interact with CD8α/α on T cells. This was first demonstrated by Sanders and colleagues, where they showed that .211-HLA-G cells adhered to the CD8 transfected COS7 cells (213). Interestingly, a recent report has shown that ILT2 and ILT4 were competing with CD8α/α for the HLA-G binding (161). Therefore, it could be speculated that by overexpressing HLA-G in DC, alloreactive CD8+ T cells would preferentially interact with HLA-G on DC and receive tolerogenic signals rather then activating signals from classical MHC I molecules.

1.8 Immunomodulatory functions of HLA-G molecule

1.8.1 HLA-G arrests maturation of APC

One of the effects of HLA-G mediated through ILT4 on DC is the inhibition of DC maturation. Treatment of human monocyte derived iDC with HLA-G1 tetramers prevented CD40L mediated upregulation of MHC II, CD80 and CD86 costimulatory molecules (214). The effect was inhibited by the pre-treatment of the iDC with 27D6 mAb which specifically blocks ILT4 binding to HLA-G (214). Furthermore, the same authors show that the co-culture of purified allogeneic $CD4^+$ T cells with DC treated with HLA-G1 tetramer reduced the number of activated $CD4^+CD25^+$ T cells, however increased $CD4^+CD25^+CTLA\text{-}4^+$ T cells which were generally considered to have regulatory properties (215-217). These cells produced low IL-2 and IFNγ and moderate levels of IL-10 protein. Indeed the above $CD4^+$ T cells were true regulatory cells as they inhibited allogeneic mixed lymphocyte reaction (MLR) between DC (autologous to the generated regulatory T cells) and third party T cells. Furthermore, relative to the untreated DC, DC treated with HLA-G1 tetramers increased the number of IL-10 secreting $CD8^+CD28^-$ T cells (215). These $CD8^+CD28^-$ T cells are also termed T suppressor (Ts) cell because of their immunosuppressive property towards other T cells (168, 169).

However, a contrasting report has been published recently claiming that the addition of 1 μg/ml of recombinant human HLA-G5 was unable to inhibit TNF-α maturation of monocyte derived DC (218). Although the culture condition of DC were similar between the two reports, there could be several other factors contributing to the differences observed. This could include: 1) the type of the HLA-G used (it was reported that HLA-G5 and HLA-G6 can have different effects and different binding properties to ILT2 and ILT4 on the same cell type (219)), 2) dimerisation was shown to be important for HLA-G1

(194, 195) and HLA-G5 (220) functions thus tetramers may have a stronger affinity for ILT2 and ILT4 receptor on DC compared to the HLA-G5 which may not efficiently dimerise in the culture, 3) different maturation stimuli used and 4) different timing of HLA-G addition. Therefore further studies are essential to elucidate the conditions under which HLA-G works most efficiently to inhibit DC maturation and promote DC tolerogenic functions. This understanding of HLA-G immunobiology during alloimmune response could facilitate the development of successful HLA-G-based immunotherapy against transplant rejection.

1.8.2 The effect of HLA-G on T cells

When LCL 721.211 cell line transfected with HLA-G was used as a stimulator in MLR, it inhibited T cell proliferation in a HLA-G dependent manner, which was demonstrated by the use of anti-HLA-G mAb (221). This was the first evidence which demonstrated inhibition of T cell proliferation by membrane bound HLA-G. Further reports strengthened this observation, showing that CR1 (222) and KG1 (223) cells transfected with HLA-G were also able to inhibit $CD4^+$ T cell proliferation. Furthermore, KG1 transfected cells rendered T cell unresponsive to the subsequent allogeneic stimuli (which was similar to the T cell anergy) and generated Tr cells which were shown to suppress proliferation of secondary MLR (223). The inhibition of T cell proliferation by KG1 transfectants was dose dependent (223), supporting the rationale for overexpression of HLA-G on DC (which express low or undetectable HLA-G). Interestingly, sensitisation of T cells *in vitro* with HLA-G5 transfected cells rendered T cells incapable of proliferation to subsequent allogeneic stimuli (220). In the same report it was shown that patients with long term allograft survival had high serum levels of HLA-G5, which was previously found to

be associated with fewer rejection episodes (224). When the serum from these patients was used in T cell sensitisation it exerted the same effect as HLA-G5 transfected cells (220). Most interestingly, pre-treatment of T cells with supernatant from HLA-G5 transfected cells generated Ts cells capable of inhibiting MLR in a contact independent manner (220). In the same study, direct addition of HLA-G5 in the PBMC MLR showed that a HLA-G5 suppressive effect was primarily mediated through ILT2 and ILT4 receptors on monocytes as the use of specific anti-ILT2 and ILT4 mAb reversed the T cell inhibition.

Moreover, the direct interaction of soluble HLA-G1 with the CD8 receptor on $CD8^+$ T cells induced FasL upregulation and secretion in these T cells, which in turn induced their apoptosis via the Fas/FasL pathway (225, 226). This finding could explain why some researchers have shown reduced T cell proliferation in MLR. However, a recent study demonstrated that T cell apoptosis was not induced during the early steps of T cell activation but that the HLA-G5 mediated inhibition of T cell proliferation was due to cell cycle arrest in T cells (227). In addition to T cell apoptosis and cell cycle arrest, HLA-G5 inhibited cytotoxicity of $CD8^+$ T cells was reversed with anti-HLA-G1 specific mAb (87G). Others have also shown that HLA-G can inhibit a cytotoxic T cell response (228) and that the effect of HLA-G on inhibition of T cell cytotoxic response was concentration dependent (229). Isoforms other that HLA-G1, namely HLA-G2, G3 and G4, can also protect transfected target cells barring these molecules against acquired T cell cytotoxicity (230). Altogether, these findings demonstrate that both HLA-G1 and HLA-G5 have strong immunosuppressive properties towards DC and T cells. Importantly, HLA-G can contribute to all three mechanisms of tolerance generations and that is: induce T cell apoptosis, render T cells unresponsive to antigenic stimuli (similar to T cell anergy) and generate Tr or Ts cells. With this in mind, it is fair to say that HLA-G represents a strong candidate for

genetic manipulation of DC in order to generate DC with strong antigen specific immunosuppressive properties.

1.9 Cell-based tolerogenic therapy for transplantation

Various immunosuppressive genes (together with various gene delivery mechanisms) and different pharmacological agents are being used to generate tolerogenic DC (231, 232). Depending on the nature of the immunosuppressive gene or the pharmacological agent, DC exhibit different immunomodulatory properties. Some modified DC can induce T cell hyporesponsiveness, prolong allograft survival, induce apoptosis in $FasL^+$ T cells and even induce T cell anergy in some cases (233-237). Besides DC therapy, antigen-specific T regulatory cells are being investigated as potential cellular therapy agents for the treatment of transplant rejection (238, 239). The approach involves the generation of patient's T_{REG} cells *ex vivo* directed against donor antigens and expansion to sufficient numbers to be injected back into the transplant recipient (239). However there are limitations associated with this particular approach, including poor expansion efficiency of T_{REG} *in vitro*, durability of T_{REG} *in vivo* is untested in humans and whether the *in vitro* suppression assays employed to asses T_{REG} function reflect their function *in vivo* is currently unknown (238). Another limiting factor of this approach is selection of T_{REG} cells based on their profile. For example, the FoxP3 transcription factor is a key marker of T_{REG} cells, however its intracellular expression makes it unsuitable for cell separation for use in subsequent functional applications. Therefore studies are using a $CD4^+$ $CD25^{high}$ based selection approach to isolate T_{REG} cells, however in humans, activated T cells which do not possess T_{REG} properties can also express CD25 and FoxP3, thus making isolation of specific T_{REG} cells challenging (240). In addition, it is reported that expansion of $CD25^{bright}$

T cells using conventional CD3 and CD28 specific mAb's with IL-2 gives rise to only 50-60% FoxP3 positive cells (238). Recently another marker, CD127, has been demonstrated to be inversely correlated with Treg phenotype, thus isolation of CD127low cells together with CD25bright marker may provide a more specific enrichment approach however multiple cell separation parameters will eminently decrease yields making the expansion of T_{REG} a rate limiting step of this cell-therapy approach (241). Furthermore, DC therapy also has potential problems and these include stability of tolerogenic phenotype *in vivo*, durability of DC in humans and longevity of the tolerogenic response (hence may necessitate the need for re-administration of DC) (26). As mentioned earlier, monocyte derived DC have been used successfully in human trials for cancer treatment and no safety concerns were identified during phase I trials. Therefore, in the present study DC as potential tolerogenic therapy was explored for two reasons. Firstly, based on the safety data available in humans regarding the use of monocyte derived DC in cancer therapy there is likelihood that monocyte-derived tolerogenic DC may not pose safety concerns (34). Secondly, as reviewed below DC can induce T_{REG} under special circumstances and thus modification of DC could lead to generation of antigen specific T_{REG} *in vivo*, thus potentially overcoming technical issues of expanding and generating T_{REG} cells *in vitro* (26). In addition, use of DC is also justified by the fact that DC are involved in the initiation of alloimmune response and therefore tolerogenic DC would exert suppressive effects towards allogeneic T cells at the time of the initial contact with that alloreactive T cell. In the case of T_{REG} cells, specific suppression would have to rely on T_{REG} firstly finding and then suppressing the specific alloreactive T cells which, if not suppressed, could still exert its effector functions and lead to allograft damage.

1.9.1 Pharmacological manipulation of DC

Pharmacological manipulation of DC employed the use of a variety of agents, including the immunosuppressive drugs Cyclosporine A (CsA) and Rapamycin (RAPA) (231, 242). CsA and RAPA are known to inhibit the calcineurin and mammalian target of rapamycin (mTOR) signalling pathways, respectively, thus affecting multiple biochemical processes within the cell (243-247). Consequently, both agents were recently shown to inhibit murine and human DC maturation although studies involving human DC are somewhat limited and controversial (248). CsA and RAPA inhibited DC maturation through the downregulation of CD40, CD80 and CD86, as well as by impairing cytokine production (233, 249-252). As a result, these DC exhibited *in vitro* tolerogenic potential by inhibiting allogeneic T cell proliferation (250, 253). The *in vivo* potential of RAPA-treated DC was highlighted in an elegant study by Taner *et al*. 2005 (235). It was observed that RAPA-treated alloantigen pulsed mouse DC expressed low CD80, CD86 and MHC II, and were inferior stimulators of syngeneic T cell proliferation in MLR relative to the untreated DC (235). When these RAPA-treated DC were injected intravenously into mice one week before the transplantation, they significantly prolonged heart allograft survival in an alloantigen-specific manner. It was also demonstrated that the systemic delivery of exogenous IL-2 reversed allograft survival; this was indicative of the induction of T cell anergy by RAPA-treated alloantigen pulsed DC (235). In addition, Zhang *et al* (254) showed that the agent LF 15-0195 (an analogue of 15-deoxyspergualine) was able to inhibit CD40, CD80 and MHC II expression in bone marrow derived mouse DC. These DC exhibited tolerogenic property *in vitro* by inducing T cell hyporesponsiveness. When injected in mice 7 days prior cardiac transplant, LF 15-0195 treated tolerogenic DC were able to prolong cardiac survival and augmented the expression of

$CD4^+CD25^+CTLA4^+FoxP3^+$ T_{REG} (section **1.5.3**) cells in these animals. These DC also generated *in vitro* T_{REG} cells which prolonged allograft survival when adoptively transferred into the above cardiac transplant mice (254). Other agents such as Aspirin, Vitamin D3 analogues, and Corticosteroids have been successfully used to generate DC with tolerogenic properties *in vitro* (242). These agents were shown to inhibit expression of costimulatory molecules on DC, interfere with DC antigen uptake, induce IL-10 and inhibit IL-12 production by DC, respectively (242).

Therefore, pharmacological manipulation of DC can be used to target both indirect (Taner *et al* (235)) and direct pathways of allo-recognition (Zhang *et al* (254)) and therefore it could potentially interfere with both acute and chronic allograft rejection (see **1.6.2**). Although other agents were shown to have the potential to modify DC function, in the current study CsA and RAPA were selected as the agents of choice for two reasons. Firstly, there are a significant number of studies using murine DC as a model demonstrating potent *in vitro* and *in vivo* tolerogenic properties of CsA and RAPA modified DC. Secondly, CsA and RAPA are most commonly used in immunosuppression regimens for transplant patients and the use of these agents in human DC cultures may provide useful information on what effect these agents have on DC phenotype and function in transplant patients. Lastly, since both CsA and RAPA are approved for human use by the Food and Drug Administration (FDA) it is likely that CsA and RAPA modified DC would be more likely to be approved by the FDA relative to some other approaches.

1.9.2 Genetic manipulation of DC

A variety of vectors, both viral and non-viral, are available for the transfer of genetic material into cells. Non-viral gene techniques include electroporation (255, 256), ultrasound (257), ballistic gene transfer (256), cationic liposomes and more recently the use of nanoparticles (258). However, while non-viral technologies are simple to manufacture and induce minimal immunogenicity, gene transfer using a non-viral approach is often inefficient and transient (259-261). Therefore, viral vectors have been developed in order to induce higher levels of transfection efficiency in cells. Advantages and disadvantages of the various vectors are summarised in **Table 1.2**.

Currently, Adenoviral vectors are primarily used for genetic manipulation of DC, since they provide increased transfection efficiency compared to the non-viral alternatives. Furthermore, as retrovirus requires cells to undergo active division for infection, terminally differentiated DC are therefore poorly transfected using these vectors. On the other hand, Adenoviral vectors are able to infect non-dividing cells and can be efficiently grown to high titres, making them supreme candidates for DC transfection. Importantly Adenoviral transfection does not disrupt DC function (262) although DC maturation has been reported in some cases (263, 264). Although, human monocyte-derived DC lack coxsackie adenovirus receptors (265, 266), which are the primary cell attachment molecule for adenoviral serotype 5 vectors (267), transfection of DC has been improved to levels greater than 90% by combining the adenoviral vector with cationic liposomes during DC transfection (268). Recently, the modification of adenoviral vectors to express the fibre protein from group B adenoviruses has facilitated high levels of DC transfection by permitting binding to CD46 molecule on the cell-surface of DC (269, 270). Upon binding to DC, internalisation of adenoviral vectors is facilitated by $\alpha v\beta 3$ or $\alpha v\beta 5$ (271, 272).

Although adenoviral vectors provide high transfection efficiency, the primary limitations of these vectors are the induction of strong anti-viral immune responses characterised by augmented TNF, IL-1 and IL-6 secretion and CTL activation, which can result in the rapid elimination of adenoviral transfected cells and particles (273-275). As a result of the rapid induction of T cell mediated immune responses against the adenovirus Adenoviral mediated gene transfer has been limited in many *in vivo* models (276). However, the presence of immunomodulatory proteins can attenuate this response. In particular systemic CTLA4-Ig treatment attenuates anti-viral immunity, thereby enhancing the persistence of adenoviral vectors *in vivo* (277). Importantly, direct transfection of DC with CTLA4-Ig increases the survival of the cells in lymphoid tissues of MHC class II mismatched allogeneic recipients (278), providing evidence that CTLA4-Ig can act as a "stealth" gene to mask the immunogenicity of adenoviral vectors. Therefore, in our system we may anticipate that HLA-G could provide a "stealth" effect and potentially mask the strong immunogenicity of Adenoviral vectors while at the same time conferring tolerogenic properties to DC.

However, despite the disadvantages, Adenoviral vectors were shown not to cause insertional mutagenesis and there is a clinical experience using these Adenoviral vectors (273-275, 279-281). This provided confidence for the use of Adenoviral gene delivery approach for manipulating DC. For instance, myeloid DC transduced with Adenoviral vectors containing cDNA for CTLA-4-Immunoglobulin (CTLA-4-Ig) showed strong inhibition of T cell proliferation and inhibition of cytotoxic T cell responses *in vitro* (282). This was also shown in our laboratory in both human and ovine DC models, transduced with adenoviral constructs encoding CTLA-4-Enhanced Green Fluorescent protein (CTLA-4-EGFP) (283). Others have demonstrated that transduction of monocyte derived

DC with FasL resulted in DC population capable of inducing apoptosis in activated Fas-expressing $CD4^+$ and $CD8^+$ T cells via a cell contact dependent manner (284, 285). In addition, our laboratory has successfully transduced IL-10 in human monocyte derived DC using adenoviral gene delivery system. These DC expressed high IL-10 and prolonged human skin allograft survival in humanised NOD/SCID model of skin transplantation (see below) (236). Other groups have also demonstrated that IL-10 transfection of murine DC with adenoviral vectors containing IL-10 prolonged heart allograft survival (286). Other genes such as indoleamine 2,3-dioxygenase (IDO) (287) and TGF-β (288) have also been effectively used to generate tolerogenic DC capable of inhibiting T cell proliferation *in vitro*. From the above studies, it can be concluded that Adenoviral gene delivery approaches were able to induce a high expression of immunomodulatory genes and confer minimal cytotoxicity in target DC. Furthermore, a non-viral approach of gene silencing using antisense phosphorothioate-modified oligonucleotides to target CD40, CD80 and CD86 in DC has also successfully been employed to generate tolerogenic DC which are soon to be used in Phase I clinical trials (**discussed in 1.3**).

Therefore, genetic manipulation of DC to induce allograft acceptance is an attractive strategy in that it can induce allospecific hyporesponsiveness, while sparing the non-reactive T cells. Although promising results have been obtained in small animal models, there is a need to extend these findings into large animal models which have greater clinical significance.

Gene Therapy Vector	Advantages	Disadvantages	References
Non-Viral	Low immunogenicity Low production costs Good safety profile	Transient gene expression Low transfection efficiency Lack of clinical experience	(255-261, 289)
Adenoviral	No insertional mutagenesis High transfection efficiency High titres may be generated Infects dividing and non-dividing cells Clinical experience	Preferential targeting of the liver Strong immunogenicity (limits re-administration) Moderate production costs	(273-275, 279, 280)
Retroviral	Clinical experience Prolonged transgene expression Transgene expressed in progeny cells	Difficult manufacture Transfection of non-dividing cells is limited Potential of insertional mutagenesis	(290-295)
Lentiviral*	Infects dividing and non-dividing cells High transfection efficiency	Difficult manufacture Potential for insertional mutagenesis Lack of clinical experience	(296, 297)
Adeno-associated Viruses	Long-term transgene expression Low toxicity	Difficult manufacture Potential for insertional mutagenesis Strong immunogenicity (limits re-administration) Lack of clinical experience	(298-302)

Table 1.2. Advantages and disadvantages of gene therapy techniques

Several delivery approaches can be used to deliver genes into cells. The first approach involved the use of non-viral vectors. These vectors are cheap to manufacture, however they have poor transfection efficiency. Viral vectors on the other hand, can induce high transfection efficiency but they also induce strong antiviral immune response and have a potential to cause insertional mutagenesis. There are also significant safety concerns with the use of Retroviral based gene delivery as these vectors are replication-competent. However, Lentiviral vectors have been developed (from Retroviral vectors) in order to overcome the requirement of cell division for transfection.

1.10 The pre-clinical Ovine Model of Renal Transplantation

Although rodent models have been crucial in the development of novel therapies and acquiring new knowledge of immunological pathways, the direct translation of these studies to clinical therapies are rare (303). This has been attributed to the differences between human and rodent immune system. In contrast to human, mice exhibit reduced prevalence and diversity of memory T cells (304-306) and lack expression of MHC Class II molecules on the vascular endothelium (307), a feature which has particular relevance to the rejection or acceptance of vascularised allografts (308). Furthermore, there are also significant differences in T_{REG} cell function between the mice and human (309). Although large animal models still do not mimic the human immune system perfectly, they do however eliminate the issues posed by the mouse immune system and still present as important for the validation of therapies prior to clinical use. Thus, it is widely accepted that rodent models provide important "proof of concept" but testing in large animal models is an essential step before commencing clinical trials (310). On that note, The Transplantation Immunology Laboratory at The Queen Elizabeth Hospital (QEH, Adelaide, South Australia) has developed an ovine model of renal transplantation (311). This model was based on the initial work by Pedersen and Morris and involved the heterotopic transplantation of the kidney to the neck region where it is anastomosed to the carotid artery and jugular vein (312). In this model the kidney was able to maintain normal renal function in the presence of immunosuppression however following the withdrawal of immunosuppressive agents, the kidneys exhibited rejection with both histological and physiological features similar to that of human kidney allograft rejection (313).

Ideally, non-human primates have a similar immune system to humans and they can provide the closest matched models of human disease. However, the use of primate models is frequently limited by significant costs and socio-ethical concerns (314). Therefore, the

sheep model represents an advantageous model for pre-clinical testing because of low costs associated with the animal purchase and husbandry, the docile nature of sheep, and the well-characterised immune system.

1.11 Study rationale and Hypothesis

Organ rejection is currently managed with the use of immunosuppressive agents which are largely non specific and have adverse side effects (**1.2**). The most desired outcome for the transplant clinician and the patient is the induction of clinical tolerance towards allograft (**1.2**). Although several agents are being investigated in clinics as a potential tolerance induction strategy, these agents lack allospecificity (**1.2**). Current successful tolerance induction protocol relies on the establishment of microchimerism of donor cells in the recipient (**1.2**). DC microchimerism was shown to be present in a tolerant patient, suggesting the potential implication of DC in tolerance induction (**1.2**). *In vitro* manipulation of DC using pharmacological and genetic approaches generated tolerogenic DC capable of prolonging allograft survival in animal models in the absence of immunosuppression (**1.3, 1.9.1**). It is proposed that these pharmacologicaly or genetically modified DC would interact with the alloreactive T cells in an alloantigen specific manner and induce an antigen-specific tolerogenic response, in contrast to conventional immunosuppression therapy. Based on the murine studies, it is believed that it is possible to create tolerogenic human DC (either autologous or allogeneic) *in vitro* and inject them into the recipient at the time of transplantation (similar to the bone marrow co-transplant study) in anticipation that these DC may induce donor specific tolerance (**1.3, 1.9.1**). Tolerogenic human DC, generated using genetic manipulation *in vitro*, are currently investigated in a single phase I clinical trial for their ability to suppress the immune responses in Type I

diabetes mellitus (**1.3**). The lack of other clinical trials could suggest that there is a deficiency in potent human tolerogenic DC being generated.

In the present study, the aim was to investigate the role of specific pharmacological (CsA and RAPA) and genetic manipulation (induction of HLA-G) on the ability to generate potent human tolerogenic DC. Selection of the CsA and RAPA was based on previous studies using murine models, where it was demonstrated that manipulation of murine DC with CsA or RAPA generated tolerogenic DC capable of prolonging allograft survival (**1.9.1**). However the ability of these agents to generate tolerogenic human DC is unclear. Furthermore, these two agents are approved by the FDA and are currently used in transplant patients; thus if CsA and RAPA were found to generate potent tolerogenic human DC, then this approach of generating tolerogenic DC may not pose a significant safety issue in clinical trials (**1.9.1**). On the other hand, HLA-G was selected because of its potent immunosuppressive properties *in vitro* towards both DC and T cells, and its association with a better allograft outcome in transplant patients (**1.7.4**). HLA-G is also believed to protect semi-allogeneic foetus from maternal immune system attack and thus it was rationalised that HLA-G presence on DC may exert tolerogenic immune responses similar to those during pregnancy and thus enable allograft acceptance (315).

Therefore, in the current study two general hypotheses are set out to be investigated. Firstly, it is hypothesised that pharmacological manipulation of human monocyte derived DC, with Rapamycin in particular, will generate tolerogenic DC capable of inhibiting T cell proliferation. Secondly, it is hypothesised that genetic manipulation of human monocyte derived DC with Adenoviral vectors containing HLA-G molecule would induce tolerogenic DC capable of inhibiting T cell proliferation through a HLA-G dependent mechanism.

Both hypotheses will also be tested using ovine DC because the host laboratory has developed a pre-clinical ovine model of kidney transplantation which could be used to

evaluate, for the first time, the clinical potential of manipulated DC in a large animal model.

1.12 Project Aims:

The key aims of this study:

a) To examine the ability of CsA or RAPA to generate tolerogenic human DC *in vitro*. To address the above aim, CsA or RAPA will be added during DC differentiation, maturation or directly to mature DC cultures (the latter has never been investigated). The following parameters will be measured:

   a) DC viability following CsA or RAPA treatment
   b) Ability of CsA or RAPA DC to induce T cell hyporesponsiveness in a mixed lymphocyte reaction
   c) DC phenotype of costimulatory molecules as well as inhibitory receptors ILT-2, 3, 4 and HLA-G
   d) Cytokine profile expression in DC following CsA or RAPA treatments
   e) Ability of CsA or RAPA treated DC to induce T cell anergy or T_{REG} cells

b) To investigate the ability of RAPA to generate tolerogenic ovine DC. By using ovine DC, it is possible to extend the *in vitro* observations and analyse the effect of tolerogenic DC *in vivo* using a chimeric NOD/SCID mouse model of vascularised ovine skin transplantation. The extension of this study would be to use a pre-clinical ovine model of kidney transplant to further study the potency of tolerogenic ovine

DC, thus simulating the potential effect of human DC *in vivo*. The following parameters will be tested:

a) DC viability following RAPA treatment
b) Ability of RAPA DC to induce T cell hyporesponsiveness in a mixed lymphocyte reaction
c) DC phenotype of costimulatory molecules
d) Cytokine profile expression in DC following RAPA treatments
e) Ability of RAPA treated DC to induce T cell anergy
f) Analysis of the ability of RAPA-treated DC to suppress vascularised skin allograft in NOD/SCID model of transplantation

c) To investigate the ability of HLA-G induction in human monocyte-derived DC to confer tolerogenic properties to the transfected DC. In order to address this aim the following will be performed:

a) To generate adenoviral vectors containing HLA-G1 or HLA-G5 cDNA
b) To characterise HLA-G integrity and DC phenotype following DC transfection
c) To measure the effects of HLA-G towards alloimmune responses specific to T cells (T cell proliferation, T cell trogocytosis and T cell capacity to present antigens) following the co-culture of transfected DC and allogeneic T cells.

Soluble HLA-G (HLA-G5) in this context will act on T cells before they encounter antigen. Recent studies showed that pre-conditioning of T cells with HLA-G5 in the absence of costimulation inhibited T cell proliferation in response to the subsequent APC challenge (220). Conversely, membrane HLA-G1 would only interact with alloreactive T cells in the context of antigenic stimulation by DC. Thus HLA-G1 would induce antigen-specific suppression in contrast to HLA-G5 which would target T cells non-selectively. Furthermore, since HLA-G5 is not a membrane bound molecule, it would serve as a control for trogocytosis experiments where it would still provide signals to T cells (like HLA-G1) during co-culture, however would not be transferred to T cells.

CHAPTER 2
MATERIALS AND METHOD

2.1. General Methods

2.1.1. Cell Culture

2.1.1.1. Ovine and Human Peripheral Blood Mononuclear Cell (PBMC) Extraction

2.1.1.1.1 Human

Buffy coats were prepared from heparinised peripheral blood obtained from healthy donors (Red Cross Blood Service, Adelaide, Australia) and PBMC were isolated by differential centrifugation through a Lymphoprep density gradient.

Blood was aliquoted into 50 mL V-bottom tubes (12.5 mL per tube) with 25 mL PBS and underlayed with 12 mL of Lymphoprep. Tubes were centrifuged for 20 min at 1100g with the brake turned off. The mononuclear cell layer was harvested and resuspended in PBS. Cells were centrifuged for a further 10 min at 1100g. Cells were repeatedly (4 times) washed in 45 mL PBS and centrifuged at 510g for 10 min to remove platelets. Pellets were resuspended in 2 mL complete RPMI media and a cell count performed using a 1:2 Trypan Blue dilution on a haemocytometer.

2.1.1.1.2 Ovine

Heparinised ovine blood (15 ml per 50 mL V-bottom tube) was diluted with 20 ml PBS and underlayed with 12 mL of Lymphoprep. Tubes were centrifuged for 45 min at 1350g with the brake turned off. The PBMC layer was collected and resuspended in PBS. Cells were repeatedly washed (4 times) in 45 mL PBS and centrifuged at 510g for 10 min to remove platelets. Pellets were resuspended in 2 mL complete RPMI media and a cell count performed using a 1:2 Trypan Blue dilution on a haemocytometer.

2.1.1.2. Human Monocyte Derived Dendritic Cells

Monocytes were selected by adherence to plastic. Briefly, $5x10^7$ PBMC were panned for 1h at 37°C in 10 ml RPMI plus 1% FCS in 75 cm^2 plastic tissue culture flasks (Sarstedt, Germany). Non-adherent cells were removed and the remaining adherent cells were cultured in complete medium supplemented with 400 U/ml IL-4 and 800 U/ml GM-CSF for 5 days to generate immature DC (iDC). The addition of 10 ng/ml TNF-α to the iDC for a further 2 days generated mature DC (mDC).

2.1.1.3. Nylon Wool Isolation of T Cells.

Following the removal of monocytes by adherence (**2.3.1.2**), nylon wool purified T cells (NWT) were obtained by applying the non-adherent cells to nylon wool columns equilibrated with RPMI, as previously described (316). The non-adherent cells were incubated in the columns for 30 min at 37°C to adsorb B cells and the enriched NWT cells were obtained by elution with RPMI plus 10% FCS. Cells were washed twice in PBS prior to use.

2.1.1.4. Mixed Lymphocyte Reaction

PBMC were extracted from peripheral blood from two ovine or human individuals (**2.2.1.1**). PBMC were co-cultured in 96-well round-bottom plates (Sarstedt, Germany) with 1 x 10^5 cells from each individual in S10g media. The total volume for each well was 200 μL. In case of the DC-MLR, autologous or allogeneic DC were used in place of one PBMC population. Plates were incubated for 4 days in a 37°C, 5% CO_2 enriched and humidified incubator. Wells were individually pulsed with 1 μCi methyl [^{3}H] thymidine and incubated for a further 18h. Cells were harvested using a Microtitre Tomtec Cell Harvester (Turku, Finland) onto Wallac gridded filter mats (Wallac, USA). Filter mats were treated

with β-scintillant and tritium incorporation in DNA was measured using a Wallac MicroBeta® Scintillation Counter (USA). Results were expressed as the mean of triplicate wells +/- standard deviation. Unpaired two-tailed student *t-test* was used for statistical analysis. The data was shown to have normal distribution using D'Agostino-Pearson noramility test.

2.1.1.5. Cell Lines

Human embryonic kidney 293 (HEK 293) cells were grown in DMEM, until 70% confluence was achieved. At this time, cells were detached using citric saline solution and washed in PBS containing 5% FCS. Cells were then passed through an 18 gauge needle in order to break the cell clumps and used to seed three new flasks of the same dimensions. All cells were grown at 37°C, 5% CO_2.

2.1.2. Molecular Biology Methods

2.1.2.1. Total RNA Extraction

Total RNA was extracted using TRIZOL® reagent according to the manufacturer's instructions. Briefly, 200 µl of TRIZOL reagent was added to 1-4x10^6 cells. Suspension was then vortexed for 5 s, and the 40 µl of chloroform was added. Suspension was vortexed again for 15 s and incubated for 10 min at room temperature before it was spun again at 11,000g for 5 min. Aqueous layer was then collected and 100 µl of isopropanol was added, and the sample was placed at -70°C for at least 2h to precipitate RNA. After precipitation, samples were thawed and spun at 11,000g for 20 min at 4°C. Supernatant was carefully removed and the RNA pallet was washed with 75% ethanol and spun again at 11,000g for 20 min. Supernatant was removed again and the RNA pallet was air dried and resuspended in 40 µl of secure citrate solution. RNA sample was heated at 60°C for 10 min to activate

the citrate solution. The purified RNA was quantified by absorbance at 260 nm using NanoDrop 1000 (Thermo Scientific, USA). Sample was then stored at -70°C.

2.1.2.2. Reverse Transcription (RT)

One microgram of RNA was then added to 4 μL Oligo dT, heated at 60°C for 5 min and snap cooled on ice. 33 μL RT-mastermix (**Table 2.1**) was added, giving a total volume of 40 μL per tube.

Table 2.1. Reverse Transcription Master Mix

RT Component	**Volume/reaction**
Sterile H_2O	19 μl
5 x First Strand Buffer	8 μl
10mM dNTPs	4 μl
RNAsin	1 μl (40U)
MMLV reverse transcriptase	1 μl
	33 μl

Tubes were then vortexed, pulsed and incubated at 37°C for 1h. The reactions were inactivated by heating the samples at 70°C for 10 min, snap cooled and pulsed. The volume was made up to 100 μl with sterile H_2O (Baxter, Australia) and cDNA was stored at -70°C until further use.

2.1.2.3. Polymerase Chain Reaction (PCR)

Details of primers are presented in **Appendix 1**. For all PCR reactions *Tth* DNA Polymerase was used. PCR mastermix (**Table 2.2**) was prepared in a DNA free room and 22.5 μl of the mix was aliquoted into PCR tubes. Two drops of sterile mineral oil were also added in order to prevent evaporation. Lastly, 2.5 μl of cDNA was added to each tube

giving a final volume of 25 µl per reaction. PCR tubes were then vortexed, pulsed and placed in a Perkin Elmer DNA Thermal Cycler (USA) where the PCR reactions were performed.

Table 2.2. PCR Master Mix	
PCR COMPONENT	**Vol/Reaction**
Sterile Water	16.4 µl*
10x Tth Buffer	2.5 µl
25 mM $MgCl_2$	2.5 µl*
dNTP (0.2 mM)	0.5 µl
Forward Primer (100 µM)	0.25 µl*
Reverse Primer (100 µM)	0.25 µl*
Tth Polymerase	0.1 µl
cDNA	2.5 µl
TOTAL VOLUME	25 µl

* Although standard master mix composition is shown, volumes of indicated reagents may vary depending on different primer sets. The specific amounts of the above indicated components for each primer set used is summarised in **Table 2** (**Appendix 1**).

2.1.2.4. Agarose Gel Electrophoresis

For the PCR products 2.5 µl of 6x loading buffer was mixed with 12.5 µl of the PCR product and electroporated through 2% w/v Agarose gels using a Bio-Rad Minigel apparatus. Restriction digest products (10 µl) were mixed with 2 µl of 6x loading buffer and run on 1% w/v Agarose gels. However, Adenoviral digest products were run on 0.8% w/v Agarose gels due to the large DNA size of the vectors. DNA size markers (2 µl) pUC19 (Bresatec, Australia) or SPP1/EcoRI (Geneworks, Adelaide) were mixed with 2.5 µl of 6x loading buffer and 10 µl of water. All samples were loaded onto the gel and electroporated at 90 V for approximately 90 min. Gels were stained in 1% GelRed™

solution for 10 min and photographed under UV illumination using InGenius gel documentation system (Syngene, USA).

2.1.2.5. Endonuclease Restriction Digestion of DNA

Unless specified, 1 μg of DNA was digested in each reaction. Depending on the source of DNA, DNA concentrations were calculated using two approaches. The first approach involved comparing band intensity of DNA size markers of known concentration with the DNA of interest, viewed on Agarose gels under UV illumination. The second approach relied on performing spectrometric measurements of the DNA of interest using NanoDrop 1000 spectrophotometer (Thermo Scientific, USA). Digest reactions were setup as per **Table 2.3** and were run for 18h at 37°C.

Table 2.3: Restriction Digest Reactions

Single Digest Reaction	
DNA	1 μg
10 x Buffer	2 μl
10 x BSA	2 μl
Enzyme	1 μl (10 units)
H_2O	to 20 μl

Double Digest Reaction	
DNA	1 μg
10 x Buffer	2 μl
10 x BSA	2 μl
Enzyme 1	1 μl (10 units)
Enzyme 2	1 μl (10 units)
H_2O	To 20 μl

2.1.2.6. Agarose Gel Purification of Restriction Digest Products

Restriction digest products were loaded into multiple wells of a 1% w/v Agarose gel and electroporated at 90 V for 90 min. Exterior lanes for each digest product were excised, stained in GelRed™ and visualised under UV light. Bands of the digest product were identified and marked on the excised lanes and then used to identify the positions of the

digest product on unstained portion of the gel. Bands were then excised from the unstained gel and transferred to pre-weighed eppendorf tubes for further purification (**2.3.2.7**). DNA yield was estimated by comparing band intensity of a DNA size markers of known concentration with the purified DNA band, viewed on Agarose gels under UV illumination.

2.1.2.7. Ultraclean™ Purification of DNA

UltraClean™ DNA Purification Kit (Mo Bio Laboratories, USA) was used to purify DNA either from Agarose gels or from the solution. Purification was performed as per the manufacturer's instructions, with an assumed 50% DNA loss.

2.1.2.8. Ligation of DNA Fragments into Cloning Vectors

Ligation reactions were setup as per **Table 2.4** and incubated either for 2h at room temperature or for 18h at 4°C in 0.5 mL tubes:

Table 2.4. Ligation Reaction	
DNA Inserts	X μl
10 x Ligase Buffer	1 μl
Plasmid DNA	1 μl (50 ng)
T4 Ligase enzyme	1 μl
Sterile H_2O	To 10 μl

2.1.2.9. Preparation of Competent E.coli TG1α and DH10B Bacterial Cells

Both TG1α and DH10B *E.coli* bacteria were made competent using the same protocol. Bacteria from laboratory glycerol stocks were streaked onto LB agar plates and allowed to grow for 18h at 37°C. A single colony was then selected from the agar plate, resuspended in LB media and grown in an orbital shaker at 37°C with a rotation speed of

200 rpm. One millilitre of overnight culture was added to 25 ml LB and incubated further (37°C, 200 rpm) until the culture reached OD_{600nm} of 0.42 which corresponded to log phase of the cell growth. Cells were then chilled on ice for 15 min and centrifuged at 280g for 10 min at 4°C. Pellets were resuspended in 2 ml ice cold 0.1 M $CaCl_2$/ 20 mM $MgCl_2$ solution and incubated on ice for at least1h for up to 18h.

2.1.2.10. Transformation of Competent *E.coli* Cells

Five microlitres of ligation mix (**2.3.2.8**) was added to 200 µl of competent *E.coli* cells (**2.3.2.9**) and incubated on ice for 30min. Following incubation, cells were heat-shocked for strictly 90s at 42°C and immediately chilled on ice for a further 10 min. The solution was then transferred to 20 ml V-bottom tube, supplemented with 500 µl LB medium and incubated at 37°C, 200 rpm for 1h. Cells were briefly pulsed in a centrifuge, 400 µl of supernatant was removed to concentrate the cells and the pallet was resuspended by pulse/vortex mixing. The remaining 300 µl of the bacterial suspension was spread evenly onto two LB agar plates containing appropriate antibiotics and incubated for 18h at 37°C. Uncut plasmid with no insert was used as a positive control for the efficiency of transformation while untransformed *E.coli* cells served as a negative control.

2.1.2.11. Plasmid Mini-preparation (Mini-prep)

Transformed single bacterial colonies which grew on the appropriate antibiotic plate were carefully isolated, resuspended in 2 ml LB containing the same antibiotic and incubated at 37°C, 200 rpm for 18h. One and a half millilitre of the cell culture was centrifuged at 11, 600g for 1 min and the cell pallet was resuspended by pulse/vortex in 100 µl Mini-prep Solution-1 for 5 min, as previously published (317). Two hundred microlitres of Mini-prep Solution-2 was added to the above cell suspension, which caused

cell lysis during the 5 min incubation on ice. The reaction was neutralised with 150 µl Mini-prep Solution-3 for 5 min on ice. Cell lysate was centrifuged for 10 min at 11, 600g and the clear supernatant was transferred to a new 1.5 ml tube. DNA phenol (225µl) and chloroform (225µl) was added to the clear lysate and the solution was centrifuged at 11, 600g for 10 min. Approximately 450 µl of the upper layer of liquid was removed and plasmids were precipitated by the addition of 2 volumes (900 µl) of 100% ethanol and centrifuged at 11, 600g for 10 min. Plasmid pellets were washed with 250 µl of 70% ethanol, centrifuged for an additional 10 min and air-dried. The pallet was resuspended in 45 µl TE8 and 5 µl DNase inactivated RNaseA (200 µg/ml) and stored at -70°C until further use.

2.1.2.12. Plasmid Midi-preparation (Midi-prep)

Transformed single bacterial colonies which grew on the appropriate antibiotic plate were carefully isolated, resuspended in 2 ml LB containing the same antibiotic and incubated at 37°C, 200 rpm for 18h. This 2 ml culture was then used to seed 100 ml LB containing the same antibiotic as the initial LB agar plate and incubated for 18h at 37°C 200 rpm. Plasmid midi-prep was performed using a JetStar 2.0 Plasmid Midi Kit (Genomed, Germany) strictly following the manufacturer's instructions. Plasmid elution was divided into five eppendorf tubes (1 mL into each). Plasmids were precipitated by addition of 700 µl cold isopropanol and palleted at 11,600g for 30 min at 4°C. Plasmid pellets were washed twice with 1.5 ml of 70% ethanol, centrifuged at 11,600g for 20 min after each wash and air-dried. Plasmid pellets were resuspended in 30 µl sterile milliQ water and pooled into a single eppendorf tube. Plasmid concentration was determined by measuring the absorbance of the plasmid containing solution (relative to milliQ water background) at 260 nm using NanoDrop 1000 (Thermo Scientific, USA).

2.1.2.13 DNA Sequencing

Dideoxy based DNA sequencing with chain-terminating inhibitors was performed at the Sequencing Facility in the Department of Haematology at the Flinders Medical Centre (318). cDNA (the gene of interest) was cloned into a desired vector and sequenced in the forward and reverse directions using gene-specific primers (**Table 2.1**). Consensus sequences were constructed by alignment of forward and reverse primer sequence data and verified against published data.

2.1.3. Adenoviral Methods

2.1.3.1. Preparation of Electrocompetent BJ5183 Cells

Ten millilitres of LB media supplemented with streptomycin (30 μg/mL) was inoculated with a single bacterial colony form of BJ5183 *E.coli* cells and incubated for 18h at 37°C, 200rpm. One millilitre of the culture was seeded in a 1 L conical flask containing 125 mL LB streptomycin media and incubated at 37°C, 200rpm until the OD_{550nm} reached 0.8 (which corresponded to a log phase growth of the bacteria). The culture was then divided into 4 Sorvall tubes and chilled on ice for 1h. Cells were centrifuged at 400g for 10 min at 4°C, resuspended in 30 mL sterile, ice cold 10% glycerol and re-centrifuged. The 10% glycerol wash was repeated once more and following the centrifugation, all but 2.5 mL of supernatant removed. Cells were resuspended, pooled into one tube and centrifuged again for 10 min at 400g. This time, all but 625 μL of the supernatant was removed and this was used to resuspended the bacteria. Twenty microlitre aliquots of now electrocompetent BJ5183 cells were made, snap frozen on dry ice and stored at -70°C for further use.

2.1.3.2. Generation of pADEasier-1 BJ5183 Bacterial Cells

Electrocompetent BJ5183 cells were electroporated with pAdEasy-1 plasmid using a Bio-Rad Gene Pulser and 2 mm gap electroporation cuvettes (Bio-Rad, USA). Curvettes were chilled on ice as the Gene Pulser was set to 2500 V/200 Ohms/25 μF. pAdEasy (100 ng) was then added to 40 μL of electro-competent cells and chilled on ice for 1 min. Cells and DNA were mixed by pipetting, placed in a curvette and the mix was levelled by gentle tapping to reduce electric arcing. Cells were electro-shocked for 5 milliseconds and immediately resuspended in 1 mL SOC media, transferred to a 50 mL V-bottomed tube and incubated at 37°C, 200 rpm for 1h. The culture was spread onto 6 LB ampicillin plates (25 μg/mL) and grown for 18h at 37°C. A random colony which grew on the ampicillin plates was carefully selected and made competent as per section **2.3.3.1** DNA was extracted from a aliquot of electrocompetent pAdEasier-1 cells as per section **2.3.2.12** and subjected to *Hind* III endonuclease digestion (**2.3.2.5**) in order to confirm the integrity of the pAdEasy-1 plasmid. A correct digestion pattern confirming the intact structure of pAdEasy-1 in the BJ5183 cells was shown in **Figure 5.7**.

2.1.3.3. Electroporation of BJ5183 cells with pAdTrack-CMV

The pAdTrack-CMV vectors containing the gene of interest were linearised (**2.3.2.5**) with *Pme* I restriction enzyme. Electrocompetent pAdEasier-1 cells (**2.3.3.1**) were then electroporated with linearised pAdTrack-CMV vector as in section **2.3.3.2**. Following the electroporation pAdEasier-1 cells were grown on LB agar plates supplemented with kanamycin (30 mg/ml) instead of ampicillin in order to select for successfully transformed bacteria containing the pAdTrack-CMV vector.

2.1.3.4 Screening of Colonies for Homologous Recombination

As shown by the schematic diagrams of the adenoviral vectors (**Figure 6.1**), only pAdTrack-CMV confers kanamycin resistance gene. pAdEasier-1 cells which did not successfully recombined with pAdTrack-CMV were therefore unable to form colonies on kanamycin plates. To note, linear forms of pAdTrack-CMV are not successfully replicated and thus cannot confer kanamycin resistance unless homologous recombination occurs with pAdEasy1. However, false positive colonies could occur after recircularisation of the pAdTrack-CMV. The smallest colonies of electroporated pAdEasier-1 cells that grew on kanamycin plates were selected for endonuclease restriction screening since replication of the large recombinant vector would be expected to slow down the colony growth. Mini-preps of selected cultures (**2.3.2.11**) were digested with *Pac* I in Buffer 1 (NEB, USA) in order to screen for successful homologous recombination. Both pAdEasy-1 and pAdTrack-CMV contain one and two *Pac* I restriction sites respectively. Thus, bacteria which contained successfully recombined vectors would yield 33.5 kb and either 4.5 or 3 kb fragments post *Pac* I digestion. This was depended on whether recombination occurred at the left arm homology region or the origin of replication.

2.1.3.5. Transformation of DH10β E.coli Cells

BJ5183 cells are prone to high rates of homologous recombination which could effect the integrity of the recombined Adenoviral vector and thus DH10β strain of E.*coli.* (capable of high efficient plasmid propagation and extremely low recombination) were used to grow large amounts of recombined Adenoviral vector. DH10β cells were made chemically competent (**2.3.2.9**) and transformed with undigested mini-prep samples from section **2.2.2.5**. Transformed colonies which grew on the kanamycin plates were selected, midi-preps (**2.3.2.12**) were performed and vectors were digested with *Pac* I to re-determine the recombinant properties of the plasmid. In addition, PCR technique was used to confirm the presence of HLA-G1 and HLA-G5 in the recombined vector.

2.1.3.6. LipofectAMINE™ Transfection of Adenoviral Constructs into HEK 293 Cells

The Human Embryonic Kidney 293 (HEK 293) cell line was used to generate Adenoviral particles. HEK 293 is a genetically modified cell line engineered to express the E1 gene, which is necessary for packaging of adenoviral particles (319). Eight micrograms of the recombinant viral plasmid were linearised with *Pac* I (**2.3.2.5**). Linearised plasmids were ethanol precipitated for 18h at -20°C by the addition of 10% NaAc (3 M) and two volumes of 100% ethanol. Following the incubation, the precipitate was centrifuged at 4°C for 30 min at 11000g. DNA pallet was washed once with 70% ethanol, centrifuged for 5 min and resuspended in 30 μL sH_2O. Each linearised vector (4 μg) was mixed with 10 μL sH_2O, 20 μL of the cationic liposome LipofectAMINE™ (GibcoBRL, USA) and 500 μL of DMEM supplemented with 1% glutamine. The mixture was then mixed by pipetting, incubated for 30 min at 37°C to allow for the DNA/LipofectAMINE™ complexes to form. Seventy percent confluent monolayer of HEK 293 cells in 25 cm^2 flasks, were washed once with plain DMEM and then incubated with 2.5 mL DMEM supplemented with 1% glutamine for 10 min at 37°C humidified incubator. The DNA/LipofectAMINE™ complexes were then added to the flasks and incubated for a further 4 h. Media was removed and replaced with 6 mL complete DMEM. Flasks were incubated for 12-14 days and viewed daily under a Nikon TM300 Inverted Fluorescent Microscope (Japan) for GFP expression. At day 10 of the culture an additional 2 ml of complete DMEM were added to the flask in order to provide extra nutrients.

2.1.3.7. Preparation of Adenoviral HEK 293 cell lysates

Twelve to fourteen days following transfection, HEK 293 cells were detached from the flask using a rubber policeman and transferred to 50 ml tubes. Cells were centrifuged at 1200g for 10 min, supernatant was decanted and the cell pallet was resuspended in 2 ml

sterile PBS. Cell suspensions were snap frozen in liquid nitrogen and thawed at 37°C. This cycle was repeated four times and at the last cycle a 10 μL aliquot was placed on a slide and visualised under the microscope to confirm cell lysis. Cellular debris was removed by centrifugation at 1200g for 10 min.

2.1.3.8. Infection of HEK 293 Cells and Scale-up Viral Production

- Round one of Adenoviral production

Media was decanted from 80-90% confluent HEK 293 cell monolayer grown in 25 cm^2 flasks. Four hundred microlitres of crude adenoviral extract obtained in section **2.3.3.7** was added to the flask and incubated for 1h at 37°C humidified incubator. At the end of incubation, 5.5 ml of complete DMEM was added and flasks were incubated at 37°C and 5% CO_2 until at least 50-70% of the cells had rounded up and detached, due to cytoskeleton disruption, as a result of viral production. The remainder of the attached cells was gently scraped with the rubber policeman and cell lysates were prepared as per section **2.2.2.7**.

- Intermediate round of Adenoviral production

Round one above was repeated 2 to 3 times in order to generate enough viral particles to be used in the final round of viral production. During each subsequent infection, the number of flasks that were infected were doubled. At the end of this round cell lysates from 5-6 infected 75cm^2 flasks were prepared.

- Final round of Adenoviral production

Viral titres were calculated from the cell lysated prepared in the intermediate round using fluorescence based quantification of Adenoviral titres Assay (described below). Ten million of HEK 293 cells plated in 75 cm^2 were infected with $1x10^7$ viral particles per cell.

A total of fifteen 75 cm^2 flasks were infected using the crude adenoviral extracts. The flasks were incubated at 37°C and 5% CO_2 until at least 50-70% of the cells had rounded up and detached (usually 3 days post infection).

2.1.3.9. MustangQ Purification of Adenoviral Particles

This protocol was adopted from the Pall Corporation catalogue 2005, with minor modification. Briefly, three 75 cm^2 flasks of HEK 293 cells from final round above were pooled in one 50 ml V-bottomed tube and centrifuged at 1200g for 10 min. The cell pallet was resuspended in 2 ml of 0.3M NaCl solution and the cell suspension was subjected to four cycles of freeze/thaw lysis **2.3.3.7**. Cell debris was removed by centrifugation at 1200g for 10 min, cell lysates were pooled and sequentially filtered through 5 μm, 1.2 μm and 0.8/0.2 μm sterile filters (Pall Corp, UK). Following 0.8/0.2 μm filtration, 100 U/ml of proprietary DNase/RNase mixture (Benzonaze) (MERCK, Australia) was added to the filtrated cell lysate and incubated for 30 min at room temperature. This step degrades DNA and RNA which otherwise would compete with Adenoviral particles for binding to positively charged MustangQ membranes. During incubation, MustangQ membranes were preconditioned by applying several solutions through the membrane in the following order: 3 ml of 1M NaOH, 3 ml of 1M NaCl and 5 ml of 0.3M NaCl. After DNA/RNA digestion, lysate was filtered once more through 0.8/0.2 μm filter and passed through preconditioned MustangQ membrane at a flow rate of 1 ml/1 min. The membrane was washed once with 3 ml of 0.3M NaCl prior to elution of the purified virus with 3 ml of 0.6M NaCl.

2.1.3.10. Fluorescence Quantification of Adenoviral Titres

Within the present study, Adenoviral vector acquired GFP cDNA from pAdTrack-CMV during homologous recombination, and this enabled rapid quantification

of Adenoviral titres using GFP fluorescence as a marker of Adenoviral infection, as previously reported (320). Briefly, HEK 293 cells were plated in 96 well flat-bottom plates with $2x10^4$ cells per well in 100 μl complete DMEM. The cells were incubated at 37°C 5% CO_2 for 18h to allow for cell adhesion. Ten-fold viral dilutions were prepared in DMEM supplemented with 10% normal horse serum, 0.05% yeast extract and 2 mM glutamine. The media was decanted from the confluent wells and the 50 μl of viral dilutions ranging between 10^{-7} to 10^{-11} were added to each well with 10 wells in total prepared per dilution. To some wells 50 μl of viral-free media was added which served as a control for background fluorescence. The plates were incubated for 48 h at 37°C and the wells were examined daily by fluorescent microscopy for the presence of fluorescent cells. The viral titre was calculated by dividing the number of wells with fluorescent cells at the highest dilution by the total volume in all wells and multiplying by the dilution factor.

2.1.4. Flow Cytometry

2.1.4.1. Cell surface staining

Flow cytometric analysis was performed using either phycoerythrin (PE) or fluorescein isothiocyanate (FITC) conjugated primary mAb. In situations where directly conjugated primary mAb were unavailable, detection of unconjugated primary mAb was enabled using PE or FITC conjugated secondary mAb specific to the IgG of the host species in which primary mAb was raised.

Cells were washed in FACS wash buffer and blocked with heat inactivated rabbit serum for 20 min at 4°C. Primary antibodies (50 μl of either saturated supernatant or 1–2 μg/ml purified primary antibody) were then added and cells were incubated for 30 min at 4°C. In the case of unconjugated primary mAb, cells were washed in an FACS wash buffer then incubated for 30 min at 4°C with FITC- or PE- conjugated secondary mAb.

Cells were then equilibrated for a further 5 min at room temperature and fixed in 1 ml FACS lysing solution (BD Biosciences, USA). Background staining was established by using isotype-control mAb. Antibody staining was detected using either Becton Dickinson FACScan or FACSCanto and the data was analysed using FASCDiva Software version 4.1.

2.1.5. Histochemistry

2.1.5.1. Biopsy Preparation

Isolated tissues were embedded in Optimal Cutting Temperature (OCT) compound in cryostat moulds. Tissues were then frozen in a dry ice and stored at -70°C until required. Once required, tissues were equilibrated at -20°C, cut using a cryostat onto slides and fixed in acetone for 10 min at 4°C. Slides were air dried, wrapped in aluminium foil and stored at -70°C until further use.

2.1.5.2. Hematoxylin and Eosin Staining

Slides were thawed, hydrated briefly in distilled H_2O and stained in hematoxylin for 5 min. Excess hematoxylin was removed by washing with running tap water for 2 min. Slides were dipped twice in acid alcohol and washed for a further 4 min in running tap water. After a brief dip in 70% EtOH, slides were stained for 30 s in eosin. Excess eosin was removed by sequential dipping in two changes of 95% EtOH and incubation in absolute EtOH for 5 min. Slides were dehydrated well and incubated in SubX clearing agent for 20 min. Following incubation, the slides were air dried and cover slips were mounted using Sub X mounting medium. The cover slips were then left to set at room temperature overnight.

2.13.5.3. Immunohistochemistry

- Immunoperoxidase staining

The slides were thawed and rehydrated for 20 min with 3% serum (of the same species in which secondary mAb was raised) in PBS at room temperature. Avidin/Biotin blocking kit (Vector Laboratories, USA) was used to block endogenous avidin and biotin. The slides were washed in PBS for 10 min before a primary mAb was added overnight at 4°C in a humidified chamber. Sections then were washed for 10 min in PBS followed by a 30 min incubation at room temperature with a biotinylated secondary mAb. The wash step was repeated again before sections were incubated with a 1:1 preparation of Avidin DH and biotinylated horseradish peroxidase for 60 min according to the manufacturers instructions (ABC kit, Vector Laboratories, USA). Sections were washed and incubated in the dark at room temperature for 7 min with diaminobenzidine substrate solution, counterstained with Harris' haematoxylin and mounted with a cover slip. Positive staining was represented by brown colouration.

- Immunofluorescence staining

In case of immunofluorescence staining, the slides were thawed, blocked with 3% serum before primary mAb was added for 2h at room temperature. Sections were washed in PBS and secondary mAb conjugated with a fluorescence tag was added for 1h. DAPI counterstain was performed by adding 100 ml of 15 mM solution per section for 5 min at room temperature in the dark. Cover slips were mounted, following the PBS wash, using a fluorescence mounting medium (DAKO, USA) and allowed to set at 4°C overnight.

2.2 Centrifuges

- All tissue culture centrifugation was performed in a Beckman GP Centrifuge (USA).

- Centrifugation of all eppendorf, treff and PCR tubes was performed in an Orbital 100 Phoenix Centrifuge (USA).

- Centrifugation of all bacterial cultures was performed in a Sorvall RC-5B Refrigerated Superspeed Centrifuge (USA)

CHAPTER 3

RAPAMYCIN DOWNREGULATES THE INHIBITORY RECEPTORS ILT2, ILT3, ILT4 ON HUMAN DENDRITIC CELLS AND YET INDUCES T CELL HYPORESPONSIVENESS INDEPENDENT OF FOXP3 INDUCTION

Publications

"Rapamycin downregulates the inhibitory receptors ILT2, ILT3, ILT4 on human dendritic cells and yet induces T cell hyporesponsiveness independent of FoxP3 induction" Immunol Lett. 2008 Oct 30;120(1-2):49-56.

- The following abstracts have been published:
  - Fedoric, B *et al.*. Immunology and Cell Biology, Vol. 84 Issue 3 Page A1 June 2006
  - Fedoric, B *et al.*. American Journal of Transplantation, Vol. 7 Supplement 2 Page 410 May 2007

Presentations

Presented at TSANZ Annual Scientific meeting 2006 in Canberra and at the American Transplant Congress 2007 in San Francisco, USA

3.1 Introduction

Conventional approaches to treat transplant rejection have involved the development of immunosuppressive agents that target T cell proliferation to inhibit alloimmune responses (247, 321, 322). In particular, Cyclosporin A (CsA) a Calcineurin inhibitor (244, 323, 324), and Rapamycin (RAPA) an inhibitor of the mammalian target of Rapamycin (mTOR) (245, 325) affect T cell proliferation by limiting IL-2 synthesis or IL-2 receptor-mediated signalling, respectively (245, 323-326). Recent reports have claimed that these agents can also modify the alloimmune response by interfering with DC function (**reviewed in 1.2 and 1.3**) (242, 327, 328). A number of studies using CsA and RAPA have been performed in murine DC, however studies examining the ability of CsA and RAPA to generate human tolerogenic DC are not forthcoming (329). It is believed that DC based tolerogenic therapy will provide antigen specific treatment in contrast to the conventional immunosuppressive regimen used in the transplant patients (**reviewed in 1.9**) (26, 238). Indeed, treatment of DC with immunomodulatory molecules such as IFN-α and IL-10 produced tolerogenic DC associated with the induction of Immunoglobulin-like transcript 3 (ILT3) and ILT4 and generation of antigen specific T_{REG} cells *in vitro* (167). Although it is known that CsA and RAPA can inhibit positive costimulatory molecules in mouse DC and as shown in limited studies in human DC, the effect of the immunosuppressants RAPA and CsA on inhibitory receptors has not been described to date.

ILT2, ILT3 and ILT4 molecules are members of the Immunoglobulin (Ig) gene super-family and the specific ligand interactions with these molecules initiate a cascade of intracellular signalling that is associated with the immunotyrosine based inhibitory motifs

(ITIM) (157, 158, 164). As discussed earlier in section **1.7.2**, signalling through ITIM leads to the de-phosphorylation by SHP-1 phosphatase and calcium-dependent downregulation of NF-κB, which subsequently results in the reduced expression of CD80 and CD86 on DC. It has also been reported that the interaction of ILT3 and ILT4 on DC with their ligands on T cells induces T cell anergy and/or induction of allospecific T regulatory cells (164, 167). While the ILT3 ligand on T cells is currently unknown (157) there is evidence that ILT2 and ILT4 mediate immunomodulatory effects by interacting with HLA-G (160, 220).

The present study examines the ability of the immunosuppressants CsA and RAPA to generate human tolerogenic DC *in vitro* with a particular emphasis on the ability of these agents to affect ILT2, ILT3, ILT4 and HLA-G expression. These inhibitory molecules have been implicated in tolerogenic mechanisms both *in vitro* and *in vivo* and therefore knowledge about the effect of CsA and RAPA on the above inhibitory molecules may assist in determining what occurs in transplant patients receiving CsA and/or RAPA. This study further investigates the ability of RAPA to induce tolerogenic DC when added directly to mDC. The latter approach has not previously been examined.

Our data highlights that the addition of RAPA at the beginning of DC culture downregulates positive costimulatory molecules CD40, CD80 and CD86 as well as the inhibitory receptors on DC. Additionally, these RAPA-treated DC exhibited tolerogenic properties throught their low allostimulatory capacity and not their ability to increase the number of $FoxP3^+$ T cells. Lastly, RAPA treatment of mature DC generated tolerogenic DC that are capable of inhibiting T cell proliferation. The mechanism of inhibition of these DC may primarily be through the induction of IDO in DC since the expression of positive costimulatory molecules was not affected during this treatment approach.

3.2 Materials and Methods

3.2.1. DC preparation and treatment with immunomodulatory agents

Human DC were generated using buffy coat from healthy blood donors (Australian Red Cross Blood Service, Adelaide, Australia) as previously published (316). In brief, Peripheral Blood Mononuclear Cells (PBMNC) were isolated from the buffy coat using Lymphoprep^{TM} (Nycomed, Oslo, Norway) density gradient separation. PBMNC were then resuspended in complete medium, which consisted of RPMI 1640 culture medium (Sigma-Aldrich, Saint Louis, MO, USA) supplemented with 10% (v/v) FCS (Commonwealth Serum Laboratories, Melbourne, Australia) and 1% glutamine (Multicel, Castle Hill, Australia). Each experiment consisted of $5x10^6$ PBMNC that were panned onto six-well plates (Greiner Bio-One, Frickenhuasen, Germany) for 45 min at 37^{o}C. The non-adherent cells were removed while the adherent cells (monocytes) were differentiated *in situ* into immature DC (iDC) in the presence of 400 U/ml (10^{-5} U/mg) of IL-4 (eBioscience, San Diego, USA) and 800 U/ml of Granulocyte Macrophage Colony Stimulating Factor (GM-CSF) – Leucomax^{TM} (Sandoz Australia, North Ryde, Australia) for 5 days. The iDC were then treated with TNF-α (10 ng/ml) (R&D, McKinley Place, MN, USA) for 48 h to produce mature DC (mDC). All cultures were incubated under 5% CO_2 at 37^{o}C, and cells at different stages of DC differentiation and maturation were used in the experiments.

Cyclosporin A (Neoral®, Sandoz Pharmaceuticals, Vienna, Austria), Rapamycin (Rapamune®, Wyeth Pharmaceuticals, Baulkham Hills, Australia) and IFN-α (Roferon-A®, Roche Products, Dee Why, Australia) were diluted in RPMI. An outline of the treatment approaches are depicted in **Figure 3.1**. In the first approach, treatment commenced either at the monocyte stage prior to differentiation or at the immature DC

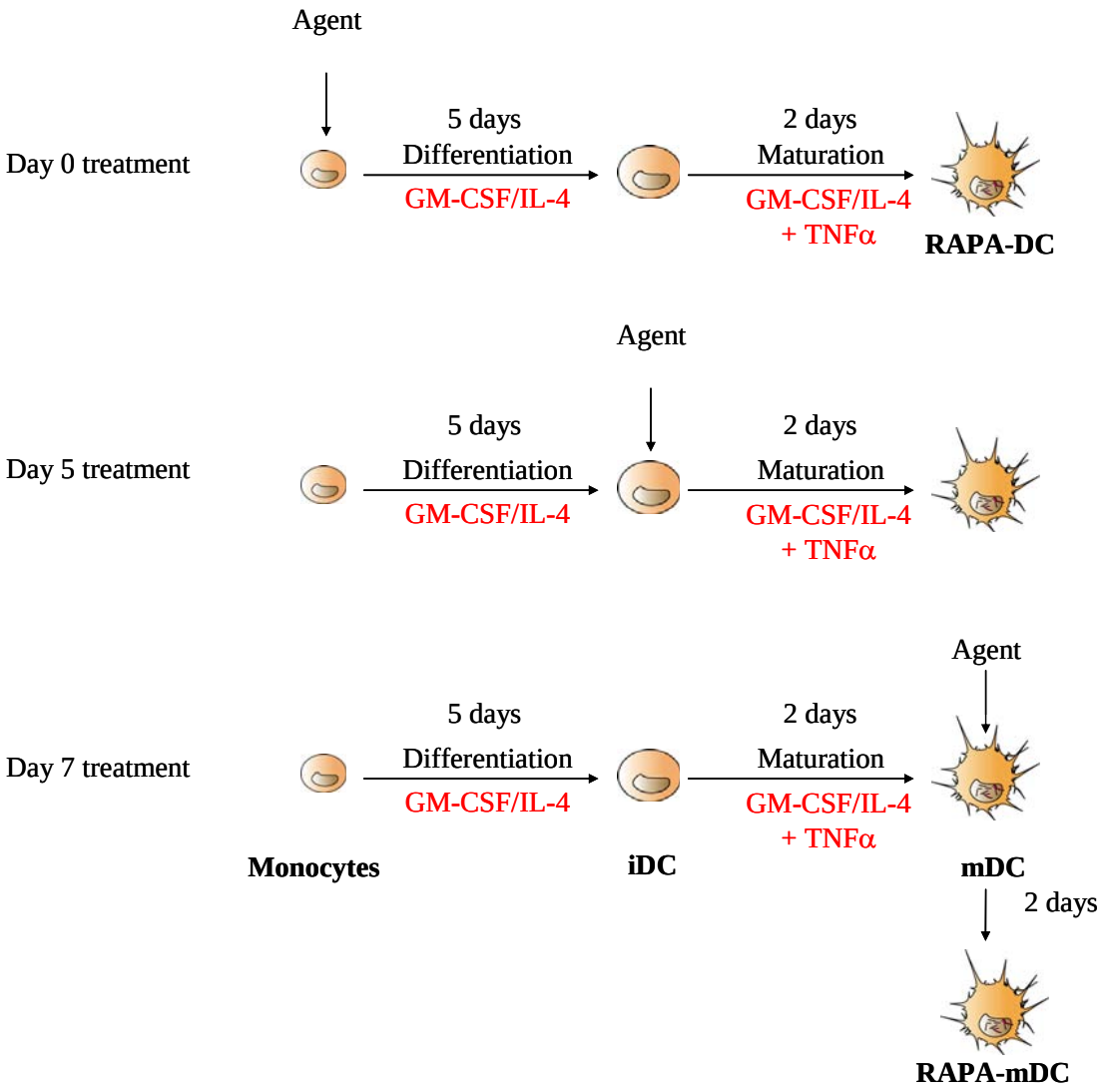

Figure 3.1. Outline of DC treatment approaches. Monocytes were cultured in the presence of GM-CSF and IL-4 for 5 days to generate Immature DC (iDC). TNF-α maturation stimulus was added at day 5 for 48h in order to mature DC (mDC). During day 0 treatment agent was added at beginning of monocyte culture for a period of 7 days. In day 5 treatment agent was added at day 5 post culture in presence or absence of TNF-α for 48h. During day 7 treatment agent was added to mDC on day 7 post-monocyte culture for 48h in the presence of TNF-α.

stage preceding maturation. All agents were present for 7 days in culture. In the second treatment approach, purified RAPA (Sigma-Aldrich, USA) was used instead of the RAPA formulation above. Pure RAPA was added to the mature DC (day 7) for 48 h. This was compared to DC which received RAPA at the monocyte stage prior to differentiation or at the immature DC stage preceding maturation. Relative to the first treatment approach where the length of the exposure of cells to RAPA was for a maximum of 7 days, the second approach consisted of cells receiving RAPA at day 0 and were exposed to RAPA for 9 days in total.

3.2.2 Flowcytometry

Cells obtained at different stages of DC differentiation and maturation were firstly incubated with ethidium monoazide (EMA) (Molecular Probes, Eugene, OR, USA) for 20 min at 4^{o}C to enable subsequent live-gate analysis following monoclonal antibody (mAb) staining. The following primary mAbs were used for cell surface labelling: RM3.54 (MHC II), MY-4 (CD14) (Beckman Coulter, Fullerton, CA, USA), anti-CD40 (Santa Cruz Biotechnology, Santa Cruz, CA, USA) anti-CD80 (Immunotech, Marseille, France), anti-CD83, anti-CD86 (Serotec LTD, Oxford, UK), HP-F1 PE-conjugated (ILT2) (Beckman Coulter, Fullerton, CA, USA), ZM3.8 (ILT3) and 42D1 (ILT4) (Dr Marco Colonna, Washington State University, St Louis, USA), 87G (HLA-G) (Abcam, Cambridge, MA, USA). The following isotype matched control mAb were used in order to determine background staining: X63 (IgG1), 1D4.5 (IgG2a), normal rat IgG2a (Santa Cruz Biotechnology, Santa Cruz, CA, USA). Unconjugated mouse primary mAb were detected with FITC-conjugated anti-mouse IgG1 secondary mAb (Southern Biotech, Birmingham, AL, USA). For ILT4 staining, primary mAb (42D1) was labelled with biotinylated rabbit anti-rat IgG (Vector Laboratories, Burlingame, CA, USA) and then

detected with Streptavidin-PE (Becton Dickinson, San Jose, CA, USA). After the secondary antibody staining step, the cells were fixed in 2% paraformaldehyde (BDH, Kilsyth, Australia) and analysed using a Becton Dickinson FACScan (San Jose, CA, USA). Cells were selected according to their size, complexity and viability.

3.2.3 Mixed lymphocyte reaction (MLR)

Allogeneic responder T cells were enriched by passage of monocyte-depleted PBMNC through a packed nylon-wool column (Boehringer Mannheim Biochemica, Indianapolis, USA), as previously described (316). DC that were pre-treated with immunomodulatory agents were washed 3 times in PBS to minimise transfer of free agents or cytokines before they were used as stimulators in the DC-MLR. DC were added to responder T cells ($1x10^5$) in a volume of 200 μl in each well at a stimulator: responder ratio of 1:1000, 1:100 and 1:10. The mixed cell populations were subsequently cultured for 4 days in 96-well round-bottomed plates (TPP, Trasadingen, Switzerland) at 37°C and then pulsed for 20h with 1 μCi of [^{3}H]-thymidine (Amersham Biosciences Limited, Bucks, UK). Cells were then harvested onto glass-fibre filters and counted in a scintillation fluid in a Wallac Microbeta Counter (Turku, Finland). All experimental samples were counted in replicates of five and the results reported as counts per minute (cpm).

3.2.4. FoxP3 analysis in T cells co-cultured with modified DC

T cells were cocultured with DC pretreated with immunosuppressive agents for 6 days. Aliquots of 5 x 10^5 cells from the coculture were stained using the FoxP3 kit (eBioscience, San Diego, USA) based on the manufacturers instructions. Essentially, cells were permeabilised and fixed prior to blocking with normal rat serum before incubating with a PE-conjugated rat anti-human FoxP3 mAb. An isotype-matched control mAb was used to

determine background activity. Data was acquired using a Becton Dickinson FACScan and analysed using CellQuest^{TM} software.

3.2.5 RT-PCR analysis

RNA was extracted using Illustra RNAspin Mini Isolation Kit (GE Healthcare, UK). Briefly, RAPA treated DC ($1x10^6$) were lysed in RA1 buffer/2-mercaptoethanol mixture. Cell lysate was equilibrated with 70% ethanol and centrifuged through the RNAspin column at 13,000g for 1 min. Following the attachment of RNA to the column, DNAse I was loaded onto the RNAspin column and incubated for 15 min at room temperature to digest genomic DNA. DNAse I was subsequently inactivated with RA2 buffer and RNA was washed two times with RA3 buffer. RNA was eluted in 40 μl of sterile water and quantified by absorbance at 260 nm using NanoDrop 1000 (Thermo Scientific).

Reverse transcription was performed with MMLV (Molony Murine Leukaemia Virus) reverse transcriptase (GibcoBRL, Grand Island, NY, USA) on 1 μg of total RNA.

Semi quantitative RT-PCR for IL-10, IL-12p40, IDO, PKCb, RelB and GAPDH was performed in quadruplicates using Rotor-Gene^{TM} 2000 (Corbett Research, Sydney, Australia) and the results were analysed using Rotor-Gene^{TM} Analysis Software V5.0 (Corbett Research, Sydney, Australia). Specific cDNA was amplified with Tth polymerase and specific primers, which were custom synthesised by Proligo (Lismore, Australia) (**Table 1, Appendix 1**). The specific cycling conditions are summarised in **Table 2, Appendix 1**. The results were normalised with GAPDH as the housekeeping gene. The GAPDH normalisation was also confirmed using the total RNA. Using melt curve analysis, it was determined that there was no detectable genomic DNA contamination within the RNA samples.

3.2.6 Statistical analysis

Unpaired students' *t-test* was conducted using SPSS Software V12.0 with statistical significance at $P < 0.05$. The data was shown to have normal distribution using D'Agostino-Pearson noramility test.

3.3. Results

3.3.1 Baseline expression profile of costimulatory molecules on DC during their differentiation and maturation

Baseline phenotypic changes in DC during differentiation and maturation were determined by indirect immunofluorescence staining for ILT2, ILT3, ILT4, CD14, CD80, CD86 and MHC II on pre-DC, iDC and mDC on 2, 5 and 7 days of culture, respectively.

As displayed in **Figure 3.2**, the loss of the CD14 monocyte marker (50%+ve pre-DC vs 0%+ve mDC) and the increased expression of the maturation marker CD83 (0%+ve iDC vs 75%+ve mDC) in mDC indicated that the differentiation of monocytes to DC had occurred. Associated with the differentiation and maturation of DC, the surface expression of positive costimulatory molecules CD40 (MFI of 132 for iDC vs 300 for mDC) CD80 (MFI of 20 for iDC vs 45 for mDC) and CD86 (MFI of 19 for iDC vs 34 for mDC) increased as indicated by the mean fluorescence intensities. The MHC class II molecule also showed increased expression in mature DC (MFI of 120 for iDC vs 270 for mDC). In contrast to the positive costimulatory molecules, the inhibitory receptors showed a decrease in cell numbers and a reduction in the expression for ILT2 (MFI of 207 for iDC vs 108 for mDC), ILT3 (MFI of 30 for iDC vs10 for mDC), ILT4 (MFI of 54 for iDC to 30 for mDC) and HLA-G (MFI of 6.7 for pre-DC to 0 for mDC).

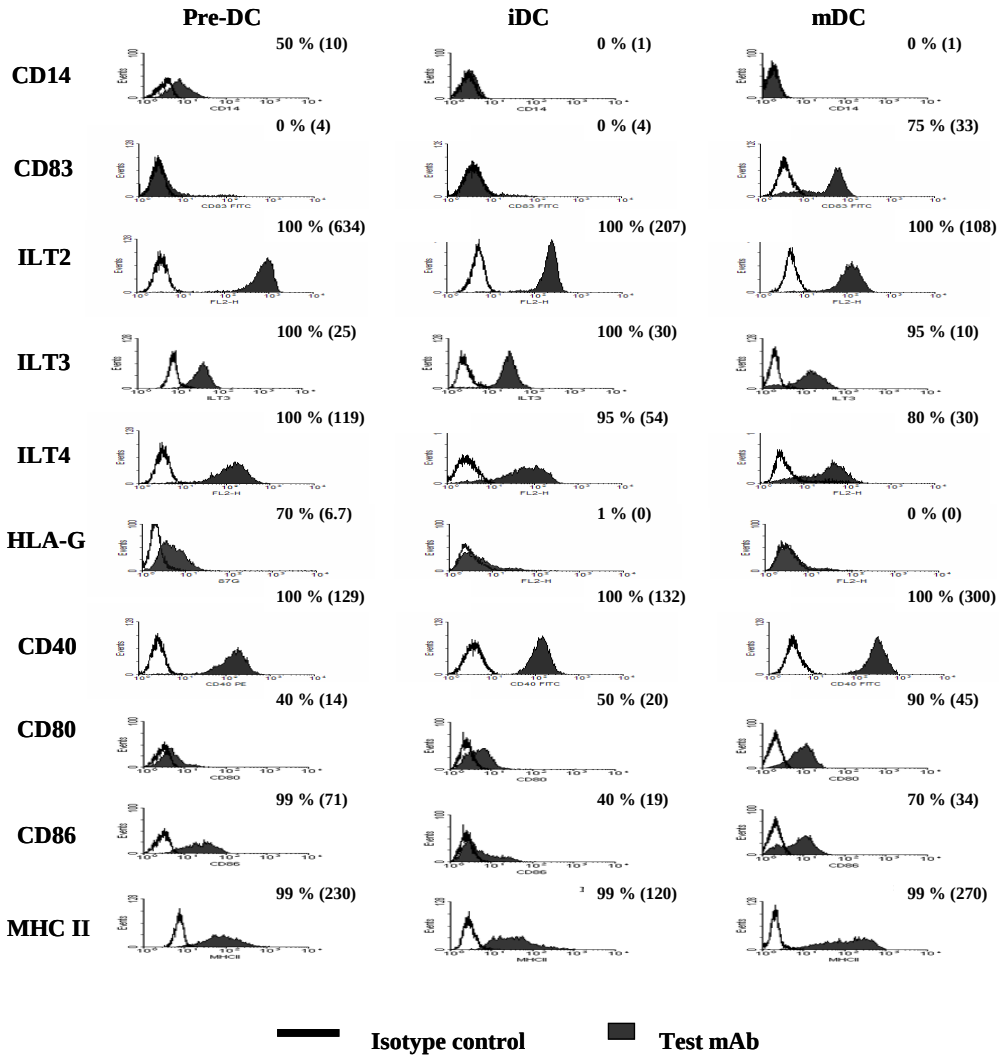

Figure 3.2. Expression profile of cell surface molecules during DC differentiation and maturation: Adherent monocytes were differentiated with IL-4 and GM-CSF for 5 days and then the resulting iDC were matured for 2 days with TNF-α. Cells were labelled at day 2 (pre-DC), day 5 (iDC) and day 7 (mDC) with mAb directed against CD14, ILT2, ILT3, ILT4, HLA-G, CD40, CD80, CD83, CD86 and MHC II. The open histogram represents isotype-matched control mAb while the filled histogram represents test mAb. Percentage of marker positive cells and the Mean Fluorescence Intensity (in parenthesis) are reported with each histogram. Data are representative of three different experiments.

3.3.2 Rapamycin downregulates the expression of both positive costimulatory molecules and inhibitory receptors during DC differentiation

In this set of experiments, the immunomodulatory agents were added either at day 0 prior to DC differentiation and the expression of cell surface molecules was determined on day 2 (pre-DC), day 5 (iDC) and day 7 (mDC). In another set of experiments, agents were added at day 5 after DC differentiation and flowcytometry was performed on day 7. The concentration of the immunosuppressive agents CsA (100 nM) and RAPA (10 nM) used during the DC differentiation and maturation protocol were based on optimal concentrations that showed inhibition of T cell proliferation. IFN-α was used at a concentration of 1000 U/ml previously reported by Manavalan *et al.* 2003 [22].

The flowcytometric analysis (**Figures 3.3 and 3.4**) showed that CsA had minimal effects on the expression of both positive costimulatory molecules and the inhibitory receptors regardless of the time of addition of the agent.

At the mDC level, RAPA treatment inhibited CD40, CD80 and CD86 expression and produced no effect on CD83 compared to untreated controls (**Figure 3.4**). RAPA treatment also showed a concomitant downregulation of the inhibitory molecules ILT2, ILT3 and ILT4 in iDC and mDC (**Figure 3.3**). The addition of RAPA on day 5 however, did not exhibit any changes in the profile of these molecules on DC.

While IFN-α treatment induced the expression of CD80 and CD86 on iDC and mDC, downregulation of CD40 and CD83 in mDC occurred. Interestingly, IFN-α treatment induced CD83 expression at the pre-DC and iDC stage even in the absence of the maturation cytokine TNF-α compared to the untreated control. Furthermore, IFN-α upregulated HLA-G and downregulated ILT2 and ILT4 expression in both iDC and mDC when added at day 0, whereas ILT3 was induced in iDC when added on day 5 with no other effects noted.

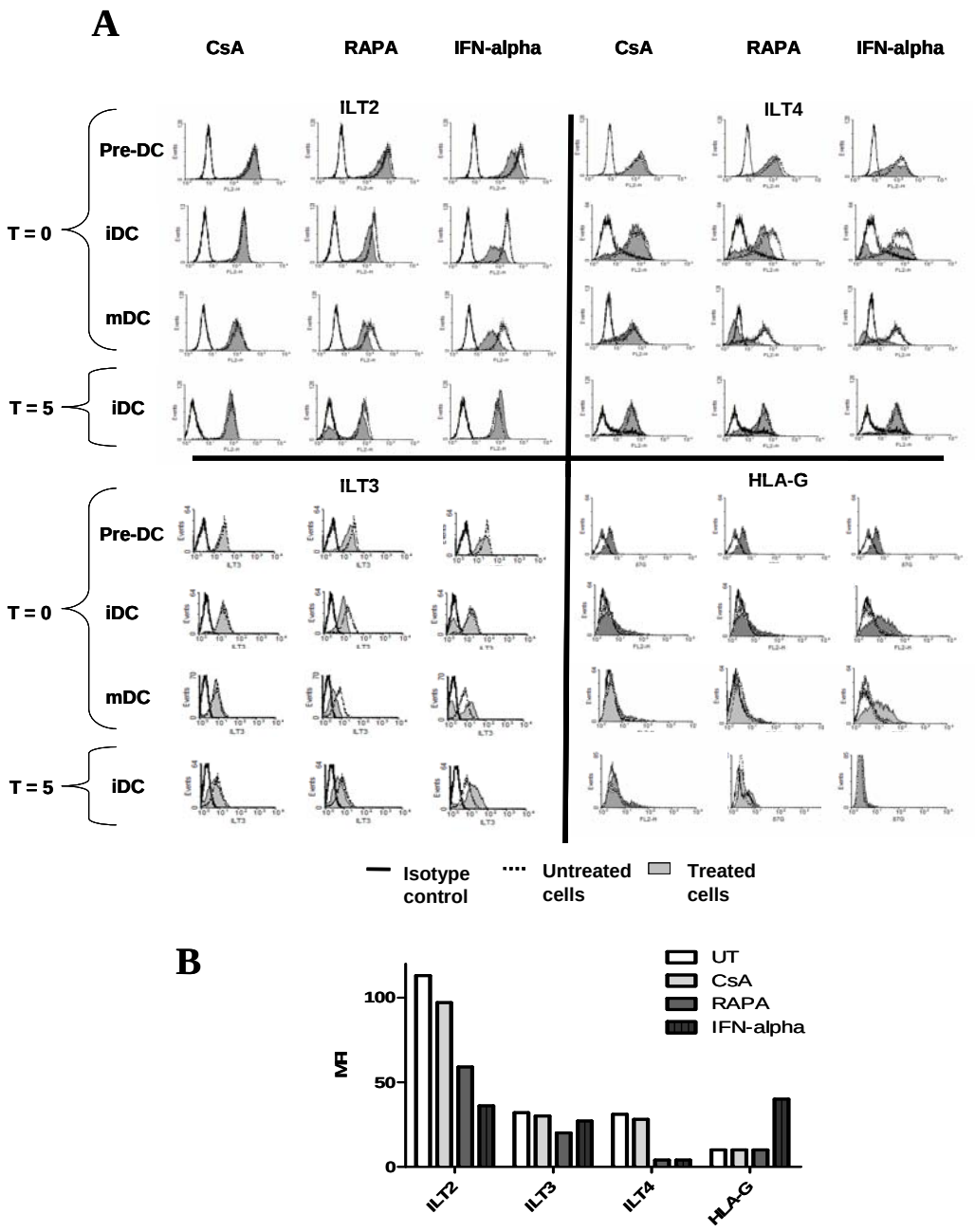

Figure 3.3. Rapamycin downregulates the expression of inhibitory receptors during DC differentiation: (A) Cells in culture were treated with either CsA, RAPA or IFN-α at days 0 and 5 and the expression of the inhibitory receptors was demonstrated by labelling with mAbs against ILT2, ILT3, ILT4 and HLA-G after 2 days (pre-DC), 5 days (iDC) and 7 days (mDC). The histograms show isotype-matched controls (black line); treated cells (gray filled area); and untreated cells (dashed line). (B) Comparative changes in the Mean Fluorescence Intensity (MFI) profile of inhibitory receptors in CsA, RAPA and IFN-α treated mDC. Data are representative of three different experiments.

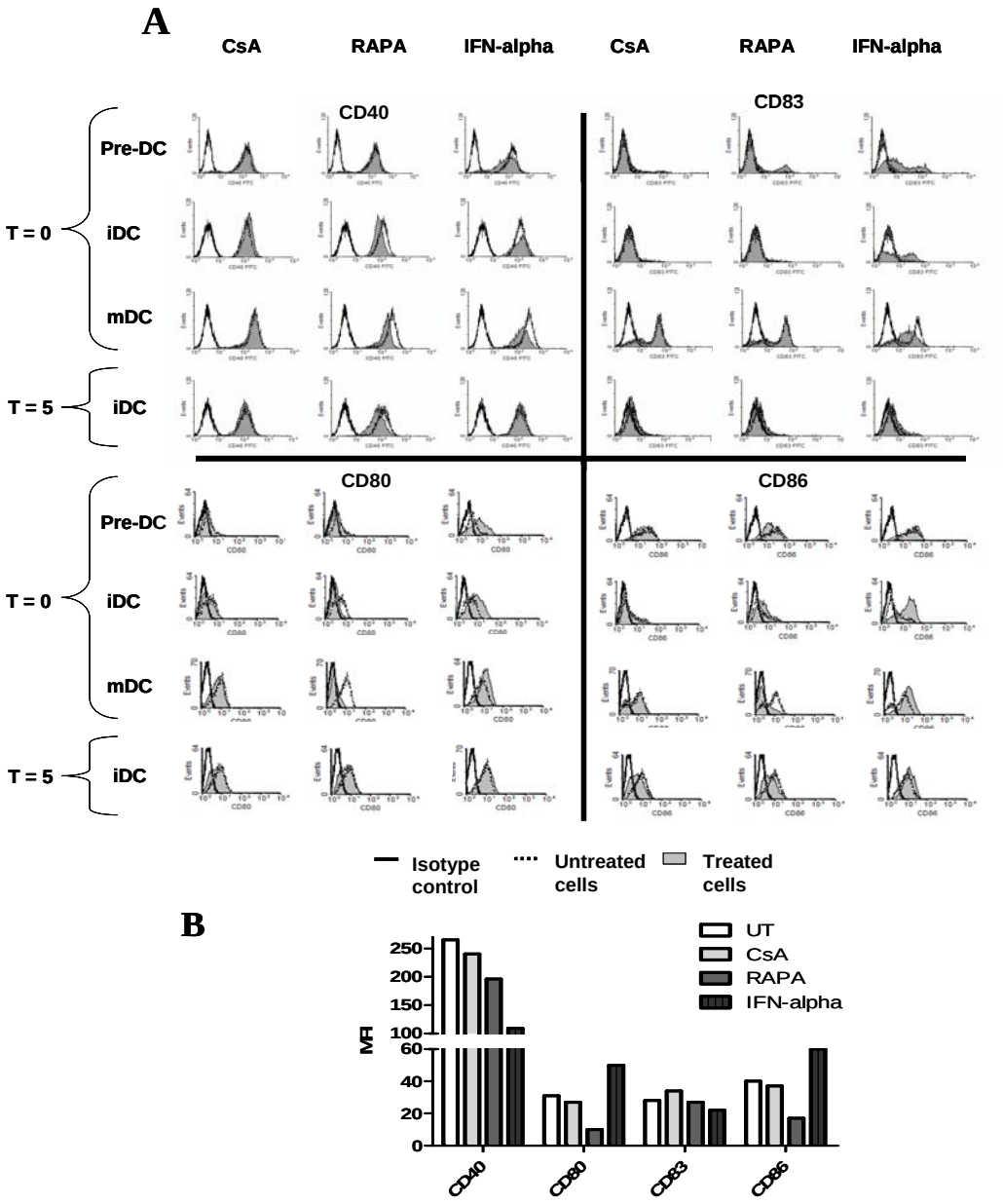

Figure 3.4. Rapamycin downregulates positive costimulatory molecules during DC differentiation: (A) Cells in culture were treated with either CsA, RAPA or IFN-α at days 0 and 5 and the expression of positive costimulatory molecules were demonstrated by labelling with mAbs against CD40, CD80, CD83, CD86 and MHC II after 2 days (pre-DC), 5 days (iDC) and 7 days (mDC). The histograms show isotype-matched controls (black line); treated cells (gray filled area); and untreated cells (dashed line). (B) Comparative changes in the Mean Fluorescence Intensity (MFI) profile of positive costimulatory molecules in CsA, RAPA and IFN-α treated mDC. Data are representative of three different experiments.

3.3.3 Rapamycin-treated DC inhibit T cell proliferation in a DC-MLR with moderate changes to FoxP3 expression in T cells

In this set of experiments, the effect of immunosuppressive agents on DC function was studied. Firstly, the effect of day 0 treated DC on T cell proliferation was assessed in a DC-MLR. The modified DC were washed thoroughly prior to use as stimulators in the MLR to minimise any residual agent. In **Figure 3.5**, the MLR showed that, in comparison to the untreated mDC, RAPA-treated mDC inhibited 40% of T cell proliferation (P =0.001) in a stimulator: responder ratio of 1:100. CsA-treated mDC showed no effect on T-cell proliferation whereas IFN-α-treated DC enhanced T cell proliferation by 30% compared with untreated DC (P=0.003) in a stimulator: responder ratio of 1:100. Inhibition of T cell proliferation by RAPA-DC was not due to induction of IL-2-responsive T cell anergy since the addition of exogenous IL-2 did not restore T cell proliferation relative to the control cells (**Figure 3.5C**).

The potential of modified DC to generate T regulatory cells was assessed by quantifying the percentage of FoxP3 expressing T cells and the level of protein induction by MFI values after co-culture for 6 days. **Figure 3.5** showed that RAPA-treated DC produced 19% FoxP3 positive T cells with an MFI of 53 in comparison to untreated DC which produced 25% positive cells with an MFI of 65. CsA-treated DC also showed similar effects.

3.3.4 Rapamycin-treated mature DC inhibit T cell proliferation in a DC-MLR with minor changes to FoxP3 expression in T cells

In this set of experiments, the functional consequence of RAPA addition to mature DC was studied. Firstly, the effect of RAPA treated DC on T cell proliferation was assessed in a

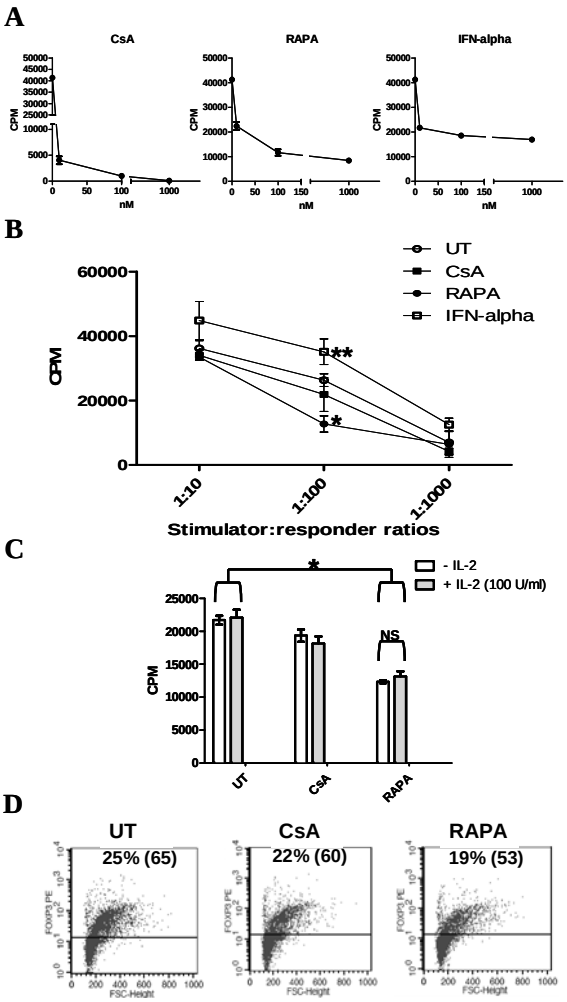

Figure 3.5. RAPA-treated DC induce T cell hyporesponsiveness in a MLR with minor changes to FoxP3 expression in T cells: (A) DC ($1x10^3$) were added to responder T cells ($1x10^5$) at a stimulator: responder ratio of 1:100 in the MLR. Cultures were also treated with varying concentrations of CsA, RAPA and IFN-α. After 4 days of culture, wells were pulsed for 20h with 1 μCi of [^{3}H]-thymidine and the incorporated radioactivity were expressed in cpm as a mean (± SD) of 5 replicate wells per group. (B) Pre-treated DC ($1x10^3$) were added to responder T cells ($1x10^5$) at a stimulator: responder ratio of 1:100 in the MLR. Statistical significance was shown for: RAPA vs UT (*P = 0.001), IFN-α vs UT (**P = 0.003). Data are representative of three different experiments. (C) DC ($1x10^3$) were added to responder T cells ($1x10^5$) at a stimulator: responder ratio of 1:100 in the MLR. Cultures were also treated with IL2 (100 U/ml) at the beginning of the cell culture. The data are representative of two individual experiments (*P = 0.03). (D) FoxP3 protein analysis in T cells co-cultured with either UT-DC, CsA-DC or RAPA-DC. T cells ($1x10^5$) were co-cultured with DC ($1x10^3$) in 96-well round bottomed plates and after 6 days of co-culture FoxP3 flowcytometric analysis was performed. The data are representative of four different experiments.

DC-MLR. The RAPA treated DC were washed 3 times in PBS prior to use as stimulators in the MLR to minimise any carryover of RAPA. In **Figure 3.6**, the MLR showed that, in comparison to the untreated mDC, RAPA-treated mDC inhibited 40-45% and 40-50% of T cell proliferation (P =0.04) in a stimulator: responder ratio of 1:10 and 1:100, respectively. When compared to day 0 and day 5 DC, all of the treatment groups had similar inhibitory strength. No significant differences were observed at 1:1000 ratio, a feature probably related to the sensitivity of the assay. We aimed to investigate if RAPA treatment was inducing apoptosis in DC, which could potentially explain our finding. Using the trypan blue to exclude dead cells, the results demonstrated that there was no significant difference in the number of DC recovered from each plated well after 5-day incubation. The potential of RAPA modified mature DC to generate T regulatory cells was assessed by quantifying the percentage of FoxP3 expressing T cells and the level of protein induction by MFI values after coculture for 6 days. **Figure 3.6** showed that RAPA-treated DC produced 21% $FoxP3^+$ T cells with an MFI of 1252 in comparison to untreated DC which produced 49% positive cells with an MFI of 1150.

3.3.5 Rapamycin treatment of mature DC does not affect the expression of positive costimulatory molecules on these DC

In this set of experiments, RAPA was added at day 7 (mDC) for 48 h, when flowcytometry was performed.

When added to mature DC at day 7, RAPA treatment did not inhibit CD40, CD80 and CD86 expression compared to untreated controls (**Figure 3.7A**). Similarly, this was observed with day 5 treatment, while RAPA addition at day 0 still inhibited positive costimulatory molecules expression. Forward and side scatter properties demonstrated obvious morphological differences in RAPA DC treated at day 0, when compared to UT DC, RAPA mDC (day 5) and RAPA mDC (day 7) (**Figure 3.7B**). When compared to the

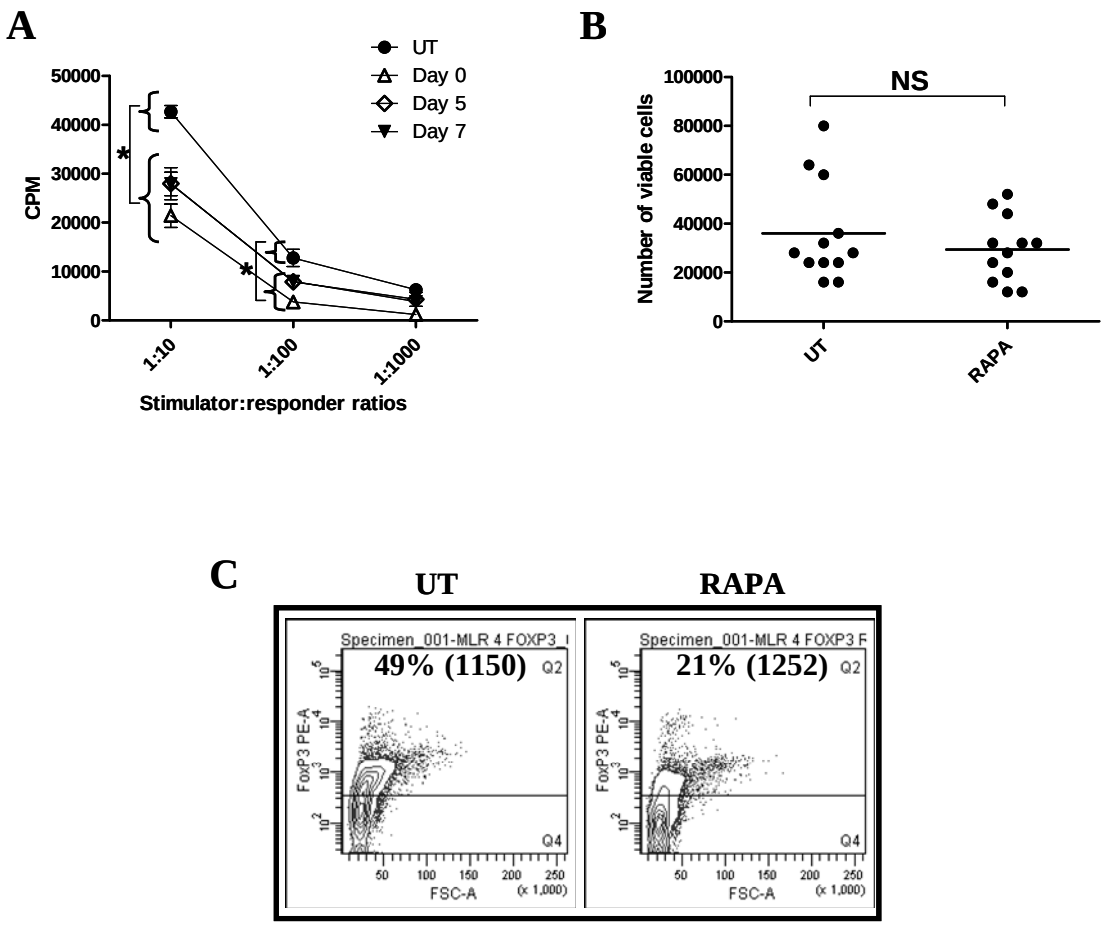

Figure 3.6. RAPA-treated mature DC also induce T cell hyporesponsiveness in a MLR with minor changes to FoxP3 expression in T cells: (A) DC cultures were treated with RAPA (10nM) either at the start of DC differentiation (from day 0 for 9 days), during DC maturation (from day 5 for 4 days) and post DC maturation (from day 7 for 2 days). In this experiment all DC also received TNF-α maturation for 48h. Varying amounts of DC ($1x10^2$-$1x10^4$) were added to responder T cells ($1x10^5$) at a stimulator: responder ratios of 1:1000, 1:100 and 1:10 in the MLR. After 4 days of culture, wells were pulsed for 20 h with 1 μCi of [^{3}H]-thymidine and the incorporated radioactivity were expressed in cpm as a mean (± SD) of 5 replicate wells per group. (B) Viability of RAPA-DC was assessed using trypan blue dye. At the end of the treatments (at day 9), UT and RAPA-mDC were harvested, washed three times in PBS and seeded at $8x10^5$ cells per well in 200 μl final volume in 96-well round bottomed-plate. Following 5 day incubation, cells were resuspended by pippeting and 10 μl aliquot from each well (12 wells for each treatment) was counted for presence of live cells (C) FoxP3 protein analysis in T cells co-cultured with either UT-mDC, RAPA-mDC (day 0), RAPA-mDC (day 5) or RAPA-mDC (day 7). T cells (1×10^5) were co-cultured with DC (1×10^3) in 96-well round bottomed plates and after 6 days of co-culture FoxP3 flowcytometric analysis was performed. *$P < 0.05$ for RAPA treatment vs. UT DC, NS indicates that the data is not significant. The data are representative of four different experiments.

A

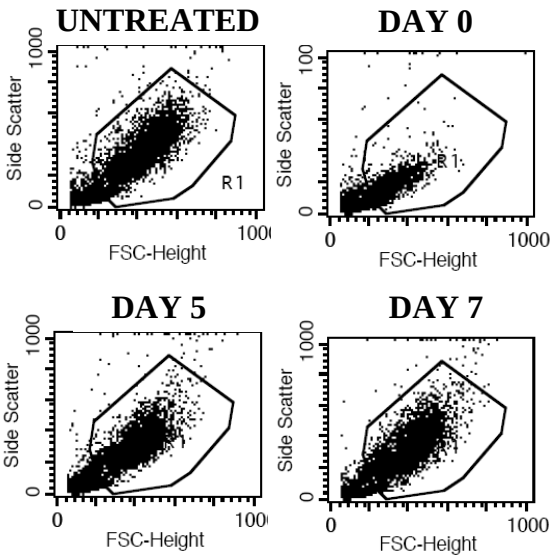

B

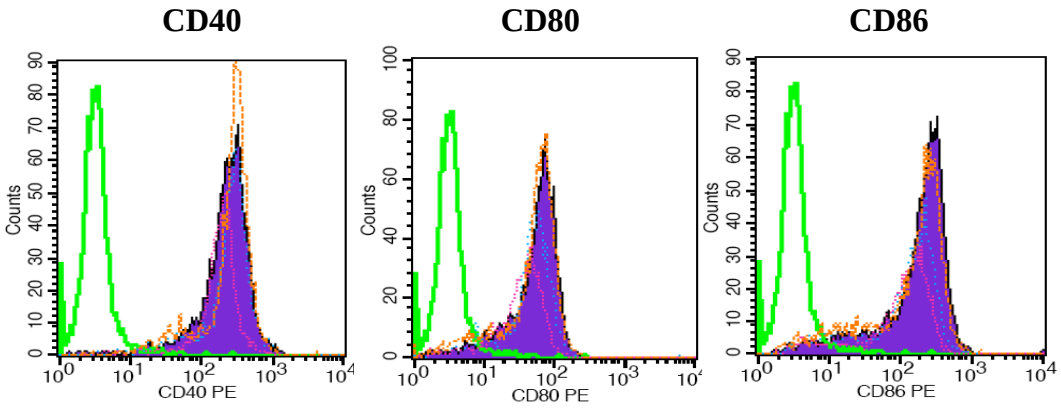

Figure 3.7. RAPA treatment of mature DC does not inhibit the expression of CD40, CD80 and CD86 on DC: (A) DC cultures were treated with RAPA (10nM) either at the start of DC differentiation (from day 0 for 9 days), during DC maturation (from day 5 for 4 days) and post DC maturation (from day 7 for 2 days). In this experiment all DC also received TNF-α maturation for 48h. Forward and side scatter dot plots are shown for each of the treatment groups. (B) CD40, CD80 and CD86 protein analysis in DC was performed. Green = isotype control, Purple fill = UT mDC, Pink = RAPA (day 0), Blue = RAPA (day 5) and Orange = RAPA (day 7). The data are representative of 2 different experiments.

UT DC, RAPA treated DC at day 5 or day 7 did not exhibit profound changes in morphology.

3.3.6 Rapamycin treatment of mature DC at day 7 induces the expression IDO mRNA on these DC

In order to elucidate mechanism of action for RAPA-treated mature DC, RNA from day 7 treated DC was extracted, reverse transcribed and quantified. The results in **Figure 3.8** indicate that all RAPA treatments (day 0, day 5 and day 7) induce very strong IDO mRNA levels. Relative to the UT DC, RAPA-treated mature DC (day 7) expressed 70% induction of IDO mRNA. Even greater differences were observed for day 0 and day 5 treated DC. Furthermore, IL-10 was reduced by a minimum of 50% in all RAPA treatments, while IL-12p40 was significantly induced by 50-70%. Interestingly, PKCβ (activator of RelB) was induced in all three treatments (30% for day 7 DC, and 80% for day 0 and day 5 DC) while RelB induction was exclusive to day 0 treated DC (60% induction vs. UT DC). The results are representative of 3 experiments for IL-10, IL-12p40 and IDO ($P < 0.05$), and 2 experiments for PKCβ and RelB.

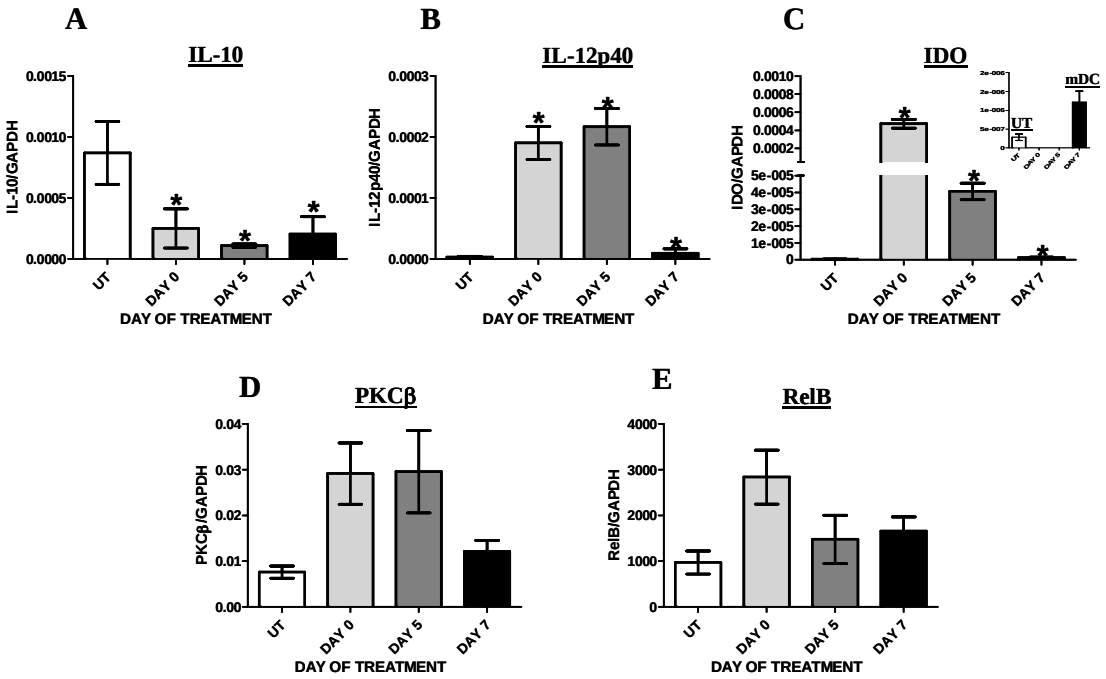

Figure 3.8. RAPA treatment of DC induces significant amount of Indoleamine 2,3-deoxygenase (IDO) mRNA: DC cultures were treated with RAPA (10nM) either at the start of DC differentiation (from day 0 for 9 days), during DC maturation (from day 5 for 4 days) and post DC maturation (from day 7 for 2 days). In this experiment, all DC also received TNF-α maturation for 48h. mRNA was extracted, reverse transcribed and subjected to PCR amplification of (A) IL-10, (B) IL-12p40, (C) IDO, (D) PKCβ and (E) RelB. Results are expressed as copy numbers of target gene / copy numbers of GAPDH. Insert in figure (C) highlights mDC and UT treatment groups enabling visualisation of the extent of IDO difference. The data are representative of at least 2 different experiments (*$P < 0.05$).

3.4 Discussion

The differentiation of monocytes to dendritic cells with the cytokines IL-4 and GM-CSF provides an *in vitro* model to assess the ability of immunomodulatory agents that interfere with the process of differentiation and maturation of these cells. The seminal work of Randolph *et al* (50, 51) has shown that monocytes do indeed undergo differentiation *in vivo* into DC and therefore, the *in vitro* model is a representation of the *in vivo* process. The baseline data reported in our study shows that during DC differentiation and maturation the positive costimulatory molecular profile increases in expression which is attributed to the NFκB/RelB (330-332) pathway, whereas the inhibitory receptors concomitantly decrease on the cell surface (**Figure 3.2**). The present study has collectively analysed the inhibitory immunoglobulin-like transcripts ILT2, ILT3 and ILT4 with regard to DC differentiation, and the reduction in the profile of these molecules during DC maturation is likely to facilitate the increased immunogenicity of mature DC. On the other hand, the increased expression of ILT3 and ILT4 on DC treated with IFN-α/IL-10 confers tolerogenic properties upon these cells as defined by inhibition of allogeneic T cell proliferation and generation of allospecific T regulatory cells (167). In addition, the immature status of DC depicted by the lower expression of costimulatory molecules such as CD40, CD80 and CD86 may also facilitate the tolerogenic behaviour of iDC. However, the studies by Rastellini's group showed that the *in vivo* tolerogenic property of iDC was ameliorated by the subsequent maturation of DC depicted by the upregulation of costimulatory molecules that led to the rejection of allogeneic pancreatic islet transplants (129). Our *in vitro* study corroborates that in addition to the upregulation of the costimulatory molecules, the downregulation of inhibitory receptors is an effective means for DC to maintain their stimulatory capacity and requires further clarification in future *in vivo* studies.

It has become apparent from the studies of Lehtonen *et al* that the transcription factor, IFN regulatory factor 4 (IRF4) is induced during DC differentiation and maturation. Moreover, Nakajima *et al* have demonstrated that the transcription factor PU.1 regulates ILT2/ILT4 and the observation that IRF4 binds to PU.1highlights a potential mechanism for the regulation of ILT2/ILT4 during DC maturation (333, 334). It may thus be proposed that the reduction in PU.1 as a result of its interaction with IRF4 may contribute to the downregulation of ILT2/ILT4 cell surface expression during the course of DC differentiation and maturation as reported in our study.

While studies have shown that the immunomodulatory molecules such as IL-10 and IFN-α induce the inhibitory molecules ILT3, ILT4 (167) and HLA-G (335), data on the role of immunosuppressants on the expression and function of these molecules is not forthcoming. There is however some limited evidence that immunosuppressive agents may influence the *in vivo* expression of ILT3 and ILT4 (164, 167) as well as HLA-G in liver/kidney transplants (205, 220, 336, 337). Due to the limited data, in this study we define the specific effect of clinically relevant doses of the currently used immunosuppressants CsA and RAPA (338, 339) on the inhibitory immunoglobulin-like transcript receptors in DC during differentiation and maturation in culture. The important feature of our study is that RAPA, unlike CsA, showed the most profound effects on the molecular profile of both positive costimulatory molecules and the inhibitory immunoglobulin-like transcripts in DC. In particular, as demonstrated in **Figures 3.2** and **3.3,** when RAPA was added prior to DC differentiation the costimulatory molecules CD40, CD80 and CD86 are downregulated. Our data was supportive of Monti *et al.* (252) who reported similar effects of RAPA when added prior to differentiation followed by CD40-ligand mediated maturation of DC and was in contrast to Woltman *et al.* (340) who showed no effects on the costimulatory molecules. Additionally, we report that despite the

downregulation of costimulatory molecules, RAPA did not modify the maturation marker CD83 expressed by mDC. This may be explained by the inability of RAPA to modify IL-12 expression (341), thus maintaining high CD83 expression. In **Figure 3.8B,** we demonstrated that RAPA could induce IL-12 mRNA expression in DC, although the approach used in **Figure 3.8B** was slightly different to the one used above.

Our studies emphasise the phenomenon of the timing of the addition of RAPA prior to differentiation on the cell surface molecular profile of DC. A potential reason for this restricted "window of opportunity" for RAPA mediated effects when added at day 0 may be due to its influence on the early induction of IRF4 by GM-CSF and IL-4 as reported by Lehtonen *et al*. Thus the administration of RAPA after the induction of IRF4 may not be effective on DC differentiation/maturation as shown by the lack of responsiveness at day 5 (**Figure 3.3** and **3.3**). Additionally, Hackstein *et al.* have shown that RAPA downregulates the IL-4 receptor complex (consisting of IL-4R and the IL-2Rγ chain) in DC (233) which is likely to influence IL-4 signalling and thus limits the cytoplasmic levels of IRF4. Global gene profiling studies further suggest that a host of transcription factors in response to IL-4/GM-CSF are induced during this early phase of DC differentiation and may be subject to either direct or indirect mTOR inhibition (342-345). Surprisingly, CsA showed no effects on DC differentiation which is consistent with the observations of Woltman *et al.* (346) regardless of its observed direct effects on T cell proliferation (**Figure 3.5**).

The effect of RAPA on human DC differentiation also influences the ability of these cells to induce T cell proliferation. The reduced allogeneic T cell proliferation in response to RAPA-treated DC as stimulators is consistent with the downregulation of costimulatory molecules on DC, however its potential to increase the numbers of $FoxP3^+$ T cells in culture compared to CsA-treated DC or unmodified DC (**Figure 3.5**) was not demonstrated in our studies. Our observations, which showed that reduced costimulation in RAPA-DC

was incapable of inducing FoxP3$^+$ cells, is consistent with the reports that costimulatory strength (high costimulation) is required for the induction and expansion of FoxP3$^+$ T regulatory cells through the production of IDO from DC (347, 348). However, our data which was generated using human monocyte-derived DC were inconsistent with the observations of Thomson's group that demonstrated in a murine model of allograft transplantation that RAPA-treated DC of bone marrow origin were capable of generating FoxP3$^+$ T regulatory cells (235, 349). The discrepancy of the observations may be due to the precursor source of DC or species differences. In addition RAPA-DC did not induce a classical clonal T cell anergy response as evidenced in **Figure 3.5** by the lack of responsiveness of T cells to exogenous IL-2. However, another level of T cell anergy exists, called division arrest anergy and this represents a deeper and non-IL-2 dependent substrate of clonal anergy (102). Since in this latter anergy state T cells have blockade in IL-2R signalling, phosphorylation of the tyrosine motifs could be assessed in purified T cells following co-culture with RAPA-DC, in order to determine if RAPA-DC are able to induce this form of T cell anergy (106).

Furthermore, in the present study we also demonstrated for the first time that RAPA treatment of mature DC resulted in generation of *in vitro* tolerogenic DC capable of inducing T cell hyporesponsiveness independent of FoxP3$^+$ T cell generation. These DC were not apoptotic nor did they have any reduction in their expression of positive costimulatory molecules. PCR analysis revealed that IDO expression was significantly induced in the RAPA-treated mDC, which may provide a potential tolerogenic mechanism for these DC. The same was also true for day 0 and day 5 treated DC. IDO was shown to be expressed by DC and to lead to inhibition of T cell proliferation (350, 351). It has also been associated with T_{REG} cell generation, but we did not observe any FoxP3 induction in the RAPA groups (352-354). In contrast, FoxP3$^+$ cells were reduced in number. This however

could not be explained by the lack of costimulatory signal, since the levels of costimulatory molecules did not differ between tolerogenic RAPA-mDC and UT DC. We are unsure if RAPA-DC can produce functional IDO, as our observations were only limited to mRNA expression. Furthermore, we cannot exclude that other immunosuppressive molecules such as PDL-1 or CD200 may be acting cooperatively with IDO to generate T_{REG}, and these may have been downregulated by RAPA treatment. For example, murine DC expressing CD200 receptor (CD200R) were induced to express IDO by CD200-Ig which in turn rendered DC tolerogenic capable of suppressing antigen specific responses *in vivo* (355). In another study, CD200R ligation on DC rendered DC capable of inducing FoxP3 T_{REG} (356). Nevertheless, future studies are warranted to investigate the role of IDO protein in RAPA-modified tolerogenic DC, especially during day 0 treatment, since these DC showed the highest mRNA induction of IDO. In addition, RAPA-DC treated at day 0 showed a marked induction in PKCβ mRNA expression relative to the UT DC. PKCβ is known to induce RelB expression and downregulate NF-kappaB (357) in DC cell lines. RelB has been shown to induce non-canonical NF-kappaB pathway (358) which in turn upregulated IDO in DC (359). Therefore from our data it may be implied that induction of PKCβ in DC by RAPA may induce RelB production (in particular at day 0 treated DC) which in turn may activate non-canonical NF-kappaB leading to the IDO production by DC. To data there have been no studies looking at the relationship between RAPA and IDO induction in transplant patients. Although this may be challenging since patients often receive a cocktail of immunosuppressive agents, it may be of great importance, as IDO expressing cells are being implicated in the induction of tolerance (360). Our experimental observation suggests that in transplant patients RAPA could potentially act on DC to induce IDO expression. This may contribute to the inhibition of the alloimmune response. Furthermore, our results provided another novel finding showing that inhibition of the mTOR pathway is

responsible for the induction of IDO mRNA expression. Therefore, instead of using oral administration of RAPA, a more specific approach of inhibiting mTOR expression could be investigated. For example, aptamer-small interfering RNA (siRNA) molecules have been developed in order to deliver specific siRNA to the specific target cells (361). Cell specificity was provided through the aptamer portion of aptamer-siRNA complex. This approach resulted in functional siRNA being delivered to specific target cells and efficient mRNA knock-down (361). mTOR specific siRNA is currently available on the market and with a combination of the siRNA and aptamer technology, DC could be targeted through DC specific marker, for example DC-SIGN. Clinical trials using aptamer technology for Macular Degeneration are currently underway and several drugs have passed Phase I safety studies, and are now in Phase II or III clinical trials.

In conclusion, this study demonstrates that RAPA in comparison to CsA is more effective in generating tolerogenic DC if treated prior to differentiation. Furthermore, our studies also pre-empt that the *in vitro* data may also reflect the potential effects of RAPA on DC function *in vivo*. The *in vivo* effects on RAPA DC differentiation and maturation warrant further investigation with regard to tolerogenic mechanism that lead to the acceptance of allografts in contrast to its immunosuppressive effects on T cell proliferation. This study has demonstrated, for the first time, that RAPA can even generate tolerogenic DC when added to the mDC. Here we propose to study the effect of RAPA on *ex vivo* DC isolated from sheep. These sheep DC were previously shown by our group to express mature DC phenotype (ie. CD83 and high MHC II expression) and induce strong T cell proliferation. The effect of RAPA on DC phenotype and function will be examined both *in vitro* and *in vivo*. The latter will involve using a NOD/SCID model of vascularised ovine skin transplantation. This translational model will allow for the “proof of concept” studies to be

carried out before assessing these DC in a more complex ovine model of solid organ transplantation (**2.3**).

CHAPTER 4

THE TOLEROGENIC EFFECTS OF RAPAMYCIN TREATED OVINE DENDRITIC CELLS IN NOD/SCID MODEL OF TRANSPLANTATION

4.1 Introduction

In **chapter 3** it was reported that the treatment of mature human DC with RAPA conferred novel tolerogenic properties to DC not previously reported in the literature. To date studies have mainly reported the addition of RAPA to iDC to characterise the effect of this agent on DC differentiation and maturation (233, 235, 340). Thus in this chapter, in order to show proof-of-concept that the *ex vivo* RAPA-modified ovine DC are capable of modulating allograft rejection, a surrogate sheep model using the immunocompromised NOD/SCID mice as a host of ovine skin graft was examined upon challenge with allogeneic ovine PBMC and RAPA-modified DC. This approach will allow the evaluation of RAPA-modified DC in a small scale using the NOD/SCID model to host ovine skin/cells prior to using the large sheep model of kidney transplantation.

4.1.1 The NOD/SCID model

Immunodeficient mice (ie. human PBL-*scid*) models have been generated in order to study various human diseases *in vivo*, one of them being vascularised skin allograft rejection, (362). A feature of the PBL-*scid* mice is the lack of functional immunity which enabled efficient engraftment of human skin and lymphocytes, thus providing a murine model of human allograft rejection. Similar immunodeficient models have been used to study other human diseases, including graft versus host disease (GVHD), HIV immunobiology and cancer (363).

Although a number of different immunodeficient strains have been generated (364), the NOD/SCID strain provides a superior model for immune reconstitution (365, 366). NOD/SCID mice were derived by backcrossing the Prkdc^{scid} mutation onto the NOD/Lt strain for ten generations (366). The *scid* (severe combined immunodeficient) mutation in mice confers defective DNA-repair mechanisms and a failure to rearrange the variable,

diversity and joining (VDJ) segments of TCR and immunoglobulins (367-369). These immunological defects lead to a lack of functional T and B lymphocytes. This feature enabled successful engraftment of human cells in the *scid* mice but only for short-term. Long-term persistence of human cells was not permitted due to clearance of the engrafted cells by the mouse innate immune responses mediated via NK cells (368). In addition, the defect of VDJ recombination in *scid* mice is incomplete, resulting in the emergence of T and B cells in older animals. In comparison, the NOD/Lt strain is characterised by impairment in: functional natural killer (NK) cells (370), differentiation and function of antigen presenting cells (371) and impairment of circulating complement (372). Therefore by backcrossing the two mutated strains, the NOD/SCID strain has been formed. It is well described that NOD/SCID mice lack functional T and B cells, have poor NK cell activity, lack of circulating complement and these mice do not develop diabetes nor insulitis throughout life (365). These features enabled NOD/SCID mice to be effectively and efficiently reconstituted with immune cells when compared to the *scid* mice (373).

A NOD/SCID model of ovine vascularised skin transplant used in this study was developed by the host laboratory as per human engraftment model of Murray *et al.* 1994 (362). In their study authors transplanted partial thickness human skin grafts onto immunodeficient mice. The allograft was allowed to anastomose with mouse vessels prior to the injection of allogeneic human lymphocytes. The first onset rejection responses were similar to the rejection responses observed in human skin transplant patients, where VCAM-1 and MHC II molecules were upregulated at day 6 post allogeneic challenge on vascularised endothelium followed by profound T cell infiltration into the allograft at day 11 (362). Human $CD4^+$ and $CD8^+$ T cells localised to perivascular regions of the skin and destroyed human microvessels by day 16 post allogeneic challenge. In the present study, 8mm full-thickness sheep skin biopsies will be transplanted onto the NOD/SCID mice and

allowed to anastomose to blood vessels prior to intra-peritoneal challenge with autologous DC and allogeneic PBMC. Skin allografts will be excised on day 7 and 14 post immune challenge and analysed for the level of T cell infiltration, as per study by Murray *et al.* 1994 described above. In the current study the direct pathway of allorecognition (**reviewed in section 1.6.2**) will be examined by injecting DC autologous to the skin. However, in this NOD/SCID mice model short-term immunological responses and not long-term tolerance could be tested since ovine haematopoietic stem cells were not reconstituted and therefore ovine lymphocyte repletion does not occur spontaneously (364).

4.1.2 Ovine DC: characterisation and enrichment from lymphatic cannulation

Ovine DC obtained by lymphatic cannulation have been previously reported by our group to have mature DC phenotype (expression of CD83 and high MHC II) and strong allostimulatory capacity, similar to human DC (283). DC represent a small percentage of circulating blood MNC (~2%) and they also circulate in lymph and reside in the majority of tissues (374-376). Depending on their tissue origin, DC populations have different phenotypic and functional characteristics. In contrast to DC from lungs and intestines which exert immunosuppressive properties to T cells in the lymph nodes thus preventing strong immune response to environmental antigens (377, 378), cutaneous DC isolated from lymph are highly potent antigen presenting cells (379-381). Compared to human DC, ovine DC are not readily generated from monocytes based on our attempts. However, Chan *et al.*. 2002 demonstrated that ovine monocytes could be differentiated to MHC II expressing DC capable of inducing strong T cell proliferation and that their approach yielded a low percentage of DC (1-5%) from $CD14^{+}$ monocyte precursors (382). In the current study, ovine DC with potent antigen presenting properties were isolated from lymphatic fluid draining the skin by cannulating the lymphatic vessels.

While human lymph nodes are arranged like “beads in a chain”, sheep lymph nodes on the other hand have a number of small afferent vessels draining into a large solitary lymph node with a single efferent lymphatic vessel draining the lymph node (383-385). Although these efferent lymphatic can be cannulated, they do not contain DC as DC are retained in the lymph node (386, 387). Afferent lymph usually contains 1-10% DC, but the small diameter of the vessels makes cannulation technically difficult and minimal lymph may be collected (388). An initial study by Lascelles and Morris showed that removal of the lymph node allowed multiple afferent lymphatic vessels to anastomose to the larger efferent lymphatic vessel, which was then cannulated (389, 390). This so-called “pseudo-afferent lymph”, was shown to have a similar cellular composition of true afferent lymph. Dendritic cells could be easily enriched to >80% purity using density gradient separation (376, 391). In the current study, purified lymphatic DC will be treated for 48h with RAPA, as per the human protocol (**chapter 3**), and then analysed for any phenotypic and functional changes *in vitro*. Furthermore, these DC will be tested for their ability to inhibit allograft rejection using the NOD/SCID model of vascularised sheep skin transplantation.

4.2. Methods

4.2.1 Lymph node removal

Two-year old Merino sheep were acquired from the Institute of Medical and Veterinary Science (Adelaide, Australia). Animals were housed at the animal facility at The Queen Elizabeth Hospital under strict ethical guidelines. Animal ethics approval was obtained from the QEH and Adelaide University animal ethics committees (Ethics number 57/07). All of the procedures were performed under general anaesthetic using 1-3% Isoflurane at the oxygen flow rate of 1-1.5 L/min. Surgical procedures involving lymph

node removal and cannulation were performed by Boris Fedoric (thesis author) with technical assistance from animal facility staff. Images of the lymph node removal are outlined in **Appendix 4.1**.

Prefemoral lymph nodes were palpated and the location of the node was marked with a pen prior to making incision of approximately 5-8cm in length. Using blunt scissors, fat was teased away until the lymph node was visible. The node was then clamped and pulled upwards to allow for the visualisation of the blood vessels. Approximately 4-5 major blood vessels supplying the lymph node were generally identified and then tied off using non-absorbable 2.0 Silk (Ethicon, USA). Prior to cutting the blood supply, clamps were placed above the suture and as close as possible to the lymph node in order to prevent back-flow of blood. Ensuring the clamps and sutures were in place, blood vessels were cauterised in between the suture and the clamps. The wound was examined for any bleeding prior to closing the wound. Closure of the fascia was performed using 1.0 Vicryl absorbable sutures (Johnson & Johnson, USA) and taper needle. The same suture was used for the skin however a reverse cutting needle was used instead of a taper needle. The animals were monitored for 24-48h post operation for any abnormal changes and each examination was recorded in a clinical record sheet (**Appendix 4.4**). If there were no complications, the animals were returned to the paddock for a 6-8 week agistment period to allow pseudo-afferent vessels to develop.

4.2.2 Cannulation

This procedure was demonstrated in person to the author by A/Prof Jean-Pierre Scheerlinck (University of Melbourne, Australia). Images of the surgical procedure are shown in **Appendix 4.2**.

The sheep were returned to the QEH animal facility after 6-8 weeks and allowed to adjust to the housing conditions for 2-3 days. The sheep were then placed under general anaesthesia as above and the incision was made approximately 5 cm in length below the iliac crest. The length of the incision was 5-10 cm in length depending on the position of the lymphatic vessels. Subcutaneous fat was teased out using blunt scissors until the abdominal wall was visualised on the cephalic side. The pseudo-afferent lymphatic vessel was located caudally to the abdominal wall on the lumbar muscle, in close proximity with the iliac blood vessel and nerve (so called “bundle of three”). Retractors were placed next to the lymphatic vessel and into the lumbar muscle on the caudal side and into the abdominal wall on the cephalic side. Opening of the retractors provided better visualisation of the lymphatic vessels by positioning them proximal to the incision opening. Since lymphatic fluid flow was in the ventral to dorsal direction, a non-absorbable 6.0 Silk (Ethicon, USA) tie was placed to the most dorsal part of the lymphatic vessel. This caused swelling of the lymphatic vessel allowing better visualisation for making the incision. Using iris scissors, a small incision was made on the vessel, approximately 1cm from the silk tie. Heparinised polyvinyl tubing with an inner diameter of 0.46 mm was used as cannula tubing (CBAS-coated, Carmeda AB, Sweden). The tip of the cannula was cut at a 45° angle and inserted in the incision site in the vessel. The cannula was led down the lymphatic vessel for no more then 1.5cm (between 1-1.5cm) and once the continuous flow of lymph was ensured, the cannula was secured at that position with 3 ties using non-absorbable 2.0 Silk sutures. The retractors were taken out and skin was allowed to settle for a few minutes. The other side of cannula was then guided through a piercing needle which passed through the skin, facia and most importantly fat. The skin was pierced at the dorsal side of the incision approximately half-way between the top and bottom of the incision. This created an angle which did not allow the cannula to kink or to be under tension, both

of which would result in poor flow of lymph or cessation of flow. The wound was examined for any bleeding prior to closing the wound. Closure of the fascia and skin was performed as above. An Endotoxin-free T-75cm^2 tissue culture flask (SARSTEDT, Germany), containing 2500 IU heparin and 40 mg gentamicin sulphate, was then placed in the elastic pouch which was placed over the wound. The flask was positioned at the ventral side just below the surgical site in order to prevent wound irritation. The animal was then given the intra muscular antibiotic and allowed to wake up. All the animals were monitored daily post operation for any abnormal changes and each examination was recorded in a clinical record sheet. Flasks were collected strictly at 24 h intervals and volumes were recorded.

4.2.3 Histodenz Purification of ovine DC from lymph

Lymph was decanted into 50 ml tubes and centrifuged at 340g for 7 min. Each pallet was resuspended in 7 ml PBS and transferred to 10 ml tubes. The cell suspension was underlayed with 2 ml of 14.5% Histodenz^{TM} (Sigma, USA) in RPMI. Cells were centrifuged at 800g for 15 min with no brake. The interface layer was collected, washed twice in RPMI at 340g for 5 min and counted. This DC-rich fraction was then frozen in 10% DMSO and 20% FCS for future use.

4.2.4 RAPA treatment of ovine DC

Isolated fresh or frozen lymphatic DC were resuspended in complete media containing 400 U/ml IL-4 and 800 U/ml GM-CSF at concentration of 2x10^6 cells/ml and treated with RAPA (10 nM or 100 nM). Cells were incubated at 37°C, 5% CO_2 for 48h before DC were used in the assays.

4.2.5 Flowcytometry

The cell-surface phenotype of the Histodenz™ enriched ovine lymphatic DC was analysed by flowcytometry (**2.3.4**). Monoclonal antibodies used were either specific for ovine cell surface antigens or specific for human antigens with demonstrated cross-reactivity to their respective ovine homologue. Primary mAb used were: anti-CD1a (20.27), anti-CD4 (44.38), anti-CD8 (38.65), anti- MHC II DP (28.1), anti-CD11b (Du 12-5), anti-CD14 (VPM65), anti-CD83 (HB15A17.11), anti-CD21 (CC21), CTLA-4-Ig (anti-CD80/CD86) and isotype controls 1D4.5 and X63.

4.2.6 DC-Mixed Lymphocyte Reaction

Ovine PBMC were isolated from peripheral blood as per section **2.3.1.2**. The DC MLR was set up as detailed in section **2.3.1.4** with DC used as stimulators to responder allogeneic PBMC. DC were washed 3 times in PBS, exposed to 30 Gy of gamma radiation to prevent residual autologous T cell proliferation and added at a concentration of $1x10^5$ cells/ml to each well ($1x10^4$ cells/well). DC were then challenged with 100 μl of allogeneic PBMC at a concentration of $1x10^6$ cells/ml ($1x10^5$ cells/well). This ratio of 1:10 stimulator : responder cells consistently gave strong proliferative response.

4.2.7 DC viability

RAPA-treated or untreated DC were plated at $1x10^5$ cells/well in 200 μl of complete RPMI media in 96-well round-bottomed plate. Cells were plated in quadruplicates for each treatment and incubated for 5 days at 37°C, 5% CO_2. At day 5, DC were mixed by pipetting before 10 μl of DC from each well was mixed with 10 μl of trypan blue dye and live cells were visualised under a microscope.

4.2.8 Excision of ovine skin for engraftment in NOD/SCID

The procedure was performed by the author and the images of the procedure are outlined in **Appendix 4.3**. Animal ethics approvals for the experiments were obtained from Adelaide University and the QEH animal ethics committees (animal ethics number 57/07).

The sheep were fasted for 24 h and anaesthetised as above. Full skin thickness biopsies were excised from the non-wool bearing region of the upper thigh of the sheep using an 8 mm disposable biopsy punch (Stiefel Laboratories, Australia). Biopsy wounds were sutured using 1.0 Vicryl and antibiotic cream was applied onto the sutured skin. The animals were also administered a single intramuscular dose of antibiotics as a post-operative prophylaxis against infection. Each skin biopsy had sub-cutaneous tissue removed in order to facilitate better vascularisation of the graft, leaving approximately 0.5 mm thick graft for transplantation.

4.2.9 NOD/SCID mice

NOD/SCID mice were purchased from the IMVS (Adelaide, SA) at 4-6 weeks of age. The animals were housed in a pathogen-free environment at the the QEH Animal Facility under strict ethical guidelines. Animal ethics approvals for the experiments were obtained from Adelaide University and the QEH animal ethics committees (animal ethics number 57/07).

4.2.10 Engraftment of ovine skin onto NOD/SCID mice

Images of the grafting procedure are shown in **Figure 4.1**.

NOD/SCID mice were anaesthetized with a 1.5% Isoflurane at the flow rate of oxygen set at 0.9 ml/min. The mice were shaved at the dorsal part of thorax and skin was excised to fit the sheep skin. The sheep skin was maintained in sterile RPMI at 4°C for no

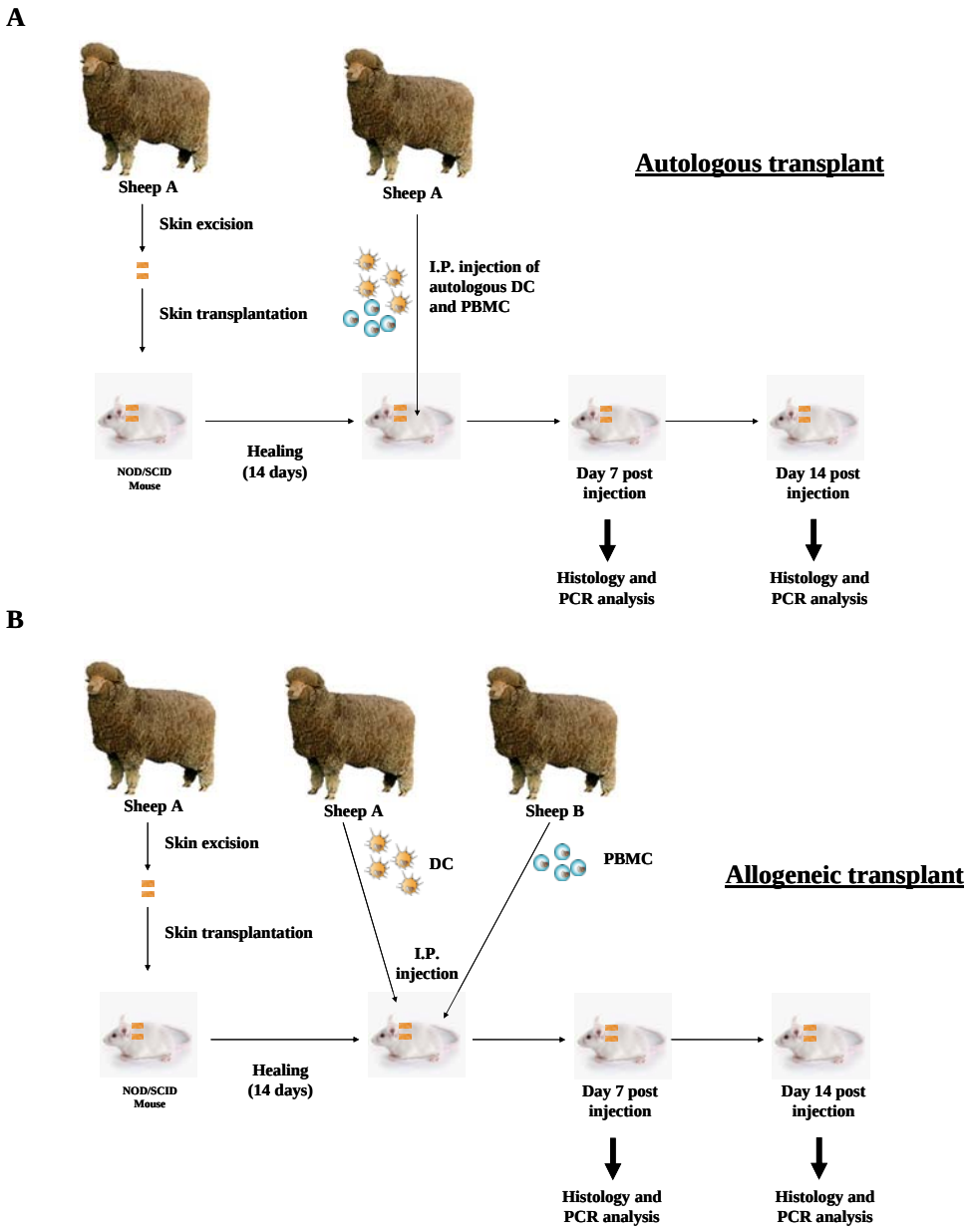

Figure 4.1. Outline of vascularised ovine skin transplantation approach in NOD/SCID mice. Skin was removed from a sheep and transplanted onto the back of the mouse. Skins were allowed to heal and anastomose to mouse microvessels for 14 days, when autologous DC (untreated or RAPA-treated; $5x10^6$ cells per mice) were co-injected intra-peritoneally with (A) autologous or (B) allogeneic responder PBMC ($5x10^7$ cells per mouse). Mice were anaesthetised and skins were removed at day 7 and 14 for the analysis of cellular rejection responses. Image of NOD/SCID mice was obtained from Charles River website, while sheep image was obtained from Pelage website.

longer then 24 h prior to transplantation. The wounds were covered with a thin layer of calcium alginate dressing SORBSAN (Steriseal, England) and the skins were secured with two layers of Tegaderm bandages (3M, Australia). Primapore bandages (Smith & Nephew, UK) were applied over the Tagaderm to provide an extra layer of protection against scratching. Primapore and Tagaderm were removed after 7 days, and healing was permitted for an additional week prior to challenge with allogeneic PBMC. The outline for the engraftment of ovine skin in the NOD/SCID experiments is illustrated in **Appendix 4.3**.

4.2.11 CFSE labelling of PBMC

Approximately $1x10^8$ PBMC were resuspended in 2 ml PBS. CFSE was added to a final concentration of 5 μM, suspension was mixed thoroughly and the cells were incubated for strictly 10 min at 37°C, 5% CO_2. Twice the volume of FCS was added to stop the CFSE uptake before cells were washed 3 times in a complete media with centrifugation (at 400g for 10 min) in 50 ml tube. CFSE labelling was visualised using FACSDiva on FL1 channel. CFSE labelling was used in order to detect responder cell infiltration within the allograft. However CFSE positive cell could not be detected in the skin as T cells may have diluted their CFSE fluorescence beyond detectable levels, as a result of proliferation.

4.2.12 Intra-peritoneal challenge with allogeneic ovine PBMC and DC

DC and PBMC were isolated as described (**4.2.3 and 2.3.1.2**) and PBMC donors were screened for their alloreactivity against the stimulator DC in DC-MLR (**2.3.1.4**). Five different responder sheep were randomly selected, bled by the Veterinary Services (IMVS, Adelaide) and were screened by MLR for alloreactivity. The combinations that gave maximum lymphocyte stimulation were used for the experiments. PBMC ($5x10^7$ cells) and DC ($5x10^6$) were mixed in the total volume not exceeding 300 μl in RPMI and immediately injected into the peritoneal cavity of the mice using 29G insulin needles. Treatment groups and animal numbers are detailed in the **table 4.1**.

Table 4.1. NOD/SCID numbers and treatment groups

DC Treatment	Lymphocytes	n =
Untreated	Autologous	4
Untreated	Allogeneic	5
RAPA	Allogeneic	5

DC were autologous to the skin donor.

4.2.13 Histological Analysis of Skin Biopsies

Engrafted skin was removed from the mice at 7 and 14 days following both autologous and allogeneic challenge and the wounds sutured with non-absorbable 4.0 silk sutures (Ethicon, USA). Each skin graft was cut in half and embedded in OCT for RNA and immunohistochemical analysis. H&E (**2.3.5.2**) and immunohistochemical staining (**2.3.5.3**) were performed to measure the level of infiltrating cells and determine rejection scores.

4.2.14 Immunohistological analysis of Skin Biopsies

Five micrometer sections were cut using cryomicrotome, briefly air-dried and submerged in cold acetone for 10 min at 4°C. Slides were firstly stained with H&E (**2.3.5.2**) to identify lymphocyte infiltrate and then subjected to either immunoperoxidase or immunofluorescence analysis to identify specific CD4 and CD8 infiltration to the graft (**2.3.5.3**). Primary sheep specific mAb used for staining included anti-CD4 (44.38), and anti-CD8 (38.65), while 1D4.5 was used as the isotype control mAb.

4.2.15 Rejection Scores

The criteria used to quantify the rejection was developed by Murray and colleagues in 1998 (392) (**summarised in the Table 4.2**) and in the present study the cellular infiltration was visualised using H&E, CD4 and CD8 staining. Two assessors, both blinded to the treatment, performed scoring and the statistical comparisons were made using the Mann-Whitney U test.

Table 4.2 Rejection scoring table

H&E Scoring	
Score	**Definition**
1	<25% scattered leukocytes
2	<25% focal infiltration
3	25-50% moderate diffuse infiltration
4	>50% infiltration
CD4/CD8 Scoring	
Score	**Definition**
1	No staining
2	Scattered discretely stained cells
3	Marked focal staining
4	Marked diffuse staining

4.2.16 RNA Extraction from skin biopsies and PCR analysis for cytokine mRNA expression

Ten to twenty 10 μm sections were cut and pooled for RNA extraction. RNA was extracted and reverse transcribed as per **2.3.2.1** and **2.3.2.2**, respectively. PCR (**2.3.2.3**) was performed on 1μg of reverse-transcribed RNA template using ovine IL-2, IL-10, IFN-γ and FoxP3 primers. Primer sequences and cycling conditions are summarised in **Appendix 2.1**. PCR products were resolved on a 2% Agarose gel, stained with GelRed™ and visualised under ultraviolet light.

4.3. Results

4.3.1 Ovine DC output from cannulated pseudo-afferent lymphatics

Lymph nodes were surgically removed in order to facilitate anastomosis of the efferent lymphatic and enable formation of the pseudo-efferent lymphatic vessel. Removal of each lymph node required 45 min and no complications were encountered. However, it was observed that the lymph nodes in different animals had different structures. For example, as evidenced in **Appendix 4.1,** the lymph node on the left had a bi-lobed structure while the lymph node on the right was single lobed. It was therefore important to clear a large area of fat and examine each lymph node prior to its removal in order to confirm the presence of any additional lobes. If a partial node was left, it would trap the DC and eliminate or reduce overall yield.

Lymph was collected at the same time each day in 24 h intervals in order to obtain data on the lymph volumes and DC yields per day. The animals were examined daily for any signs of pain, abnormalities at the surgical site, reduction of food and water intake, temperature or mood changes, ensuring good quality of life.

As shown in **Figure 4.2,** DC from the lymph were enriched using Histodenz gradient separation to at least 80% purity. DC population gated in P1 region was 98% positive for MHC II expression. Mean fluorescence intensity of MHC II was profound in DC (MFI > 10^5) while only 5% of the cells Pre-Histodenz contained high MHC II. When visualised under a light microscope in culture, ovine DC exhibited human DC-like morphology characterised by the appearance of dendrites as previously shown by Caux *et al.* 1997 (393). For *in vitro* experiments, the sheep were only cannulated for 4 weeks, but when sheep were used for *in vivo* experiments, cannulation was extended to 8 weeks. To date, there are no reports about the consequence of long term cannulation on DC phenotype and function. Here we report that following 2 months of cannulation in 3 different sheep, the number of DC per millilitre of lymph remained constant (**Figure 4.3A**). The volume of lymph varied in some sheep but the average amount of lymph produced per day was 150 ml (**Figure 4.3B**). After 2 months of cannulation, the total volume of lymph collected for one sheep was 13 litres closely followed by a second sheep producing 12 litres (**Figure 4.3C**). The total number of DC collected over the two month period ranged from $2x10^8$ – $6x10^8$ and it appeared to be dependent on the total amount of lymph produced (**Figure 4.3D**). When these DC were analysed for their allostimulatory capacity against allogeneic PBMC, the data showed that long-term cannulation did not impair DC stimulatory capacity (**Figure 4.4**). This observation was consistent with negligible changes in cell surface expression of MHC II over a two-month period (data not shown). As represented in **Figure 4.4**, some DC were better stimulators than the others which may be attributed to the level of antigenic mismatch between the animals. However, tissue typing was not performed since tissue typing reagents for sheep are not readily available.

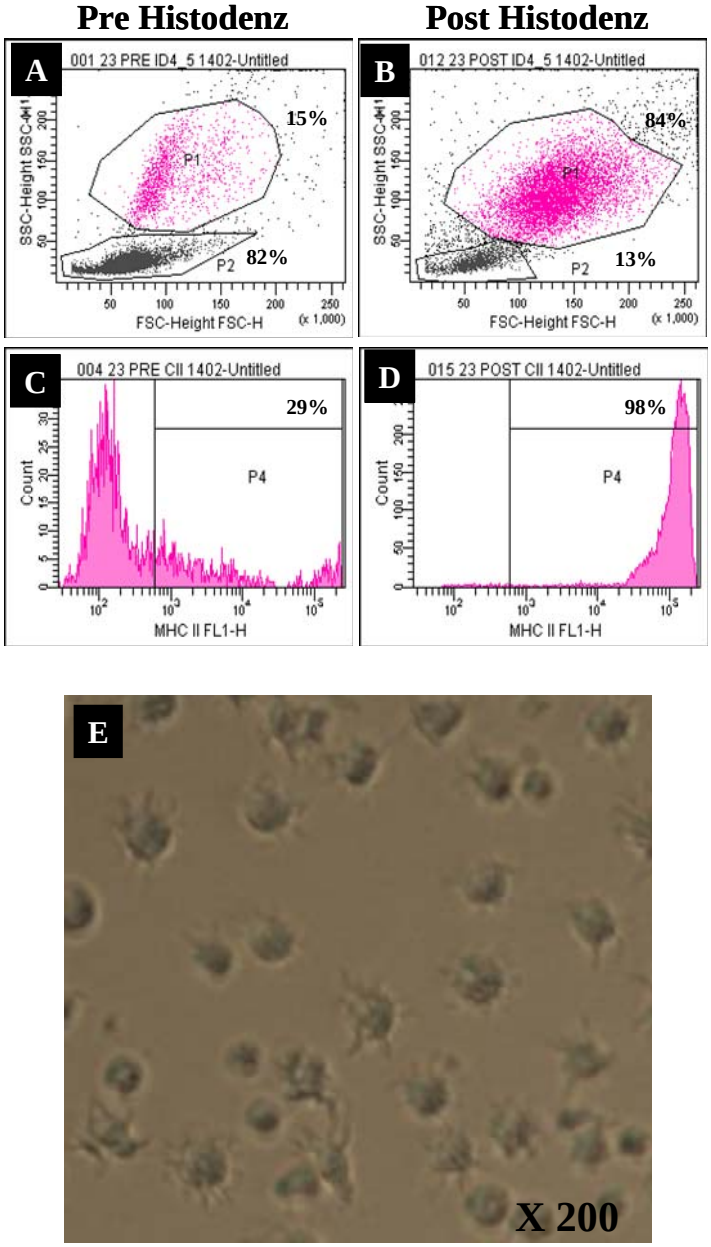

Figure 4.2. Enrichment of ovine dendritic cells using density gradient. Lymph was centrifuged to pellet the cells. The cell pellet was then resuspended in 7 ml of PBS and underlayed with 3 ml of Histodenz. (A) Aliquot of cells prior to Histodenz separation was subjected to flowcytometric analysis to determine the initial size and complexity of the cells. (B) Flowcytometric analysis of cells following the Histodenz separation. P1 gate represents the DC gated population while P2 region represents lymphocyte population. Percentage of cells in each gate are also shown (C, D) Expression of MHC Class II molecules on cells prior and post Histodenz separation, respectively. (E) Microscopic image of the sheep DC in culture.

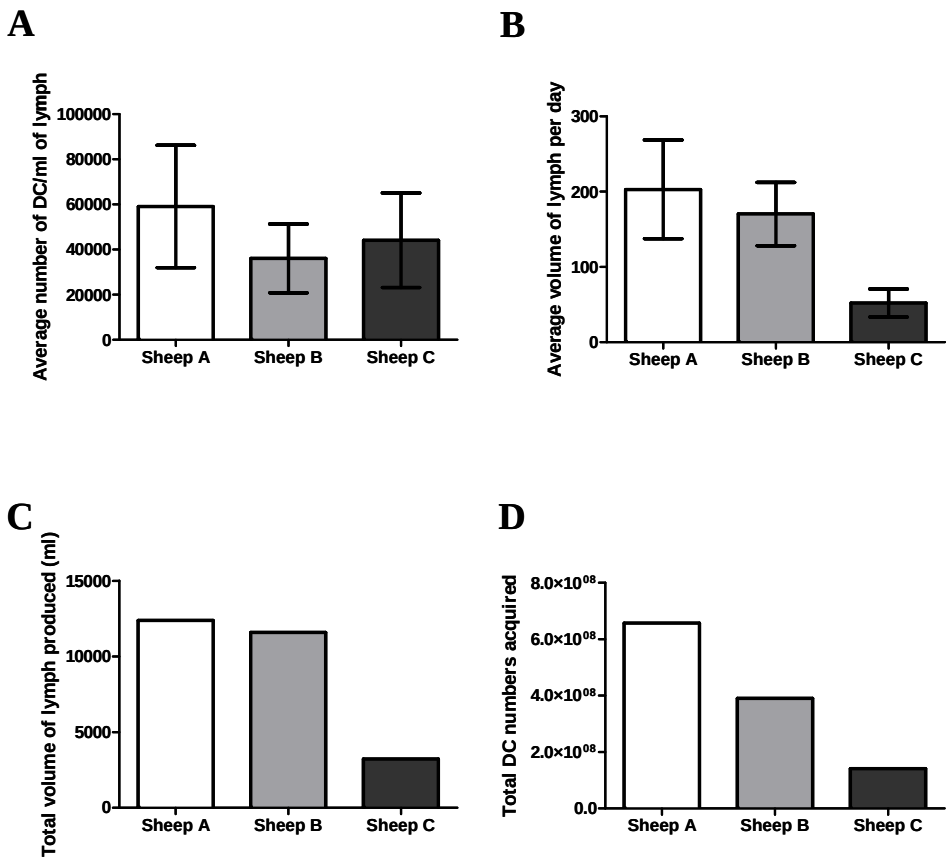

Figure 4.3. Overview of the long-term lymphatic collection. (A) Following Histodenz separation the number of cells was determined in the enriched fraction using trypan blue. (B) Lymph was collected daily at the same time for each sheep, and the average volume (ml) of lymph per 24h was recorded (C) Total volume (ml) of lymph collected over 2 months. (D) Total number of DC recovered over 2 month period.

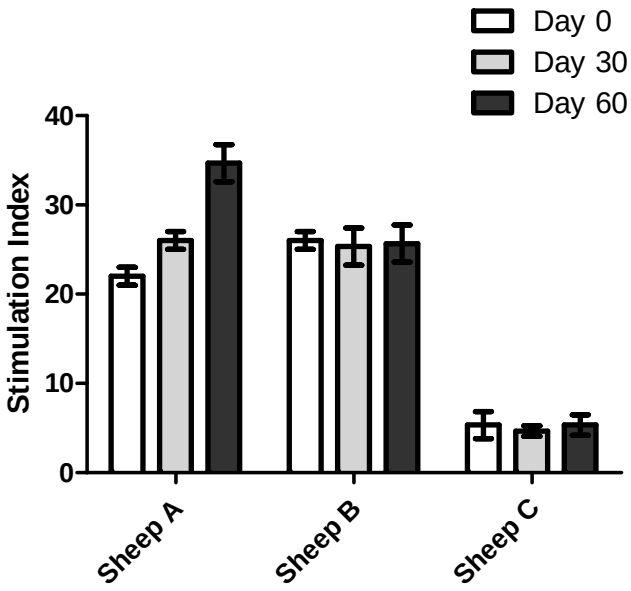

Figure 4.4. Stimulatory capacity of DC does not decrease during the 2 months of cannulation. Following the Histodenz enrichment, DC were irradiated and co-cultured with allogeneic T cells in 1:10 ratio (DC:T cells) for 5 days. At day 4 [^{3}H]-thymidine was added for 18h and the incorporated radioactivity was measured. Stimulatory index was calculated using the following formula: CPM_{MLR}/ ($CPM_{DC\ alone}$ + $CPM_{T\ cells\ alone}$). Due to the sheep being cannulated at the time of the assays, autologous PBMC could not be obtained for technical reasons to be used in autologous reaction and therefore DC and T cells alone were used to calculate Stimulation index. Error bars represent standard deviation

4.3.2 Phenotype of ovine DC obtained from pseudo-afferent lymphatic cannulation

The profiles of DC phenotypic markers were routinely examined on cells that were obtained from the lymphatic cannulation for up to 2 weeks post cannulation. **Figure 4.5** shows the typical cell surface profile of DC obtained from lymph. Most significantly, the cells demonstrated a high level of expression of the antigen presenting molecules MHC II and costimulatory molecules CD80/CD86. Although these DC exhibited high levels of MHC II, comparable to human mDC (**Chapter 3, Figure 3.2**), the CD83 was not detected in any of the sheep DC studied. In addition, DC exhibited low CD4, CD8, CD14 and CD11b expression which was consistent with previous reports (394, 395).

4.3.3 Stimulatory capacity of ovine DC

The stimulatory capacity of ovine DC were compared with PBMC in both an autologous and allogeneic setting. The data showed that the stimulation of autologous PBMC by DC (185 +/- 74 cpm) was negligible and the two way allogeneic PBMC-MLR (2500 +/- 777 cpm) was not as strong as DC which elicited a potent stimulation of allogeneic PBMC (46892 +/- 2400 cpm ($p=0.00013$)) (**Figure 4.6**). Titration of the DC stimulatory response indicated that 1:10 stimulator : responder ratio resulted in the strongest proliferation of allogeneic PBMC. In addition 1:100 ratio resulted in 50% more proliferation when compared to the PBMC (**Figure 4.6**). Therefore in our assays 1:10 (DC:PBMC) ratio will be used to evaluate tolerogenic potency of DC following RAPA modification.

4.3.4 RAPA-treated ovine DC exhibit tolerogenic properties *in vitro*

In **Chapter 3** it was demonstrated that human RAPA-DC exhibited tolerogenic properties through the induction of T cell hyporesponsiveness. In this chapter, ovine DC were treated with RAPA for 48 h, washed thoroughly, irradiated and used as stimulator cells in

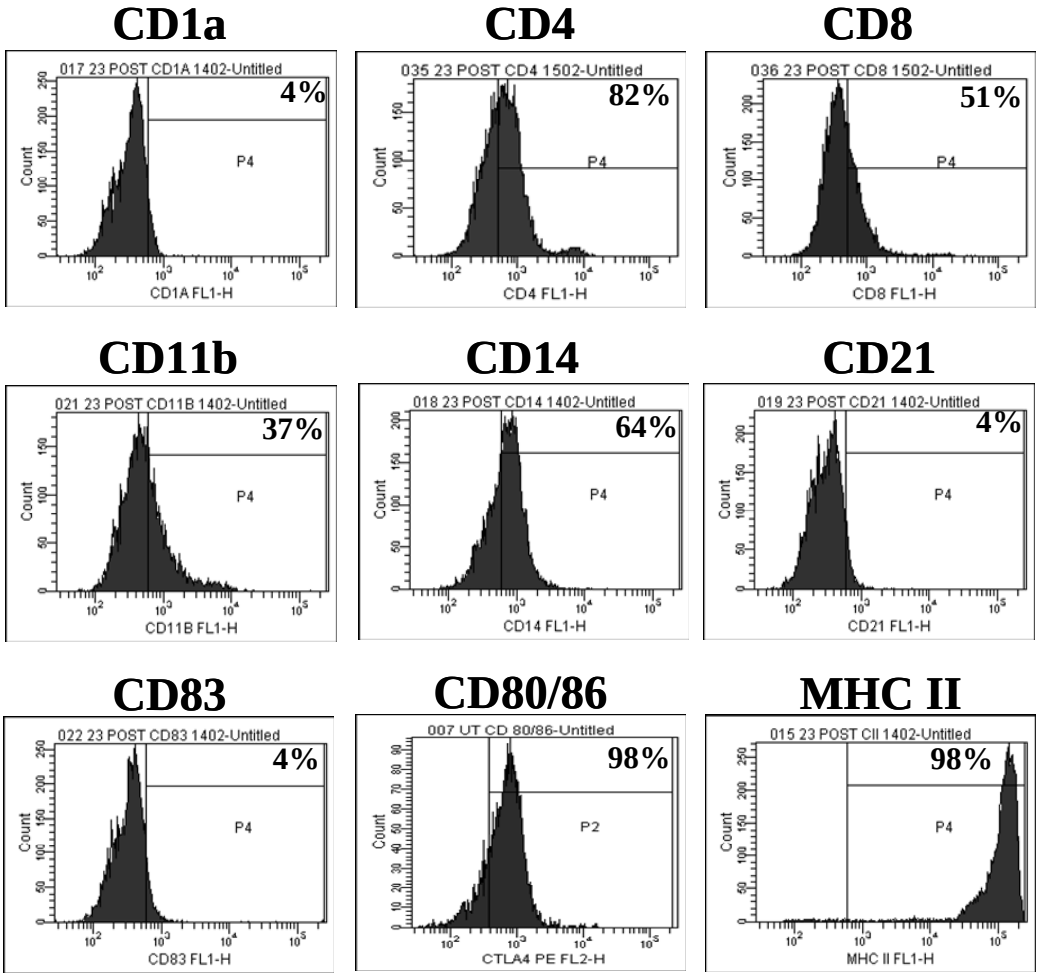

Figure 4.5. Phenotype of sheep lymphatic dendritic cells. Following Histodenz enrichment, DC were labelled with the above mAb. Isotype control mAb was used to determine the background staining and position of the negative gate. Percentage of positive cells is recorded on each histogram.

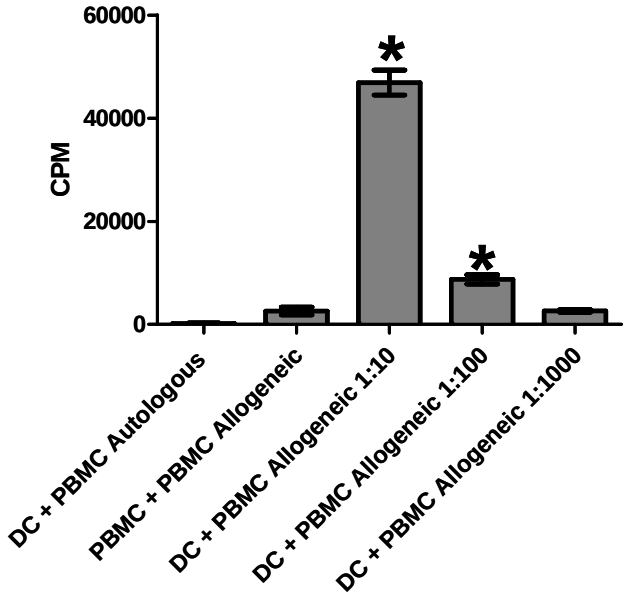

Figure 4.6. Stimulatory capacities of sheep lymphatic dendritic cells. Following Histodenz enrichment, DC were re-suspended in complete media and plated at $1x10^4$, $1x10^3$ and $1x10^2$ cells per well in 100µl. The DC were challenged with allogeneic PBMC ($1x10^5$ cells/well) in total volume of 200µl. DC were also challenged with the same amount of autologous PBMC. Allogeneic PBMC-MLR was set up by plating $1x10^4$ stimulator PBMC (autologous to DC) and challenging the stimulator cells with $1x10^5$ allogeneic PBMC (from the same responder used in DC-MLR). Cells were cultured for 5 days. At day 4 [^{3}H]-thymidine was added for 18h and the incorporated radioactivity was measured. Data are from 3 different experiments and represented as CPM (+/- SD), (*$P < 0.05$, compared to "PBMC + PBMC Allogeneic" group).

DC-MLR. The results indicated that relative to the untreated DC, RAPA (10nM) treatment of DC reduced the ability of DC to stimulate PBMC cell proliferation by 70% at 1:10 (DC:PBMC) ratio (P =0.039) (**Figure 4.7A**). The same result was obtained when DC were treated with 100 nM of RAPA. The ability of RAPA-DC to induce anergy in PBMC was investigated by adding 100 U/ml of exogenous recombinant human IL-2 (which was shown to cross-react with sheep (396)) at the beginning of DC-MLR. The results indicated that conventional T cell anergy was not induced by these RAPA-DC and there was no restoration of proliferation following IL-2 addition (**Figure 4.7B**). It was then investigated if RAPA treatment induced any morphological changes in DC. To do this RAPA-DC were collected post-RAPA treatment and analysed by flowcytometry. Forward and side scatter properties which indicated cell size and complexity, respectively, did not show any changes between RAPA-treated and untreated DC (**Figure 4.7C**). When analysed for their expression of MHC II and positive costimulatory molecules CD80/CD86, there were also no differences between the groups (**Figure 4.7D**). Finally, RAPA treatment did not induce apoptosis of DC, since similar levels of viable cells were recovered after 5-day culture from both untreated and RAPA-treated DC groups (**Figure 4.7E**).

4.3.5 Ovine skin rejection upon allogeneic challenge with DC and PBMC mixture in NOD/SCID mice

Prior to skin transplantation allogeneic responder cells were selected from the pool of 5 different sheep based on their alloreactivity to stimulator DC and the cell yields. In **Figure 4.8**, sheep R5 and R8 reacted strongest against the stimulator DC tested, however cell yields were low, which posed technical problem in obtaining large cell numbers for injection in NOD/SCID mice. Therefore, responder PBMC from sheep R7 and R2 were selected for the engraftment instead despite their slightly lower alloreactive capacity. Ovine skin allografts on NOD/SCID mice were well tolerated and showed minimal scabbing and

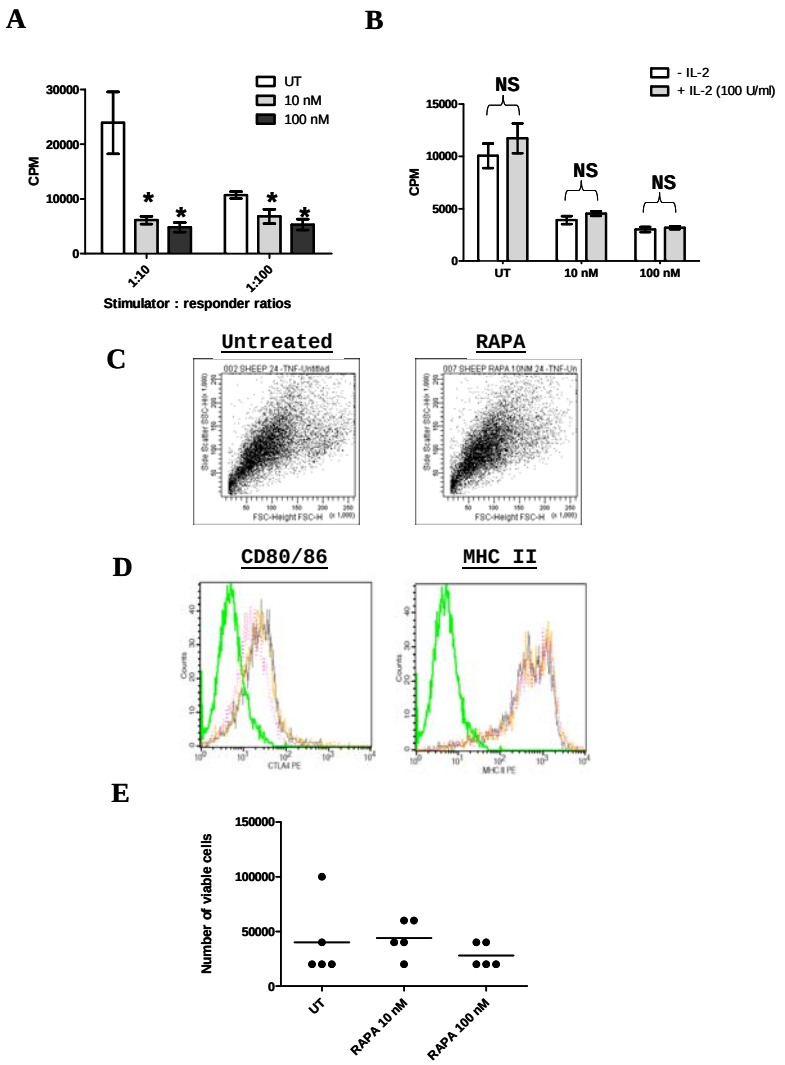

Figure 4.7. Rapamycin treatment of sheep DC inhibits their allostimulatory capacity. Following Histodenz enrichment, DC were treated with RAPA (10 and 100 nM) for 48h in presence of IL-4 and GM-CSF. (A) DC were irradiated and co-cultured with allogeneic T cells in 1:10 ratio (DC:T cells) for 5 days. At day 4 [^{3}H]-thymidine was added for 18h and the incorporated radioactivity was measured and expressed as (CPM). Error bars represent standard deviation. (B) Untreated or RAPA-treated DC were cultured with allogeneic T cells (as in (A)) in the presence or absence of 100 U/ml of recombinant human IL-2 for 5 days. Proliferation was measured as above. (C) Forward and side scatter properties of untreated or RAPA-treated DC were acquired by flowcytometric analysis. (D) Untreated and RAPA-DC were analysed for their expression of CD80/86 and MHC II molecules by flowcytometry. Isotype control is depicted by green line while untreated, RAPA (10 nM) and RAPA (100 nM) are represented by grey, orange and purple colours, respectively. (E) DC were washed 3 times in PBS and 10^5 cells were plated per well in 96-well plate. Following 5 day culture viable DC were counted using trypan blue reagent. *P < 0.05, compared to UT.

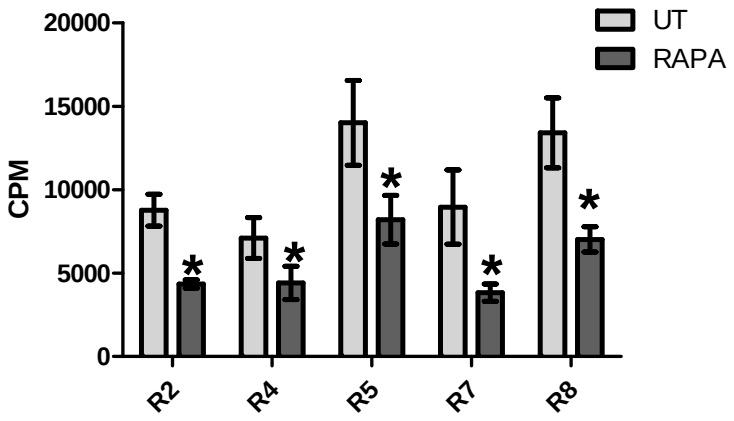

Figure 4.8. Screening for alloreactive donor and responder combinations. Following Histodenz enrichment, DC were either treated with RAPA for 48h or left untreated. DC were washed 3 times in PBS, re-suspended in complete media and plated at $1x10^4$ cells/well in 100 µl volume. DC were challenged with allogeneic PBMC ($1x10^5$ cells/well) from 5 different responder Merino sheep (R2, R4, R5, R7 and R8). Cells were cultured for 5 days. At day 4 [^{3}H]-thymidine was added for 18h and the incorporated radioactivity was measured. Data are represented as CPM (+/- SD). *$P < 0.05$, as compared to UT.

absence of necrosis (**Figure 4.9A**). Skin grafts were vascularised as demonstrated by the presence of blood vessels within the dermis (**Fugure 4.9A**). The transplanted ovine skin demonstrated a significant hyperkeratosis compared with freshly isolated ovine skin (**Figure 4.9A and 4.9B**). Injection of autologous DC and PBMC resulted in diffuse lymphocyte infiltrate in skin sections at day 7 while challenge with allogeneic PBMC caused extensive lymphocyte infiltration (**Figure 4.9A and 4.9C**). Strong infiltration of lymphocytes in the interstitial/epidermal region were characteristic of the allogeneic response (**Figure 4.9C**). Usually greater infiltration was observed at day 7 than at day 14.

4.3.6 The effect of RAPA-DC on ovine skin allograft rejection in NOD/SCID mice

RAPA-DC (10 nM) autologous to the skin were mixed with allogeneic PBMC and injected into the peritoneal cavity of the transplanted mice. Strong infiltration of lymphocytes into the interstitium and epidermis were observed in all 5 animals injected with untreated DC at day 7. Representative data of H&E and immunofluorescence staining for CD4 and CD8 are shown in **Figure 4.9C, 4.10C and 4.10E**, respectively. In comparison to the untreated group, the RAPA-DC group showed marked reduction of lymphocyte infiltration in the 3 out of 5 animals at day 7 (**Figure 4.9D, 4.10D and 4.10F**). In the majority of animals the level of lymphocyte infiltration decreased by day 14 and therefore no differences were observed between the two groups. In order to quantify the overall differences in the rejection between untreated-DC and RAPA-DC groups rejection scores were calculated based on the defined rejection criteria for H&E, anti-CD4 and anti-CD8 staining of skin sections. Individual rejection scores for each allogeneic pair is presented in **Figure 4.11**. When individual rejection scores from all 5 animals used in the study which received untreated DC, were pooled together following results were observed: H&E = (3.40 +/- 0.5), CD4 = (2.60 +/- 1.3) and CD8 = (2.2 +/- 0.8). When compared to the

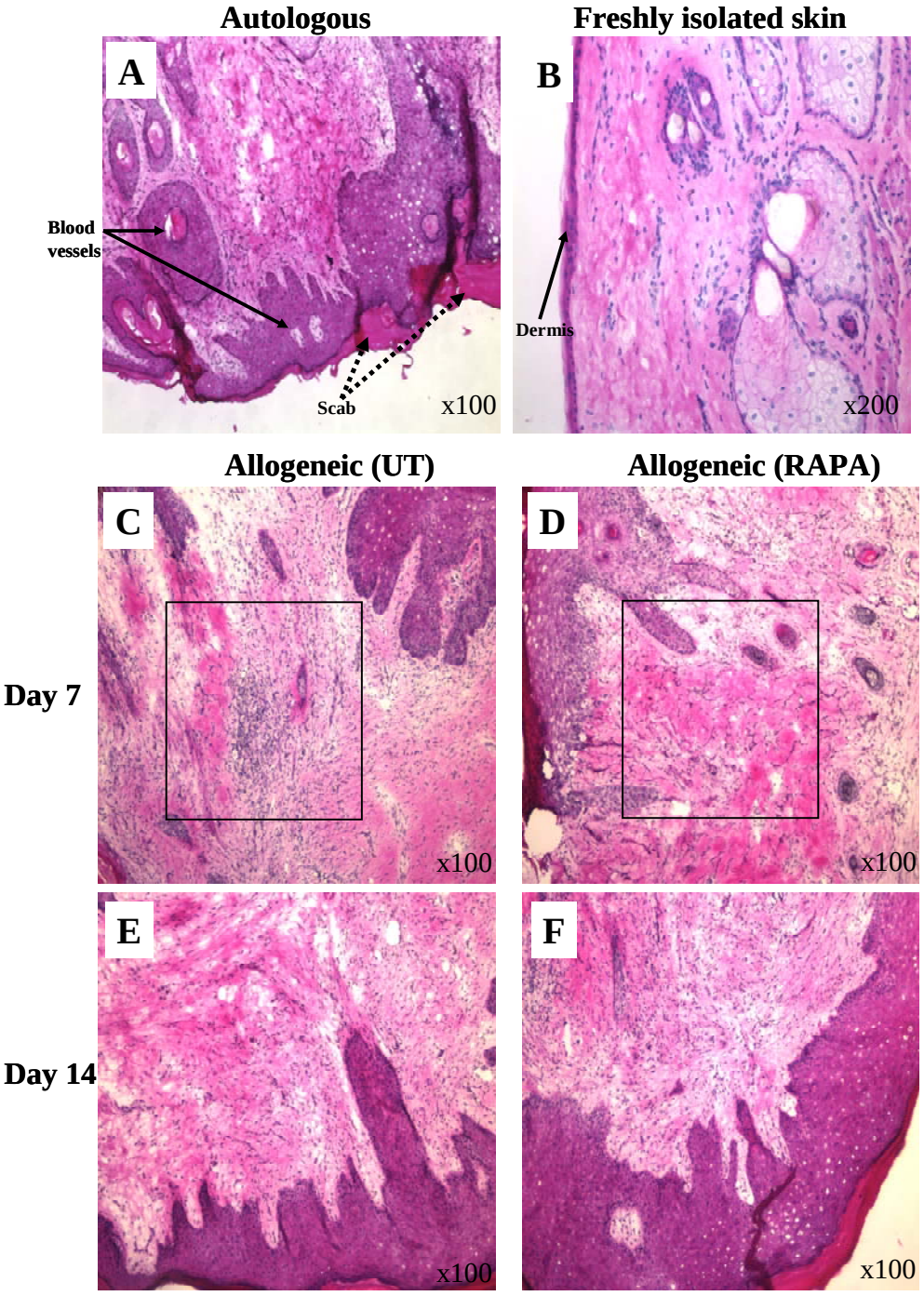

Figure 4.9. Histology of the sheep skin following the transplant. 8mm punch skin biopsy from the non-wool bearing region was transplanted on the NODscid mice. Skin was allowed to heal for 14 days, and at day 14 mice were injected with either untreated or RAPA-DC (autologous to the skin) and challenged with allogeneic CFSE-labelled PBMC. Skin was removed at either day 7 or day 14 post challenge and stained with haematoxylin and eosin red. Squares highlight similar area of interstitium/epidermis between the two treatment groups where most of the infiltration occurred. (A) Autologous transplant (B) non-transplanted allogeneic skin, (C,E) Allogeneic untreated skin at day 7 and 14 and (D,F) Allogeneic RAPA-treated skin at day 7 and 14.

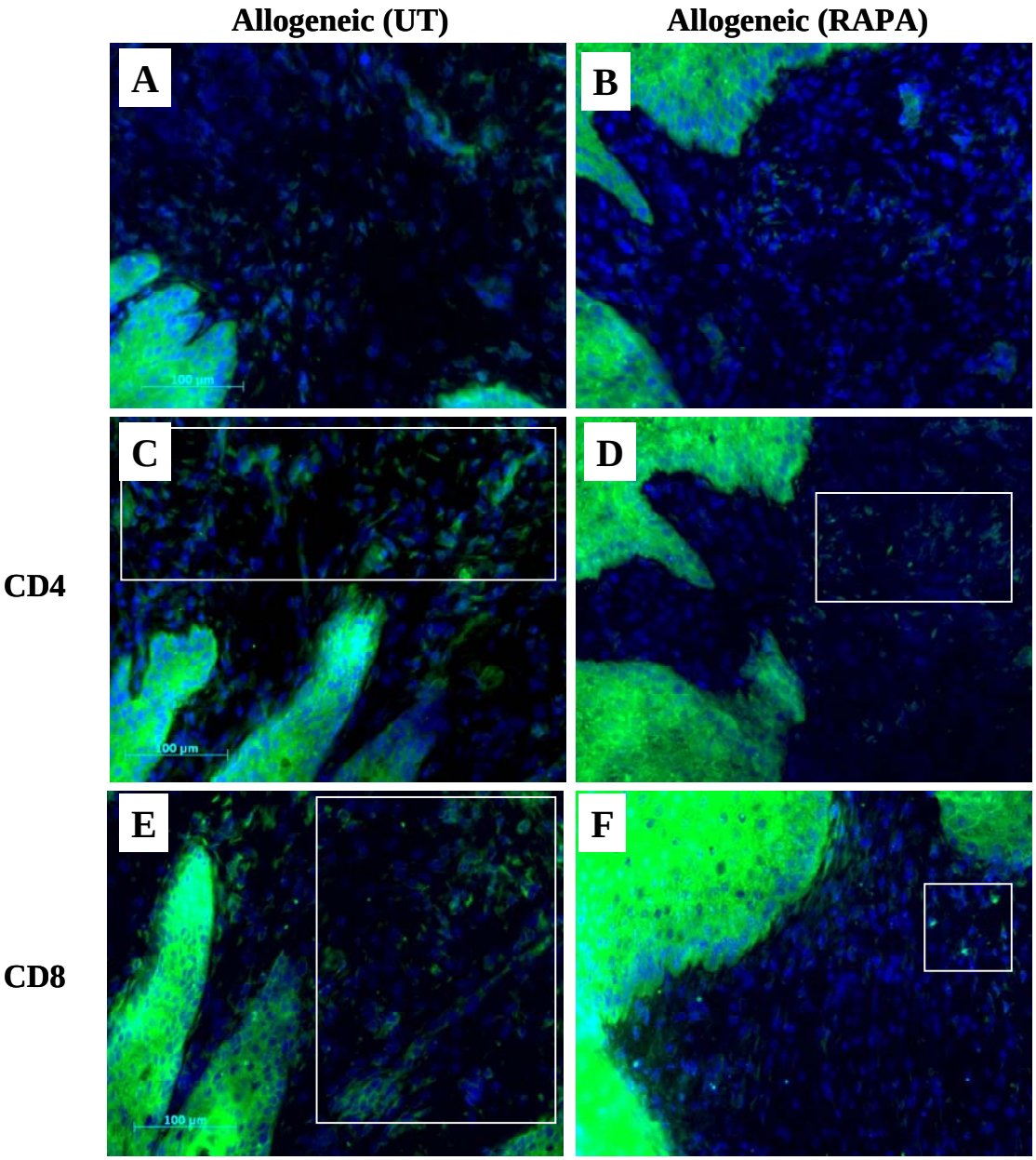

Figure 4.10. CD4 and CD8 T cell infiltration in the transplanted skin . 8mm punch skin biopsy from the non-wool bearing region was transplanted on the NODscid mice. Skin was allowed to heal for 14 days, and at day 14 mice were injected with either untreated or RAPA-DC (autologous to the skin) and challenged with allogeneic CFSE-labelled PBMC. Skin was removed at either day 7 or day 14 post challenge and stained with FITC-conjugated anti-CD4 or anti-CD8 mAb. White squares highlight area of interstitium/epidermis where majority of the CD4 or CD8 staining was observed. All the images were taken at X200 magnification. (A-E) Isotype control, CD4 and CD8 staining of allogeneic skin challenged with UT-DC, respectively, (B-F) Isotype control, CD4 and CD8 staining of allogeneic skin challenged with RAPA-DC, respectively.

untreated group, data from RAPA-DC group exhibited trend towards lower rejection scores but there were no statistically significant differences: H&E = (2.00 +/- 1.0), CD4 = (1.4 +/- 0.5) and CD8 = (1.4 +/- 0.8). Upon closer examination it was observed that only in DC from Sheep 4, RAPA treatment did not cause reduction in DC stimulatory capacity. Furthermore, DC from Sheep 4 were shown to be the weakest stimulator of allogeneic T cell proliferation *in vitro* and under these low inflammatory environment the effect of RAPA was observed (**Figure 4.111D**). However, because of the strong alloimmune responses *in vivo* RAPA effects on Sheep 4 DC (observed *in vitro*) were not evident. Thus, when the Sheep 4 results were omitted from the pooled data, a statistically significant reduction in rejection scores was observed in RAPA-treated groups versus untreated cells. The results showed the following: H&E = UT- vs. RAPA-DC (3.0 +/- 0.5 vs. 2.0 +/- 0.0), CD4 = UT- vs. RAPA-DC (4.0 +/- 1.7 vs. 1.0 +/- 0.0) and CD8 = UT- vs. RAPA-DC (3.0 +/- 1.1 vs. 1.0 +/- 0.0) (P =0.05 for all the groups). However, this RAPA effect was not observed at day 14 in the same groups.

4.3.7 The effect of RAPA-DC on cytokine response in rejecting skin

In order to evaluate the potential mechanism of the preliminary observations above, PCR analysis of the cytokine responses in the skin were performed. The level of cytokine mRNA was only detected in 1 out of five animals used in the experiment (**Figure 4.111E**). The results suggest that IL-2 expression was modestly reduced in the RAPA-DC group at day 7, but induced at day 14. On the other hand, IFN-γ was profoundly induced in RAPA-DC group at both day 7 and day 14 relative to the untreated group. Interestingly, FoxP3 expression was only detected at day 14 RAPA-DC group while IL-10 was unchanged between the treatment groups.

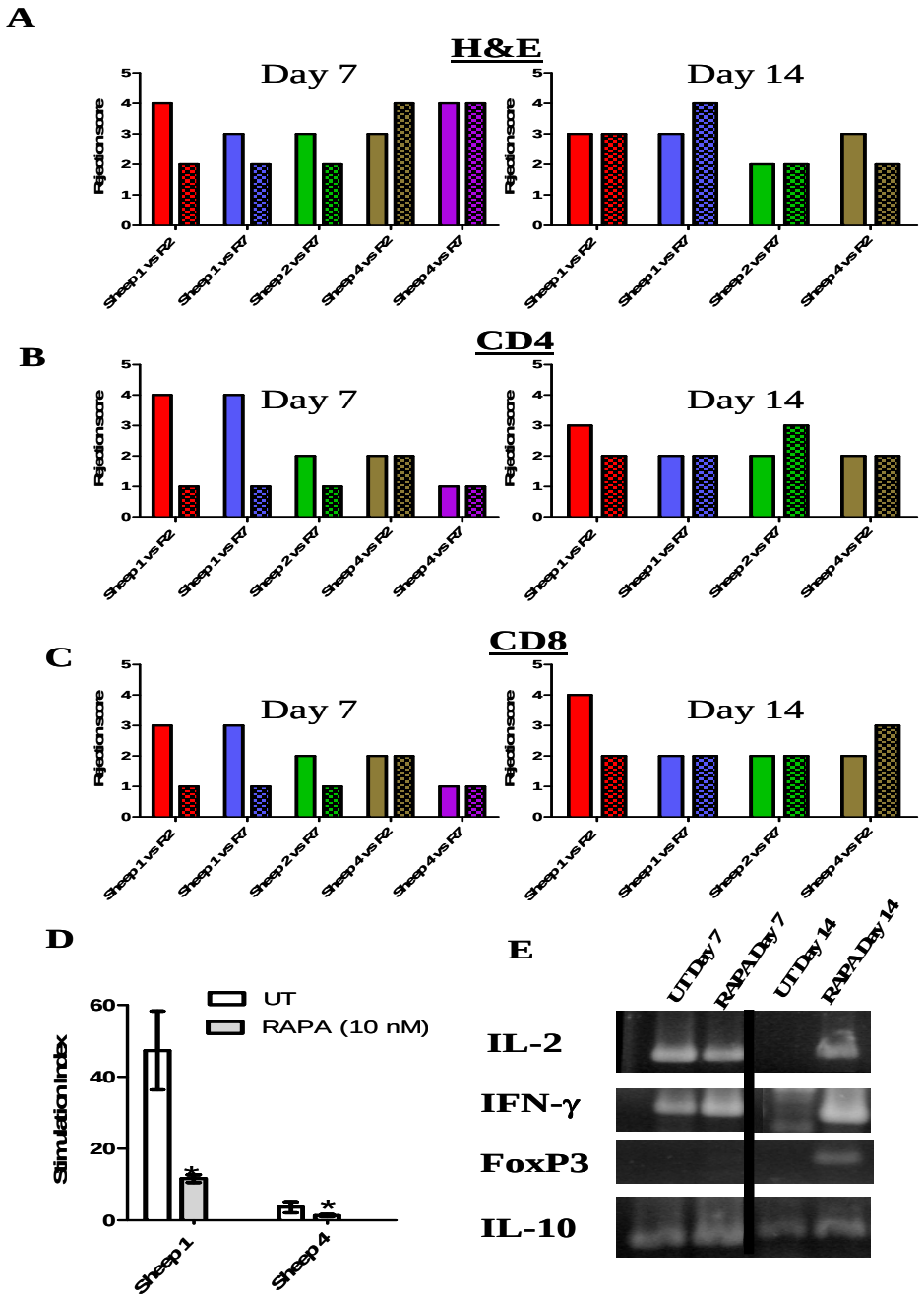

Figure 4.11. Rejection scores and cytokine profiles in the transplanted skin. 8mm punch skin biopsy from the non-wool bearing region was transplanted on the NOD/SCID mice. Skin was allowed to heal for 14 days, and at day 14 mice were injected with either untreated or RAPA-DC (autologous to the skin) and challenged with allogeneic CFSE-labeled PBMC. Skin was removed at either day 7 or day 14 post challenge and rejection scores were calculated based on staining with (A) heamotoxilin and eosin red, (B) CD4 or (C) CD8 monoclonal antibodies. Rejection scores for each allogeneic pair are shown in different colours. RAPA-treated group is distinguished by the dashed bar compared to the UT group which is represented without a pattern. (D) Comparison of stimulatory capacity between Sheep 1 and Sheep 4 DC in MLR assay. Experiment was performed as per Figure 4.6. (*P = 0.05) (E) PCR analysis for cytokine responses in the skin. 1μg of reverse transcribed template RNA from sheep skin was used as template.

4.4 Discussion

Ovine DC were successfully obtained by cannulation of the afferent pre-femoral lymphatics, treated with RAPA (10 nM) and used in skin transplantation model in order to extend the *in vitro* observations from **Chapter 3**. As previously mentioned, human DC can be readily generated from monocyte precursors but the generation of ovine DC from monocytes has been limited by poor yields (1-5% of total $CD14^+$ monocytes) (382). Here we report that between $2x10^8$ and $6x10^8$ DC were obtained after 8 weeks of cannulation with a purity of no less then 80%. DC phenotype and allostimulatory capacity were not altered during the 2 month cannulation. The animals well-being was good since they did not appear to be dehydrated due to large volumes of lymph being extracted, or unwell due to the depletion of immune cells.

DC in our study expressed stable surface phenotype which was reported by others (391). These isolated DC exhibited typical mature DC features, which included high MHC class II expression, CD80/CD86 expression and the morphological presence of dendrites (393). In addition, the physical presence of DC in afferent lymph draining from the skin was suggested itself to indicate a degree of maturation (380). These isolated DC were potent antigen presenting cells since they were able to induce strong proliferation of PBMC even at 1:100 (DC:PBMC) ratio, which was in accordance with the previous observations (28).

When these DC were treated with RAPA and used in DC-MLR they inhibited PBMC proliferation by 70%. This response was shown to be independent of T cell anergy, as the addition of human IL-2 to the culture did not reverse the responder cell proliferation, which was consistent with human findings in **Chapter 3**. Human IL-2 was shown to cross-react with sheep as its systemic administration caused pulmonary permeability in lungs (396). In addition, as discussed in **Chapter 3**, T cell anergy could also be IL-2

independent which may be playing a role in this setting (102). Furthermore, as demonstrated in human RAPA-DC, treatment of ovine DC with RAPA did not result in an inhibition of CD80/CD86 and MHC II surface expression nor did it induce apoptosis in DC. As suggested in human studies, IDO expression may be responsible for the effects observed. Therefore future studies will focus on analysing the IDO responses in sheep RAPA-DC.

Using a murine model of ovine skin rejection, the ability of ovine RAPA-DC to induce T cell hyporesponsiveness *in vivo* and inhibit rejection responses was investigated. NOD/SCID mice are characteristic for their lack of functional T and B lymphocytes which facilitates the successful engraftment of most tissues (397). The advantage of this model is that it permits the vascularisation of the graft prior to immune reconstitution, thus preventing necrosis typically observed in skin allograft rejection (398-400). Previously our laboratory has confirmed these findings by demonstrating that skin grafts were functional and persisted indefinitely without signs of rejection in the absence of the immune challenge.

In the current study RAPA-DC were administered by intraperitoneal injection since this route of administration enabled more consistent reconstitution than intravenous delivery, resulting in the detection of T and B cells in the peripheral blood, peritoneal cavity, lymph nodes and spleen (401, 402). The route of administration and the number of lymphocytes were derived from previous humanised *scid* models (236, 402). It is believed that the peritoneal cavity provides a similar function to that of a lymph node in which lymphocyte interaction and activation can occur (402-405). Therefore, injection of DC (autologous to the transplanted skin) and allogeneic PBMC allows allorecognition to occur (through direct allorecognition pathway), leading to rapid lymphocyte activation and proliferation in the intraperitoneum. Activated alloreactive T cells are then able to migrate

to the skin, leading to the lymphocyte infiltration in the skin graft predominantly at the interstitial region and epidermis. The level of infiltration in this model was transient with the maximum infiltration observed at day 7 and reduced lymphocyte staining at day 14. This rapid onset of rejection may be due to co-injection of potent antigen presenting DC and PBMC in the confined space of the peritoneum. In addition, since in this model bone marrow transplant was not performed, it is possible that T cells become exhausted and undergo AICD (364) leading to the elimination of alloreactive T cells and an absence of strong alloimmune response at day 14. Furthermore, it is also possible that the attenuation of the alloimmune responses on day 14 occurs through the induction of responder T cell anergy via chronic stimulation by murine antigens (406, 407).

Despite the limitations, this model can be efficiently used to provide "proof of concept" experiments preceding the experiments in large animal models. Indeed, here we observed a potential trend that RAPA-DC were able to reduce T cell hyporesponsiveness, at day 7 by 25-50% (depending on the parameter tested; H&E vs. anti-CD4 vs. anti-CD8). This result was only observed in 3 out of 5 animals and we proposed that lack of response in the remaining two animals (injected with Sheep 4 DC) was due to the incomplete modification of Sheep 4 DC with RAPA. Moreover, it has been shown that some individuals are resistant to RAPA treatment because of mutation in mTOR pathway as well as throught the induction in p53 expression which can also confer lack of responsivness to RAPA treamtnet (408). Therefore it maybe possible that Sheep 4 displayed partial resistance to RAPA treatment, but this needs to be substantiated in further studies. As a result of weak alloimmune response between Sheep 4 DC and responder PBMC the inhibition of PBMC proliferation by RAPA-DC was still observed *in vitro* (**Figure 4.111D**). However, due to strong alloimmune responses *in vivo*, this effect was lost.

RAPA-DC (from sheep 1 and 2) were shown to reduce both $CD4^+$ and $CD8^+$ T cell infiltration within the graft, suggesting that RAPA-DC can act in non-selective manner. In addition, preliminary finding suggested that RAPA-DC reduced T cell activation as evidenced by the reduction in IL-2 mRNA at day 7 only. IL-2 mRNA expression at day 14 in RAPA-DC group may be explained by the persistence of T cells due to the low level of activation and potentially lower AICD, relative to the untreated group. Furthermore, FoxP3 expression was detected in day 14 skin grafts in the RAPA-DC group. This was interesting considering that this model is not a long-term model in which tolerance can be examined since the *de novo* generation of donor lymphocytes does not occur (364). Therefore, it maybe speculated that RAPA-DC may convert naïve T cells into FoxP3 T_{REG} *in vivo*. This finding corroborated with the expression of IL-2 and IFN-γ of which both were shown to be implicated in generation of T_{REG} cells (409, 410). In contrast, in human studies we did not observe FoxP3 induction in allogeneic T cells by RAPA-mDC. It is important to note that there are no studies on ovine FoxP3 T_{REG} available in the literature, thus they may have different developmental requirements to human.

In conclusion, it was demonstrated that like human DC, ovine DC developed strong tolerogenic properties *in vitro*, as evidenced by inducing T cell hyporesponsiveness. The data reported in this chapter has suggested that RAPA-DC were effective in inhibiting alloimmune responses in the ovine skin grafts using the NOD/SCID chimeric model however, larger numbers of animals are required to confirm the robustness of this study. Pending follow-up confirmation of the reported findings the ability of RAPA-DC to prolong solid organ transplant in the sheep model of kidney allotransplantation (reviewed in **section 1.10**) would be warranted in association with the ability of these cells to induce experimental tolerance in this model. Furthermore, in the present study we did not investigate allospecificity of the RAPA-DC function *in vivo*. As this represents the basis for

the successful tolerogenic cell therapy (**reviewed in 1.9**), experiments will have to be designed to address this question. This could be assessed by transplanting the skin from two unrelated sheep onto the single NOD/SCID mice, prior to challenging the mice with allogeneic responder cells.

CHAPTER 5
CONSTRUCTION OF ADENOVIRAL VECTORS CONTAINING THE HLA-G1 AND HLA-G5 GENE INSERTS

Presentations
Presented at The Queen Elizabeth Hospital Research Day 2006 in Adelaide

5.1 Introduction

The aim of this chapter was to generate adenoviral construct carrying HLA-G1 and HLA-G5 cDNA for delivery of these genes into DC. As discussed in **section 1.8**, HLA-G has potent immunomodulatory properties such as inhibition of T cell proliferation and DC maturation. In addition, high serum levels of HLA-G were shown to be associated with better allograft survival.

Since DC do not normally express surface HLA-G, adenoviral constructs are crucial for inducing the expression of HLA-G in DC in order to study the ability of HLA-G to confer tolerogenic properties to DC. Adenoviral mediated gene delivery is currently the most efficient way of delivering genes into DC, when compared to all other methods of gene delivery (**reviewed in 1.9.2**). Currently the combination of Adenoviral vectors and a cationic liposome (Lipofectamine) is used to transfect DC with high level of efficiency, without notably affecting DC maturation (268, 411). This approach will be employed in the present study as it would enable high transfection efficiency of DC using a lower number of viral particles, resulting in lower antigenic load of DC. Lipofectamine combination with Adenovirus has been previously used in our laboratory and it consistently yielded high transfection efficiency (80-90%) of DC (236, 283). In addition to data from our group, several other investigators have used Adenoviral vectors to successfully deliver immunosuppressive genes such as IL-10, CTLA4, TGFβ and FasL to DC (412). These cells exhibited potent tolerogenic properties *in vitro* as evidenced by their ability to inhibit T cell proliferation and induce T cell apoptosis. Importantly, immunogenic responses toward Adenoviral vectors did not present a significant problem both *in vitro* and *in vivo* as the tolerogenic potential of these genetically modified DC was still observed. This may have been attributed to the “stealth” effects provided by the transduced immunosuppressive gene (413, 414).

In the current study, immunosuppressive genes HLA-G1 and HLA-G5 will be cloned in the Adenoviral vector pAdEasy-1. HLA-G1 is a membrane bound molecule while HLA-G5 contains a premature stop codon in intron 4, which is retained in this particular HLA-G isoform following transcription (**1.7.4.1** and **1.7.4.2**). However, despite being secreted HLA-G5 still retains an identical structure to HLA-G1 and it is recognised by the specific HLA-G mAb clone 87G.

Delivery of HLA-G1 and HLA-G5 cDNA in the Adenoviral genome (pAdEasy-1) relies on homologous recombination between pAdTrack-CMV "shuttle vector", containing HLA-G cDNA, with pAdEasy-1 (320). The homologous recombination approach (**Figure 5.1**) was an advancement in Adenoviral technology as initial protocols relied on direct ligation of DNA inserts to the endonuclease digested Adenoviral genome (415, 416). Due to the large size of Adenovirus genome, the direct ligation of DNA inserts was not efficient. In addition, scarcities of unique restriction sites in Adenoviral genome were making this approach of generating recombinant Adenoviral particles technically challenging. In the current study homologous recombination between the two vectors was performed in BJ5183 *E. coli* which expressed the functional *rec*A gene, enabling generation of stable recombinants (320). Initially homologous recombination was performed within mammalian packaging cells which formed lytic plaques as a result of cytopathic effect of adenoviral particles formed that were extensively screened for the presence of recombinant viral particles. The rate of homologous recombination was insufficient in mammalian cells and therefore required multiple rounds of plaque purification (417). Production of adenoviral particles from homologous recombinants was performed in a unique packaging cell line called HEK 293 which provided complementary

A

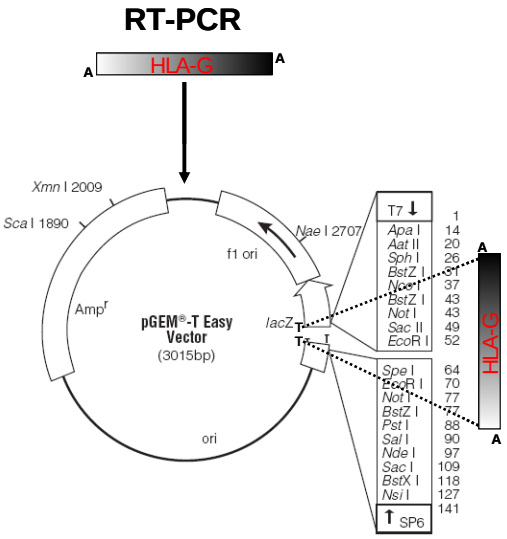
RT-PCR
HLA-G
A
A
Xmn I 2009
Sca I 1890
Nae I 2707
f1 ori
Amp^r
pGEM®-T Easy Vector
(3015bp)
lacZ
ori
T7
Apa I 14
Aat II 20
Sph I 26
BstZ I 31
Nco I 37
BstZ I 43
Not I 43
Sac II 49
EcoR I 52
Spe I 64
EcoR I 70
Not I 77
BstZ I 77
Pst I 88
Sal I 90
Nde I 97
Sac I 109
BstX I 118
Nsi I 127
141
SP6
HLA-G

B

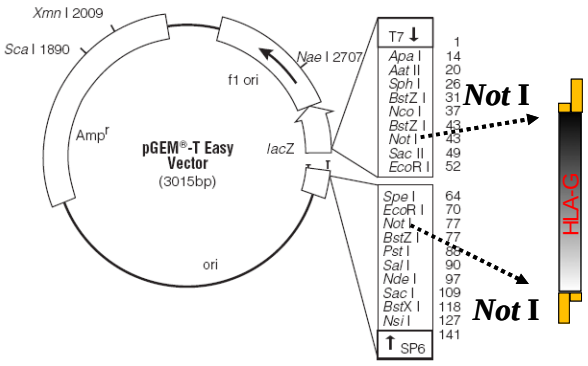
Xmn I 2009
Sca I 1890
Nae I 2707
f1 ori
Amp^r
pGEM®-T Easy Vector
(3015bp)
lacZ
ori
T7
Apa I 14
Aat II 20
Sph I 26
BstZ I 31
Nco I 37
BstZ I 43
Not I 43
Sac II 49
EcoR I 52
Spe I 64
EcoR I 70
Not I 77
BstZ I 77
Pst I 88
Sal I 90
Nde I 97
Sac I 109
BstX I 118
Nsi I 127
141
SP6
Not I
Not I
HLA-G

C

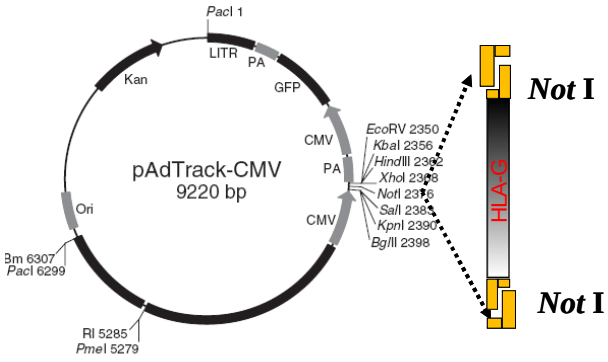
PacI 1
LITR
PA
GFP
CMV
PA
CMV
Kan
Ori
pAdTrack-CMV
9220 bp
EcoRV 2350
KbaI 2356
HindIII 2362
XhoI 2368
NotI 2378
SalI 2385
KpnI 2390
BglII 2398
Bm 6307
PacI 6299
RI 5285
PmeI 5279
Not I
Not I
HLA-G

D

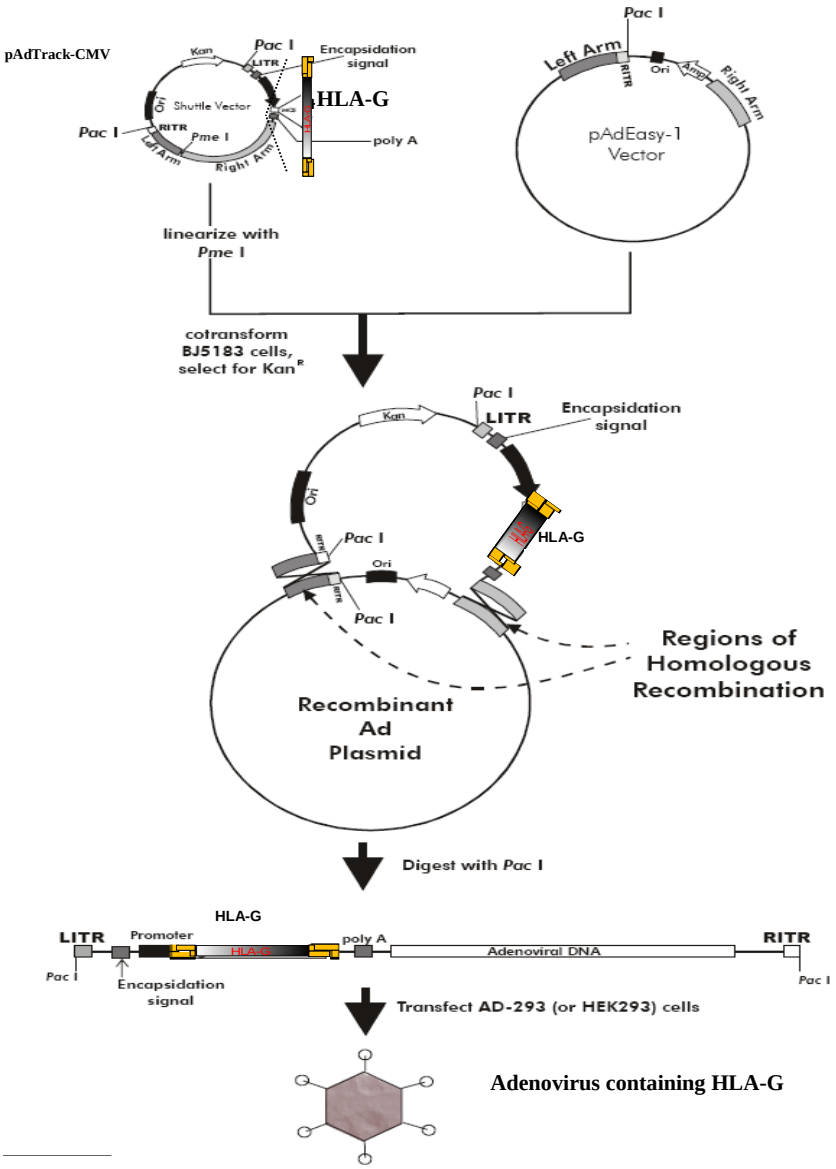

Figure 5.1 Outline of HLA-G1 and HLA-G5 cloning. (A) HLA-G1 and HLA-G were PCR amplified from Jeg-3 cells using specific primers. The specific PCR products, which contained 3' adenine overhang, were cloned into pGEM-T Easy vector containing 5' thymine overhangs (B) HLA-G was excised from pGEM-T Easy vector with *Not* I restriction enzyme and (C) cloned into *Not* I digested pAdTrack-CMV (D) HLA-G expressing pAdTrack-CMV vector was linearised with *Pme* I and homologously recombined with pAdEasy-1 in BJ5183 *E.coli*. In our system BJ5183 were designed to endogenously express pAdEasy-1 vector (pAdEasier-1) and thus no co-transformations were performed. Homologous recombination could either occur via long inverted terminal repeats (LITR) (depicted above) or Ori site. Correct recombinant was determined by *Pac* I digestion and depending on the recombination site two bands could be observed. First band was 30 kb and second band was either 3 kb or 4.5 kb indicating that recombination took place either at LITR or Ori site, respectively. Correct recombinant containing HLA-G was then used to transfect HEK 293 cells and produce Adenoviral particles.

genes, *in trans*, necessary for the replication of the replication-deficient vector pAdEasy-1 which lacked E1 and E3 genes which are required for the initiation of viral replication and invasion of host immunity, respectively (417). The E1 gene obtained from sheared DNA from the adenovirus virus type 5 (Ad5) genome was introduced into human embryonic kidney cells (HEK) by Graham and Smiley 1977, by the calcium phosphate transfection approach (319). Since the E1 gene from Ad5 became integrated in chromosome 19 (19q13.2) in HEK 293 cells it thus conferred the ability upon these cells to support the replication and packaging Adenoviral particles (418).

In this chapter we report the cloning strategy for HLA-G1 and HLA-G5 into adenoviral vectors. Briefly, HLA-G1 and HLA-G5 were isolated by PCR from Jeg-3 cells and cloned into the transition vector pGEM-T-Easy. From this vector HLA-G1 and HLA-G5 were excised using the *Not* I restriction enzyme and cloned in pAdTrack-CMV "shuttle" vector. pAdTrack-CMV containing HLA-G was homologously recombined with pAdEasy-1 vector in BJ5183 bacteria. Adenoviral particles were then produced in HEK 293 and successfully used to induce high HLA-G expression in DC.

5.2 Materials and Methods

5.2.1 Bioinformatics analysis of HLA-G1 and HLA-G5

In order to determine if the crucial restriction endonucleases used during generation of recombinant Adenoviral particles (i.e. PmeI) recognised any sequences in the open reading frame HLA-G1 and HLA-G5, NEBcutter V2.0 online software (New England Biolabs) was used. Furthermore, NEBcutter V2.0 was also used to simulate digestion of plasmids containing HLA-G cDNA prior to actual digestion. The software was also used to determine the digestion pattern of pAdEasy-1 during the generation of pAdEasier-1 cells.

Simulated PCR reactions were performed using potential candidate primers sequences on Amplify software V3.1 (Bill Engels, 2005, University of Wisconsin). The software alerted of any primer dimers, weak binding to target sequence and multiple binding sites on the sequence.

5.2.2 Primer design and PCR amplification of HLA-G1 and HLA-G5

Total RNA was extracted from Jeg-3 cells using TRIZOL® reagent and reverse transcribed on 1 μg of total RNA (**2.1.2.1** and **2.1.2.2**). PCR (**2.1.2.3**) was performed to amplify HLA-G1 and HLA-G5 using primers summarised in **Appendix 2.1**. Forward primer HLA-G1SalIF is common for both HLA-G1 and HLA-G5 while HLA-G1KpnIR and HLA-G5KpnIInt4R are HLA-G1 and HLA-G5 specific, respectively (**Figure 5.6A**). The HLA-G1 primer was designed to bind to the end of the HLA-G1 ORF flanking stop codon, while the HLA-G5 primer was designed to bind intron sequence of HLA-G transcript flanking premature stop codon (**Figure 5.6A**). The primers used to amplify HLA-G1 and HLA-G5 were designed using a published sequence (GenBank Accession: NM002127) (175, 184). The forward primer incorporated *Sal* I at 5' end of the primer while the reverse primers incorporated *Kpn* I restriction enzyme site at 5' end (underlined in **Appendix 2.1**). The restriction enzyme sites were incorporated in order to examine the correct orientation of the inserts in pAdTrack-CMV.

Master mix composition and cycling conditions for HLA-G1 and HLA-G5 are summarised in **Appendix 2.1**. Both HLA-G1 and HLA-G5 were amplified for 50 cycles, run on the Agarose gel (**2.1.2.4**) and appropriate size bands were extracted from the gels using Ultraclean™ DNA extraction kit (**2.1.2.7**).

5.3.3 Screening of bacterial colonies for HLA-G expression using PCR technique

For screening of transformed bacteria or for confirmation of HLA-G insert in the vector, 2.5 μl of 18h bacterial culture or 25 ng of plasmid were added as a template instead of cDNA. PCR were run for 30 cycles using the primer sets described above.

5.3.4 Cloning of HLA-G1 and HLA-G5

Genetic maps of the vectors are summarised in **Figure 5.1**.

5.3.4.1 pGEM-T-Easy

PCR products (containing 3'Adenine overhang) were cloned in the pGEM-T-Easy vector (containing 5' Thymine overhang) carrying the Ampicillin resistance gene and transformed into TG1α E. coli. The transformed bacteria were plated on the LB plate supplemented with Ampicillin (25mg/ml) and following 16 h incubation at 37°C, 10 visible colonies were selected and grown further in 1.5ml LB-Ampicillin for 16 h at 37°C. An aliquot (2.5μl) of bacterial culture was subjected to PCR analysis. Colonies containing HLA-G insert, as determined by PCR, were subjected to a mini-prep plasmid extraction procedure (**2.1.2.11**). HLA-G1 or HLA-G5 were then excised from the pGEM-T-Easy vector with the *Not* I restriction enzyme (**2.1.2.5**).

5.3.4.2 pAdTrack-CMV

HLA-G1 and HLA-G5 inserts excised from the pGEM-T-Easy vector were ligated (**2.1.2.8**) into the *Not* I digested pAdTrack-CMV "shuttle" vector, containing the Kanamycin resistance gene and independent GFP transcript. The ligation mix was transformed into TG1α E. coli and the transformed bacteria were plated on the LB plate supplemented with Kanamycin (30mg/ml) and following 16 h incubation at 37°C, 10 visible colonies were selected and grown further in 1.5 ml LB-Kanamycin for 16 h at 37°C.

An aliquot (2.5µl) of bacterial culture was subjected to PCR analysis. Colonies containing HLA-G insert, as determined by PCR, were subjected to a mini-prep plasmid extraction procedure (**2.1.2.11**). At this stage transcripts were sequenced using the dideoxy sequencing method (**2.1.2.13**). The correct orientation of the inserts was determined by digesting the vectors with *Kpn* I restriction enzyme (**2.1.2.5**).

5.3.4.3 Sequencing of inserts from pAdTrack-CMV vector

Sequencing was performed as outlined in section **2.1.2.13** and the primers used for sequencing are summarised in the **Appendix 2.1**. Plasmids from at least two positive colonies were sent for DNA sequencing. HLA-G1 was sequenced using HLA-G1SalIF, HLA-G1KpnIR, HLA-G_int_F, HLA-G_int_R and Gex2. On the other hand, HLA-G5 was sequenced with all the same primers as HLA-G1 apart from HLA-G1KpnIR which was replaced with HLA-G5_Int4R. The position of each primer along the sequences of HLA-G1 and HLA-G5 are depicted in **Figure 5.6A**. Sequencing data was analysed using Finch TV version 1.4.0 (Geospiza Inc) and sequence data from each primer was collated together to form one whole DNA sequence. This was then aligned using ClustalW online software (EMBL-EBI) against the consensus sequence of HLA-G1 or HLA-G5. Obtained DNA sequences were then translated into protein sequence using the online software named Translate Tool (ExPASy) in order to determine if any base changes noted in the DNA sequence resulted in the premature stop codon or significant changes in amino acid sequence. Protein sequences were then aligned against the consensus protein sequences of HLA-G1 or HLA-G5 using ClustalW software. The best matched candidate colony which did not contain any premature stop codons or significant changes in the amino acid sequence, especially in the critical residues of active domains, was selected for homologous recombination.

5.3.4.4 Homologous recombination

The pAdTrack-CMV vector containing correct HLA-G1 or HLA-G5 sequence and the correct orientation of the inserts was linearised with the *Pme* I restriction enzyme in order to expose inverted terminal repeats of the vector. The linearised plasmid was electroporated (**2.1.3.3**) in pAdEasier-1 cells (**2.1.3.2**) to facilitate homologous recombination. Electroporated bacteria were then grown on kanamycin agar plates, subjected to midi-prep plasmid extraction and then digested using *Pac* I restriction endonuclease. Homologous recombination was confirmed by examining the *Pac* I digestion pattern of the recombinant plasmids (**2.1.3.4**). Correctly recombined plasmids were then subjected to the PCR analysis (**2.1.2.3**) to confirm the presence of HLA-G1 or HLA-G5 cDNA in the Adenoviral vector. PCR positive recombinants were then transfected into DH10β *E. coli* in order to grow a large quantity of plasmid.

5.3.4.5 Production of Adenoviral particles

Correctly recombined plasmids were linearised with the *Pme* I restriction enzyme and transfected into HEK 293 packaging cell line using LipofectAMINE™ to produce Adenoviral particles (2.3.3.6, 2.3.3.8). Adenoviral particles were obtained by freeze-thaw lysis (2.3.3.7) of the transfected HEK 293 cells and purified by Mustang® Q (Pall, USA) anion-exchange membrane using the manufacturer's instructions with minor modifications (2.3.3.9). The purified virus was eluted with 3 ml of 0.6M NaCl in HEPES pH 7.4.

5.3.5 Quantification of Adenoviral Titres

HEK 293 cells ($2x10^4$ cells per well) were plated in 96 well flat-bottom plates and infected with 10-fold dilutions of purified virus as described in section **2.1.3.10** in detail. Calculation of adenoviral titres was performed as previously reported (419) (number of

wells with fluorescent cells at the highest dilution were divided by the total volume in all wells and multiplied by the dilution factor) and values expressed as plaque forming units (pfu).

5.3.6 Transfection of dendritic cells

Human iDC were transfected as previously published.(283) In brief, a hundred million of Adenoviral particles (AdV) (obtained from Dr Paul Reynolds at the Royal Adelaide Hospital, South Australia) genetically engineered to carry HLA-G1 (AdV-G1), HLA-G5 (AdV-G5) and Vector Blank (AdV-VB) were combined with 2 μg of LipofectAMINE^{TM} in 100 μl RPMI supplemented with 2 mM glutamine. After 20 min of incubation at room temperature, Adenoviral/LipofectAMINE^{TM} complexes were added to one well of a 24-well flat-bottom plate. Human iDC (1 x 10^6 cells in 100 μl RPMI supplemented with 2 mM glutamine) were added to the Adenoviral/LipofectAMINE^{TM} complex and incubated for 2 h at room temperature (with shaking at 140 rpm) to allow viral adsorption. Complete media supplemented with IL-4 (1x10^7 U/mg) and GM-CSF (1.2x10^7 U/mg) was added to DC/AdV mix and incubated for a further 48 h under 5% CO_2 at 37^{o}C to establish gene transduction.

5.3.7 RNA extraction from DC

RNA was extracted using Illustra RNAspin Mini Isolation Kit (GE Healthcare, UK). Briefly, transfected DC (1x10^6) were lysed in an RA1 buffer/2-mercaptoethanol mixture. Cell lysate was equilibrated with 70% ethanol and centrifuged through the RNAspin column at 13,000g for 1 min. Following the attachment of RNA to the column, DNAse I was loaded onto the RNAspin column and incubated for 15 min at room temperature to digest genomic DNA. DNAse I was subsequently inactivated with RA2

buffer and RNA was washed two times with RA3 buffer. RNA was eluted in 40 μl of sterile water and quantified by absorbance at 260 nm using NanoDrop™ 1000. Reverse transcription was performed on 1 μg of total RNA as per section **2.1.2.2**.

5.3.8 Polymerase Chain Reaction (PCR)

Twenty five nanograms of cDNA from DC transfectants was used for each PCR reaction. PCR reactions were performed using *Tth* DNA Polymerase enzyme (**2.1.2.3**). HLA-G1SalIF and HLA-G_IntR_R primers were used to amplify HLA-G1/-G5 sequence. Primer sequences, master mix conditions and cycling conditions are summarised in **Appendix 2.1**. GAPDH was used as a housekeeping gene and the PCR conditions are summarised in **Appendix 2.1**. HLA-G1/G5 and GAPDH were amplified for 30 and 23 cycles, respectively. PCR reactions were performed in a Perkin Elmer DNA Thermal Cycler.

5.3.9 Flowcytometry for detecting HLA-G1 expression

Two days post DC transfection, DC were harvested by gentle pipetting, washed twice with centrifugation at 800g for 10 min in FACSwash. Non-specific Fc binding was blocked by incubating cells in 10% Heat Inactivated Rabbit Serum for 20 min at 4°C. Primary mAb anti-HLA-G (87G) or isotype matched control mAb, ID4.5 (IgG2a) were added to the cells and incubated for 30 min at 4°C. Following the incubation with primary mAb, cells were washed again as above. Secondary anti-mouse mAb (conjugated to PE) was added to the cells for 30 min 4°C. Cells were then fixed using FACS Lysing Solution, acquired by FACSCanto and analysed using FACSDiva software. The gate was drawn based on forward and side scatter properties of DC in order to exclude T cells from analysis.

5.3.10 HLA-G5 ELISA

ELISA was performed as per Fournel *et al*. with minor modifications (420). Briefly, MaxiSorb microtiter plates (Nunc, USA) were coated with 87G (1µg/ml) in 0.1 M carbonate buffer, pH 9.5 for 16 h. Plates were washed 3 times in Tris-buffered saline (0.05% Tween 20). Non specific binding was blocked with 250 µl of 4% FCS for 2h at 37°C. Blocking buffer was flicked off and 100 µl of culture supernatant was added to each well and incubated for 2h at 37°C. Plates were washed 3 times before 100 µl of Biotinylated W6/32 (5µg/ml) was added for 1h at 37°C. After another wash 1/1000 dilution of alkaline phosphatase conjugated streptavidin (Roche, USA) was added for 30 min at 37°C. Alkaline phosphatase substrate (Sigma, USA) was added (50 µl per well from 1 mg/ml stock) to the washed plate for 15 minutes and reaction was stopped by adding 100 µl of 2M H_2SO_4. Tests were performed in duplicated and absorbance was recorded at 405 nm.

5.4 Results

5.4.1 PCR amplification of HLA-G1 and HLA-G5 from Jeg-3 cell line

In order to clone HLA-G1 and HLA-G5 into the appropriate vectors and generate recombinant Adenovirus, it was necessary to introduce *Sal* I and *Kpn* I restriction sites into the HLA-G cDNA sequence and to obtain large quantities of HLA-G cDNA. Forward primer containing the *Sal* I restriction site and reverse primer containing *Kpn* I were used for PCR amplification of cDNA from Jeg-3 cell lines. Following 50 cycles of PCR amplification the PCR products were run on 2% Agarose gel. The correct size of the HLA-G1 (1032bp) and HLA-G5 (974bp) cDNA were determined by comparing the migration pattern of the PCR products to the DNA fragments of known concentrations from *EcoR* I digested SPP1 vector (**Figure 5.2**). The above primers were designed to

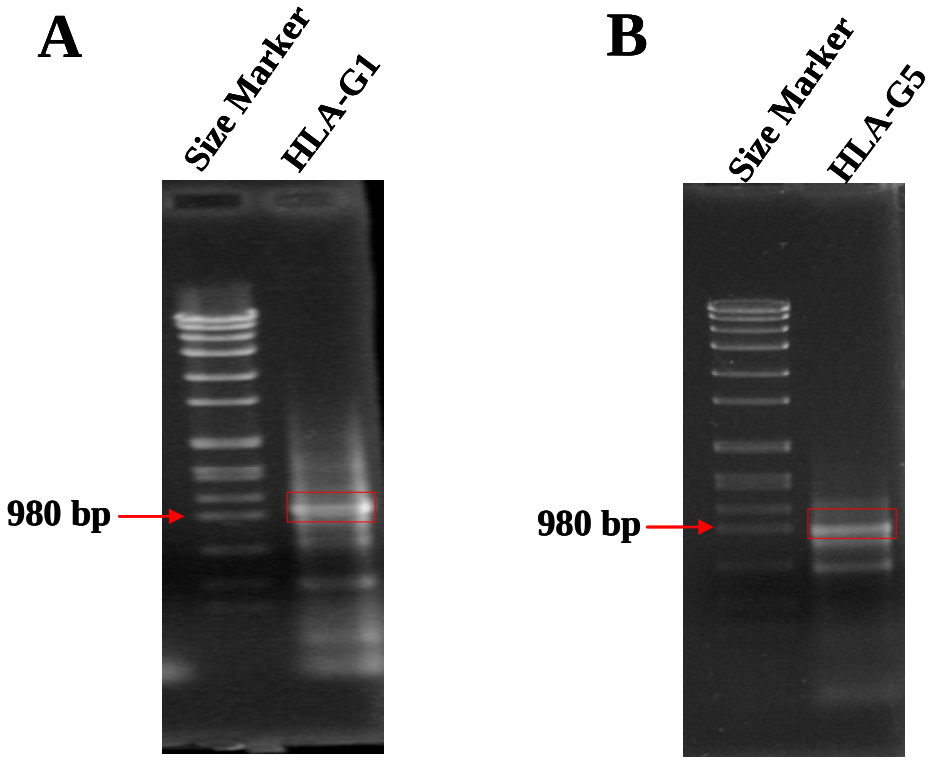

Figure 5.2. PCR amplification of HLA-G1 and HLA-G5 from Jeg-3 cell line. RNA was extracted from Jeg-3 cells, reverse transcribed and subjected to PCR amplification. For HLA-G1 the following primer pair was used HLA-G1_SalIF (forward) and HLA-G1_KpnIR (reverse). For HLA-G5 the following pair was used: HLA-G1_SalIF (forward) and HLA-G5_intR (reverse). cDNA was amplified for 50 cycles. Expected sizes for HLA-G1 and HLA-G5 are 1032 bp and 974 bp, respectively. Specific HLA-G1 and HLA-G5 products are highlighted with red square. DNA size marker is SPP1 plasmid digested with *EcoR* I.

amplify a complete open reading frame of the HLA-G gene. This resulted in amplification of smaller HLA-G isoforms depicted on the gel (**Figure 5.2**). DNA bands corresponding to the specific HLA-G1 and HLA-G5 were then excised and DNA was purified from the gel. Single DNA band matching HLA-G1 or HLA-G5 was observed on the subsequent Agarose gel following the DNA purification, thus confirming the absence of contaminating DNA isoforms (data not shown).

5.4.2 Cloning of HLA-G1 and HLA-G5 in pGEM-T Easy Vector

Purified HLA-G1 and HLA-G5 cDNA were ligated in pGEM-T Easy, in a one (50 ng) to four (200 ng) ratio of plasmid to insert, and transformed in TG1α bacteria. Bacteria which grew on the Ampicillin LB-Agar plates, due to successfully taking up the pGEM-T Easy vector conferring the resistance to Ampicillin, were screened by PCR using HLA-G cloning primers. Out of 10 colonies screened, 5 were positive for HLA-G1 and 4 were positive for HLA-G5 cDNA (**Figure 5.3A**). When bacterial cultures transformed with only the pGEM-T Easy vector were subjected to PCR, HLA-G1 and HLA-G5 cDNA were not amplified indicating that only colonies containing HLA-G were detected. Plasmids from PCR positive bacteria were extracted using mini-prep procedure, subjected to *Not* I digestion and run on 1% Agarose gel. The results indicated that HLA-G1 and HLA-G5 were successfully ligated in the pGEM-T Easy (**Figure 5.3B**). Both HLA-G1 and HLA-G5 were of the correct size as determined from DNA size marker. These *Not* I digested HLA-G fragments were purified from the gel and ligated in pAdTrack-CMV which was also subjected to *Not* I digestion.

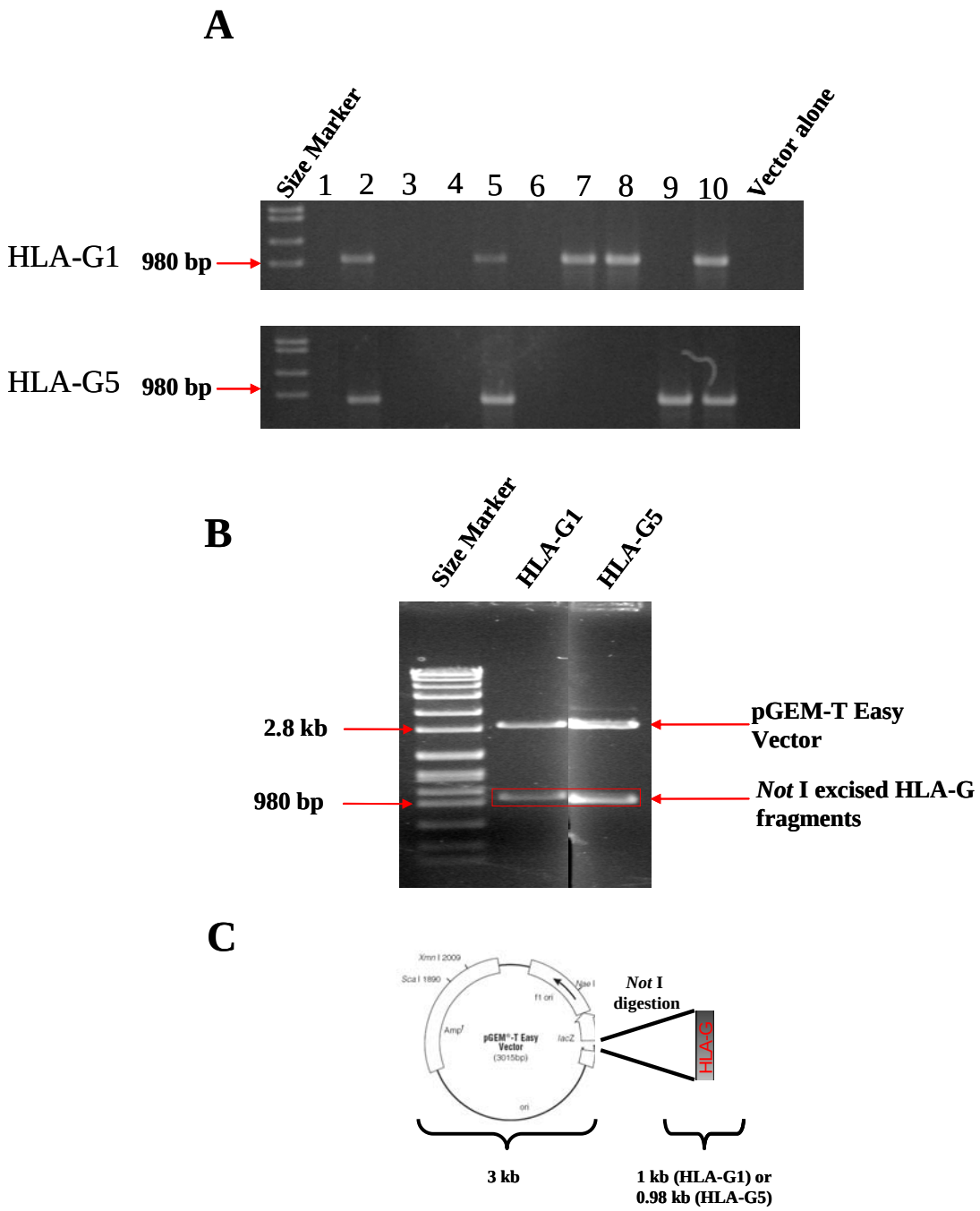

Figure 5.3. Cloning of HLA-G1 and HLA-G5 in pGEM-T Easy Vector. HLA-G1 and HLA-G5 PCR fragments were cloned into pGEM-T Easy Vector employing the 3' adenine overhangs from the PCR product and 5' thymine overhangs present in the vector. Ampicillin resistant (conferred by the pGEM-T Easy vector) colonies were selected and (A) screened for the presence of insert using HLA-G1 and HLA-G5 specific primer pairs and (B) plasmid was extracted from PCR positive colonies and subjected to *Not* I restriction in order to excise HLA-G fragments containing *Not* I sticky ends. Red squares highlight the excised HLA-G1 and HLA-G5 fragments. Size marker used was SPP1 plasmid digested with *EcoR* I (C) Pictorial representation of *Not* I digestion of pGEM-T-Easy containing HLA-G.

5.4.3 HLA-G1 and HLA-G5 cloning in pAdTrack-CMV

Following ligation of excised HLA-G1 and HLA-G5 fragments in pAdTrack-CMV and transformation of TG1α, PCR screening was performed using the primers above on the colonies growing on the Kanamycin plates. Although 30 colonies grew on Kanamycin plates only 1 out of 10 colonies screened was PCR positive for each HLA-G1 and HLA-G5. In **Figure 5.4,** PCR analysis was depicted on the positive bacterial colony after plasmid was extracted. Bacteria transformed with the pAdTrack-CMV vector alone did not give a PCR product indicating true HLA-G1 or HLA-G5 expression in the positive colony. Since the template in this experiment was a plasmid and not bacterial culture, the plasmid DNA fragments of 2.8kb and 8.5kb can also be observed in **Figure 5.4**. When these were compared between HLA-G positive and vector alone colonies, it was confirmed that the HLA-G positive colony retarded sooner (due to its size) on the 1% Agarose gel, which was indicative of HLA-G uptake by the pAdTrack-CMV vector.

5.4.4 Confirmation of HLA-G1 and HLA-G5 orientation in pAdTrack-CMV

In order for the inserted HLA-G to be successfully transcribed, the orientation of the HLA-G needed to be in the same direction as the CMV promoter. In **Figure 5.5A**, a diagramatic representation depicts the desirable orientation of HLA-G cDNA with the respect to the direction of CMV. Specifically, the start codon located on the 5' end of the HLA-G is located nearest to the CMV while the 3' end barring stop codon is located away from the CMV promoter. The five prime end of the HLA-G was engineered to express *Kpn* I restriction site, which in the desirable orientation should be located closest to the CMV promoter. In such a configuration, *Kpn* I digestion would excise complete HLA-G of approximately 1kb (**Figure 5.5A**). In case of an opposite HLA-G orientation (ie. the 180° rotation of HLA-G) the *Kpn* I restriction site would be in close proximity to another *Kpn* I

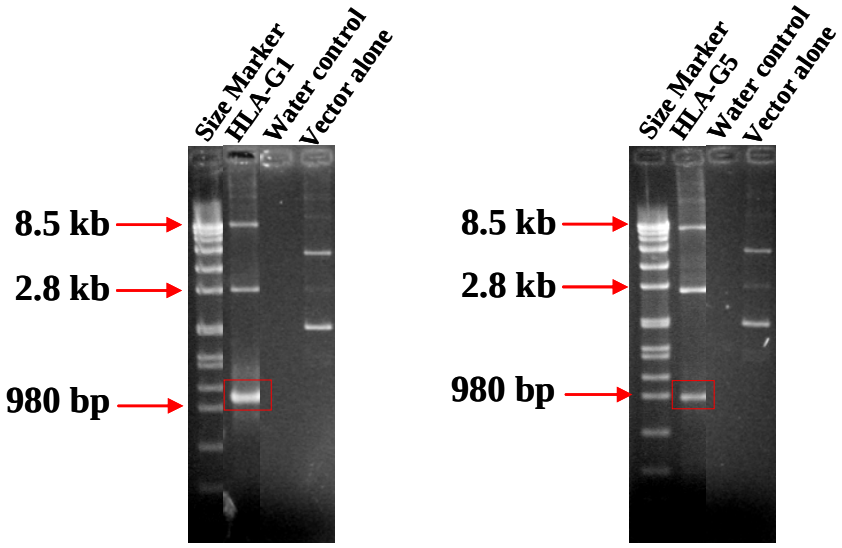

Figure 5.4. Cloning of HLA-G1 and HLA-G5 in pAdTrack-CMV Vector. HLA-G1 and HLA-G5 DNA fragments were excised from pGEM-T Easy Vector using *Not* I restriction enzyme and ligated into *Not* I digested PAdTrack-CMV vector. Kanamycin resistant (conferred by pAdTrack-CMV) colonies were selected and screened for the presence of inserts by PCR using HLA-G1 and HLA-G5 specific primer pairs. Red arrows indicate size markers while red squares indicate HLA-G1 and HLA-G5 fragments. Bands at 2.8 kb and 8.5 kb represent plasmid DNA from kanamycin resistant colony which was used as a template for testing the HLA-G presence. DNA size marker used was SPP1 plasmid digested with *EcoR* I restriction enzyme.

A

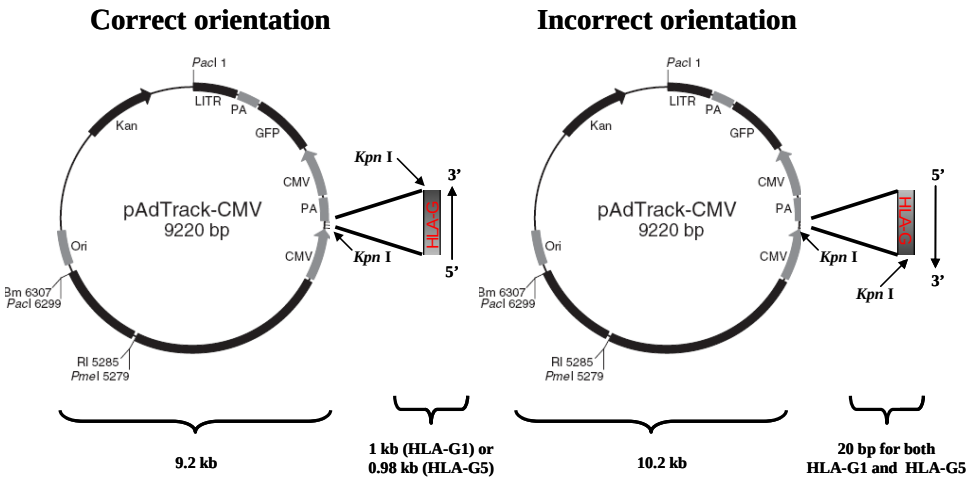

B

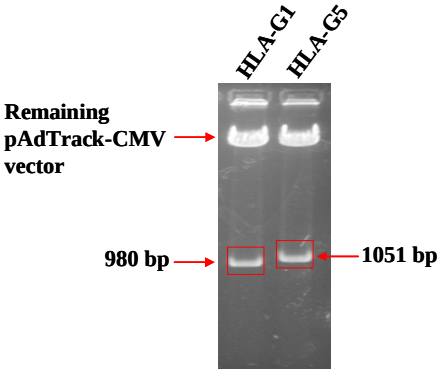

Figure 5.5. Confirmation of HLA-G1 and HLA-G5 orientation in pAdTrack-CMV Vector. pAdTrack-CMV plasmid containing HLA-G1 and HLA-G5 inserts was digested with *Kpn* I restriction enzyme in order to determine the orientation of the inserts relative to the CMV promoter. (A) Schematic representation of the location of *Kpn* I site relative to the direction of the CMV promoter and the orientation of the HLA-G cDNA in pAdTrack-CMV. (B) Agarose gel electrophoresis depicting excised HLA-G1 and HLA-G5 DNA fragments and the remaining pAdTrack-CMV vector. Red squares highlight HLA-G1 and HLA-G5 fragments.

site originally present on the pAdTrack-CMV. *Kpn* I digestion in this case would excise a fragment of approximately 30-50 bp. The above PCR positive plasmids were digested with *Kpn* I and the results confirmed the presence of ~1kb band for each HLA-G1 and HLA-G5 containing plasmids (**Figure 5.5B**). This indicated that the orientation of HLA-G inserts was correct, however the sequence analysis needed to be performed in order to analyse the integrity of the inserted HLA-G cDNA.

5.4.5 Sequencing analysis of HLA-G1 and HLA-G5 from pAdTrack-CMV

The above colonies were subjected to dideoxy sequencing and the chromatogram data was viewed using the Finch TV, aligned using ClustalW and the nucleotide sequence was translated into an amino acid sequence using Translate Tool software. The complete protein sequence of the cloned HLA-G1 and HLA-G5 were obtained and aligned against the published consensus sequence of HLA-G. The alignment analysis revealed three nucleotide substitutions in both HLA-G1 and HLA-G5 sequences: G35A, G243A, A392T. In addition, another base substitution was exclusively noted in the HLA-G5 insert at position T90C. When both HLA-G1 and HLA-G5 sequences were translated using the Translate Tool, none of the G35A, G243A, A392T base substitutions caused amino acid change except the HLA-G5 specific mutation (T90C), which resulted in Y30H substitution in amino acid sequence (**Figure 5.6**).

5.4.6 Generation of pAdEasier-1 BJ5183 E. coli

In order to increase efficiency of homologous recombination between pAdEasy-1 and pAdTrack-CMV, pAdEasier-1 cells were generated (**2.1.3.2**). The results in **Figure 5.7A** depict a theoretical *Hind* III digestion pattern of the pAdEasy-1 vector obtained using NEBcutter V2.0 software. This theoretical digestion pattern was used as a

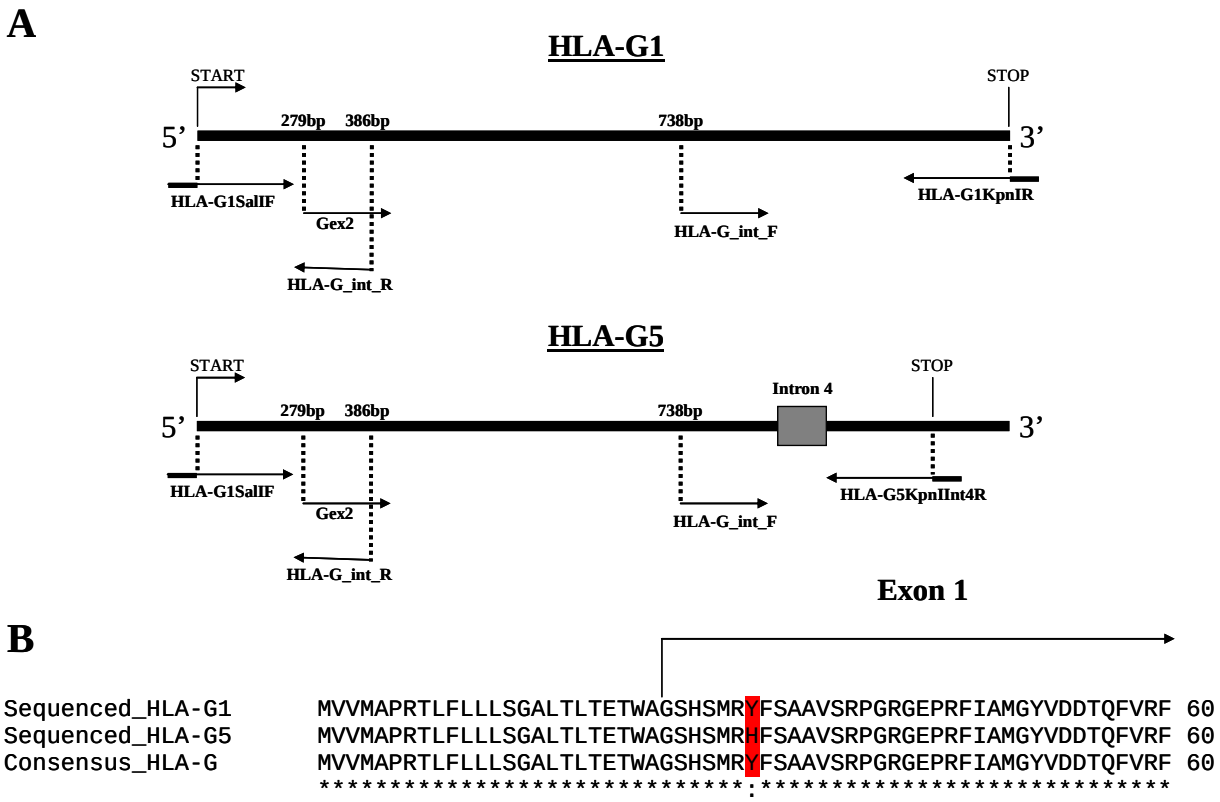

Figure 5.6. Sequence analysis of HLA-G1 and HLA-G5 inserts from pAdTrack-CMV Vector. (A) Schematic representation of the position of the sequencing primers along the HLA-G1 and HLA-G5 DNA (B) Amino acid sequence alignment of HLA-G1 and HLA-G5 depicting the location of the amino acid change in HLA-G5 sequence relative to the HLA-G consensus sequence. Highlighted in red is a specific position at which the amino acid change (Y30H) has occurred in HLA-G5. The remaining sequence is identical to consensus and therefore it is not shown.

A

#	Ends	Coordinates	Length (bp)
1	HindIII-HindIII	18478-26487	8010
2	HindIII-HindIII	32435-6402	7409
3	HindIII-HindIII	6403-11724	5322
4	HindIII-HindIII	13881-18477	4597
5	HindIII-HindIII	26488-29497	3010
6	HindIII-HindIII	29498-32434	2937
7	HindIII-HindIII	11725-13805	2081
8	HindIII-HindIII	13806-13880	75

B

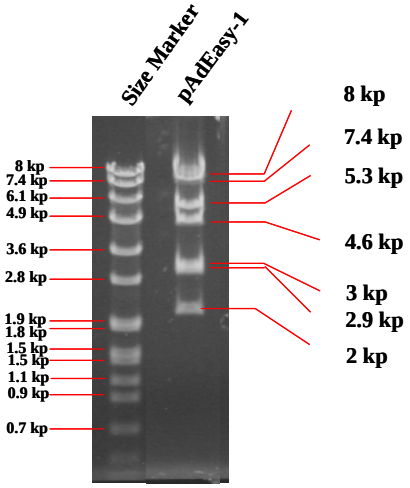

Figure 5.7. Generation of pAdEasier-1 *E.coli*. pAdEasy-1 was electroporated into electrocompetent BJ5183 *E.coli*. Ampicillin resistant colonies were then selected and plasmid DNA was extracted using alkaline lysis method. Integrity of pAdEasy-1 in BJ5183 was confirmed by *Hind* III restriction enzyme digestion. (A) Theoretical digestion of pAdEasy-1 sequence using *Hind* III was performed using NEBcutter V2.0 software and using published pAdEasy-1 sequence as the target. Digestion pattern of the pAdEasy-1 with *Hind* III restriction enzyme is represented in order from the highest to the lowest DNA band. (B) Agarose gel electrophoresis of the *Hind* III digested pAdEasy-1 plasmid from the electrocompetent BJ5183. Each pAdEasy-1 band is labelled with the red line showing specific size (in kb) of the each band. The sizes were determined by comparing the position of the *Hind* III digests with the DNA size marker.

guide before the actual *Hind* III digestion of pAdEasy-1. The pAdEasy-1 DNA was extracted from electrocompetent BJ5183, previously transformed with the pAdEasy-1 vector. Bands observed following actual *Hind* III digestion of pAdEasy-1 resembled those of the theoretical digest pattern indicating the presence of the correct pAdEasy-1 vector in the electrocompetent BJ5183 cells (**Figure 5.7B**). These transformed bacterial cells were then used for homologous recombination with pAdTrack-CMV.

5.4.7 Confirmation of homologous recombination

Pac I linearised pAdTrack-CMV containing sequenced HLA-G insert were transformed in pAdEasier-1 electrocompetent cells. Bacteria that grew on Kanamycin LB Agar plates was selected, ensuring that the smallest colonies were picked, and following 16 h incubation at 37°C, plasmid was extracted. The digestion pattern of the plasmids showed one band at 4.5kb and the other at 30kb, suggesting that homologous recombination occurred at the Ori sequence of the plasmid (**Figure 5.8B**). PCR confirmation of HLA-G1 and HLA-G5 inserts revealed that both genes were present in the recombinants (**Figure 5.8C**).

5.4.8 Detection of HLA-G1 and HLA-G5 expression

Adenoviral vectors (AdV) were generated in the current study in order to induce expression of HLA-G in DC. Following DC transfection with AdV containing HLA-G1 (AdV-HLA-G1), AdV-HLA-G5 and AdV-VB (vector blank control), mRNA from AdV transfectants was extracted, reverse transcribed and subjected to PCR. Results indicated that HLA-G mRNA transcription was evident only in AdV-HLA-G1 and AdV-HLA-G5 transfectants and not in AdV-VB controls (**Figure 5.9A**). This indicated that the presence of HLA-G1 and HLA-G5 mRNA was not due to the AdV background but due to the

specific HLA-G cDNA overexpression by the AdV-HLA-G1 and AdV-HLA-G5 vectors, respectively. HLA-G mRNA was successfully translated in DC as demonstrated by the detection of a significant amount of soluble HLA-G5 (**Figure 5.9B**) and surface HLA-G1 (**Figure 5.9C**) protein on DC relative to the control cells.

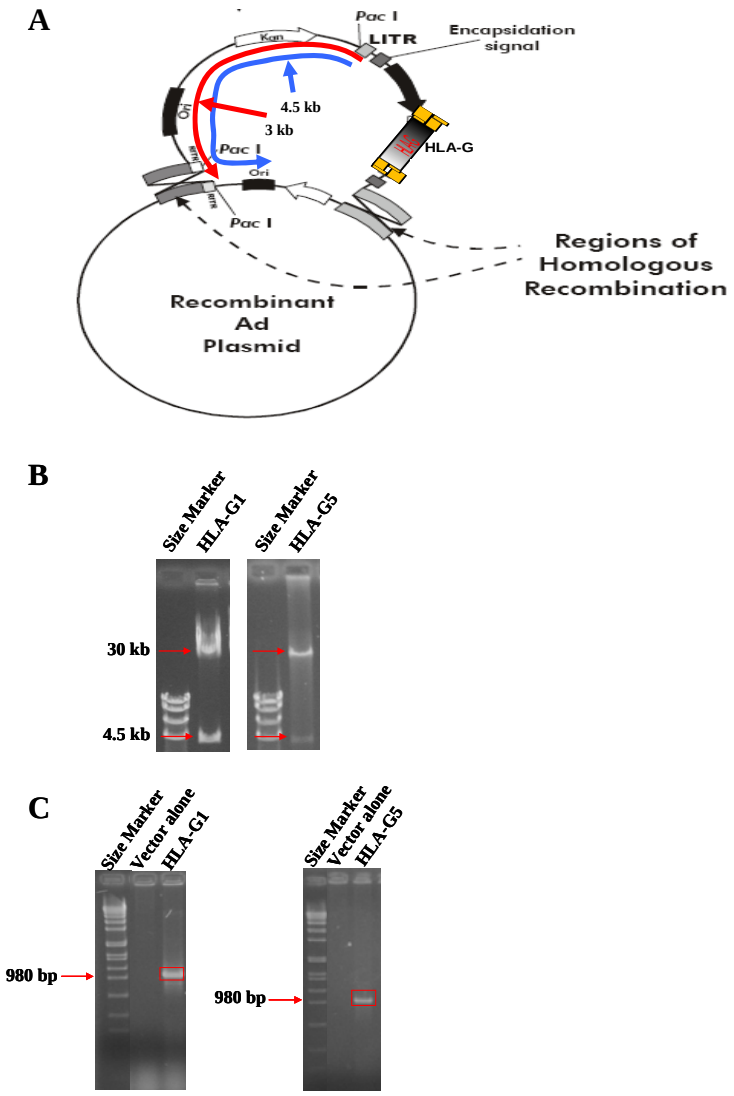

Figure 5.8. Confirmation of homologous recombination between pAdTrack-CMV containing HLA-G and pAdEasy-1. *Pme* I linearised pAdTrack-CMV was transformed into pAdEasier-1 *E.coli*. Kanamycin resistant colonies were selected and adenoviral DNA was extracted using a JetStar plasmid extraction kit. (A) Schematic representation of possible *Pac* I restriction sites following homologous recombination. Based on the site of recombination the resulting products from *Pac* I digestion could either yield 3 kb or 4.5 kb in length, depending if the recombination occurred at RTS site or at the Ori site, respectively. Red arrow highlights the 3 kb band while blue arrow indicates 4.5 kb band, respectively. (B) plasmids were digested with *Pac* I restriction enzyme and the resulting fragments were run on the 0.8% Agarose gel above. 30 kb band represents the pAdEasy-1 while the presence of 4.5 kb band indicated that the homologous recombination occurred at the Ori site. (B) PCR was performed on 2.5 ng of homologously recombined plasmid DNA. Size marker used was SPP1 plasmid digested with *EcoR* I.

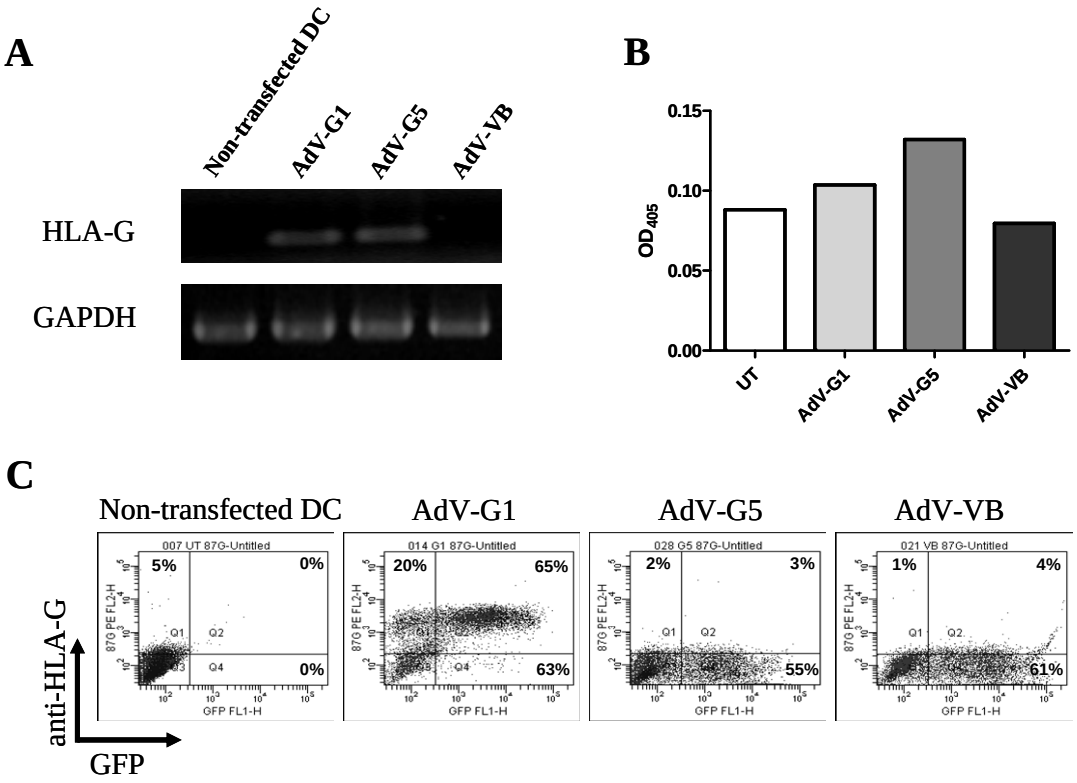

Figure 5.9. Analysis of HLA-G expression in DC transfected with AdV-HLA-G. Human DC were transfected with AdV-G1, AdV-G5 and AdV-VB or left untransfected for 48h. (A) RNA was extracted from the transfected DC, reverse transcribed and subjected to the PCR analysis using common primers for HLA-G1 and HLA-G5. GAPDH was used as a housekeeping gene to control for the DNA loading between the samples. PCR was performed for 30 cycles for HLA-G and 23 cycles for GAPDH. PCR products were then run on the 2% Agarose gel. (B) Soluble HLA-G was measured from the supernatants collected 48h post DC transfection. ELISA was performed in duplicates and data are expressed as average OD_{450} values. Data are representative of two independent experiments. (C) Transfected DC were analysed for their expression of HLA-G1 by flowcytometry using HLA-G specific monoclonal antibody (87G). Percentages of cells expressing HLA-G and GFP are shown in each quadrant on the dot plot.

5.5 Discussion

In this chapter, we were able to successfully generate recombinant human Adenoviral vectors (AdV) carrying HLA-G1 or HLA-G5 cDNA. These AdV were functional because they significantly induced both mRNA and protein HLA-G expression in transfected DC. Despite the success, our approach was initially limited by the generation of specific HLA-G primers. The primers for HLA-G1 and HLA-G5 were designed based on the published consensus sequence of the open reading frame of HLA-G1 and HLA-G5 (184, 421). They were then subjected to BLAST analysis in order to determine if they bound any other human sequences apart from HLA-G. Specifically, we would ensure that the primers designed would not bind any other sequence, especially with their 3' region. This region of the primer was shown to be important for successful PCR as minor sequence mismatch between 3' end of the primer and the DNA template resulted in the PCR failure (422). The BLAST analysis revealed no significant matches in the 3' end of the primer to other human MHC Class I sequences (data not shown). However, when cDNA extracted from PBMC was amplified using the primers above, HLA-A cDNA was amplified (instead of HLA-G) as determined by the sequencing analysis (data not shown). An alternative strategy using Jeg-3 cell line as a template for cDNA was employed, as these cells expressed HLA-G but no classical MHC Class I (423, 424). This strategy proved successful as the PCR amplified true HLA-G1 and HLA-G5 cDNA sequences. Sequencing analysis of the HLA-G1 and HLA-G5 cDNA revealed that HLA-G5 cDNA contained a point mutation T90C, which resulted in amino acid change Y30H. This mutation occurred in exon 1 of the HLA-G5 which encodes a peptide binding domain (421). It was predicted that Y30 residue may be involved in the formation of HLA-G peptide-binding pockets (425). Since ILT2 and ILT4 were shown to bind to the α3 domain of the HLA-G molecule it was rationalised that the above mutation would not inhibit HLA-G5 interaction with inhibitory ligands, and

the construct was decided to be used for further study (161, 198, 426). Furthermore, although the HLA-G5 construct contained the Y30H mutation, all of the cysteine residues, which were shown to be crucial in HLA-G dimerisation and interaction with ILT2 and ILT4 molecules (**1.7.4.2**), were preserved (194, 427).

Adenoviral constructs in this study expressed GFP for tracking the transfected cells. HLA-G1 and HLA-G5 constructs were not directly conjugated to GFP because it was thought that this may interfere with HLA-G dimerisation, β2 microglobulin association and ILT2/ILT4 interaction, all of which are important for proper HLA-G function. Recently, Gonen-Gross and Mandelboim reported to have generated the HLA-G-GFP construct which they used to show the origin of a free heavy chain of HLA-G on the cell surface (428). However the authors failed to show any data on anti-HLA-G mAb binding which would have confirmed the structural integrity of the HLA-G-GFP construct.

Although GFP is very useful for tracking of transfected cells it has been reported that murine DC expressing GFP could elicit an immune response towards GFP peptides (429). This may represent a potential problem in our system as GFP could induce additional inflammatory signals thereby masking potential suppressive effects of HLA-G. In the studies mentioned above (**1.9.2**), despite GFP antigenicity, the tolerogenic properties of transfected DC were still able to be demonstrated. It is a possibility that the co-expressing GFP could put HLA-G under additional immunological pressure which would then test the immunosuppressive limits of the HLA-G *in vitro*.

GFP expression in the Adenoviral constructs above was driven by a separate CMV promoter and therefore was independent of HLA-G1 and HLA-G5 expression. Although this enabled the expression of unconjugated HLA-G protein and the ability of tracking the transfected cells, the expression of the two did not always correlate since some GFP^+ cells were negative or low for HLA-G expression. Untransfected (GFP^-) DC could have acquired

HLA-G from transfected DC through trogocytosis and become GFP^- $HLA\text{-}G^+$ DC. Indeed, it was reported that DC can acquire MHC molecules via trogocytosis (156). Most importantly, in the transfected group the overall percentage of DC expressing HLA-G was between 85-90%.

In conclusion, functional Adenoviral vectors carrying HLA-G1 and HLA-G5 cDNA were successfully generated and used to induce high expression of HLA-G1 and HLA-G5 in DC. These genetically modified DC will be used to test the propensity of HLA-G1 and HLA-G5 to render tolerogenic capacity to DC *in vitro*.

CHAPTER 6

T CELL ACQUISITION OF HLA-G MOLECULE FROM DENDRITIC CELL (DC) BY CONTACT-DEPENDENT MEMBRANE FRAGMENT TRANSFER SUBVERTS T CELL IMMUNE RESPONSES

Publications
Manuscript in preparation to be published in Blood Journal

The following abstract has been published:

- Fedoric, B and Krishnan, R. Transplantation, Vol. 86, Issue 2S, Page 284-285 July 2008

Presentations
Presented at International Transplant Congress in Sydney 2008 (Received Young Investigator Award), TSANZ Annual Scientific meeting 2009 in Canberra and Postgraduate Research Expo at the University of Adelaide in 2008.

6.1 Introduction

This chapter examines the ability of DC to modify T cell alloimmune responses. As hypothesised in **section 2.1** genetic modification of human monocyte-derived DC to express surface HLA-G1 or soluble HLA-G5 molecules would confer DC the ability to downregulate alloimmune responses *in vitro*. The reason for selecting HLA-G was based on the number of studies demonstrating that HLA-G has strong immunosuppressive properties (**section 1.8**). It was found to inhibit T cell proliferation (430) induce T cell apoptosis (226, 431) and cell cycle arrest (227), inhibit DC maturation (214) and impair NK killing (432). In addition, HLA-G has been associated with better allograft outcomes (433, 434). Typically, HLA-G is not expressed on the surface myeloid or plasmacytoid DC from healthy individuals, although a report showed that some DC could secrete basal levels of HLA-G (203). Therefore, in **Chapter 5** we generated functional adenoviral construct to induce HLA-G expression in DC. However, in certain situations such as pregnancy DC can express HLA-G. The reports showed that monocyte derived DC from pregnant females (but not from non-pregnant females) provided a major source of soluble HLA-G (435). This selective expression of HLA-G during pregnancy is postulated to be a potential mechanism for protection of semi allogeneic foetus from maternal immune attack. Furthermore both myeloid and plasmacytoid DC derived from the cord blood, in contrast to DC derived from the peripheral blood, were shown to express both soluble and surface expression of HLA-G (436). One of the mechanisms by which HLA-G could convey its immunosuppressive effects to a diverse repertoire of target cells is through membrane transfer process called trogocytosis (147, 437).

Study by LeMaoult's group showed that T cells could acquire HLA-G from transfected cell lines (150). These HLA-G expressing T cells exhibited low proliferative capacity and were also able to inhibit proliferation of autologous T cells in the presence of

exogenous IL-2 or stimulation by APC. Therefore, it appears that T cells developed autoregulatory properties following the HLA-G acquisition.

Ability of HLA-G to be transferred via trogocytosis is due to its association with the lipid rafts on the cell membrane (150, 438). Lipid rafts are platforms within the membrane formed when sphingolipids associate with cholesterol (439). They can bind a variety of proteins (both on the intra-cellular as well as extracellular portion of the membrane) that are involved in the formation of immunological synapse (**section 1.4.4**) (439). The importance of immunological synapse in trogocytosis was demonstrated in the study where blockade of the molecules within the synapse using specific mAb resulted in the abrogation of trogocytosis (145).

The involvement of trogocytosis in the modulation of immune response has been observed both *in vitro* and in animal models (**reviewed in 1.6.3**). Lechler's group has demonstrated that human T cells can acquire antigen presenting properties (T_{APC}) from DC, a feature not normally attributed to T cells (144). These T_{APC} were able to induce significant proliferation of both autologous and allogeneic T cells (144). It was then proposed that trogocytosis may be used by the immune cells to rapidly amplify the immune responses (6). As reviewed in detail in section (**1.6.3**), recent *in vivo* data indicated that T cell trogocytosis may also have regulatory properties. Thus, depending on the immunological property of the molecules acquired T cells could either stimulate or inhibit immune responses. Therefore, acquisition of atypical molecules by T cell will result in the modification of original immune function of that cell (437).

On that note, HLA-G represents an excellent candidate to study in the context of genetic manipulation of DC due to its implication in the inhibition of alloimmune responses of several target cells (**1.7.4**). Additionally, acquisition of HLA-G by T cells (via trogocytosis) may render a distinctive inhibitory function to those cells. In addition, it

is anticipated that the use of this versatile and potent immunomodulatory molecule to genetically modify DC may also generate DC with unique and potent tolerogenic properties (reviewed in **2.1)**.

Therefore, in this chapter the *in vitro* tolerogenic potential of genetically modified DC expressing HLA-G1 and HLA-G5 will be investigated. As DC/T cell interactions constitutes a major arm of alloimmune response, this chapter will only focus on the immune changes conferred to the T cells following co-culture with HLA-G1 or HLA-G5 transfected DC.

6.2 Materials and Methods

6.2.1 Mixed lymphocyte reaction (MLR)

Prior to the MLR, DC were washed three times in PBS in order to minimise carryover of immunosuppressive agents or Adenoviral particles. These stimulator DC were mixed with responder T cells in complete medium to a final concentration of $1x10^3$ and $1x10^5$ cells in a volume of 200 μl per well, respectively (stimulator : responder ratio 1:100). The mixed cell populations were subsequently cultured for 4 days in 96-well round bottomed plates (TPP, Trasadingen, Switzerland) at 37°C. After 4 days, the mixed cultures were pulsed for 24 h with 1 μCi of [^{3}H]-thymidine (Amersham Biosciences, UK). Subsequently, cells were harvested onto glass fibre filters and scintillation liquid was added. The incorporated [^{3}H]-thymidine radioactivity was quantified using a liquid scintillation Wallac Microbeta Counter (Turku, Finland). All experiments were performed in replicates of five and the results were recorded as counts per minute (cpm).

6.2.2 Addition of purified HLA-G to the MLR

Monocytes, tolerogenic RAPA DC and mDC were generated from the same donor using the protocol described in **Chapter 3** and were used as stimulator cells. Monocytes were cultured in complete media without cytokines for 24 h post panning to allow for cells to detach. Fresh monocytes were then used in MLR against frozen allogeneic NWT cells. The same NWT cells were used for the RAPA-DC and mDC. Prior to the MLR, cells were washed three times in PBS in order to minimise carryover of immunosuppressive agents or cytokines. These stimulator cells were mixed with responder T cells in complete medium to a final concentration of $1x10^3$ and $1x10^4$ cells in a volume of 200 μl per well, respectively (stimulator : responder ratio 1:10). To some wells 1μg/ml of purified HLA-G (C42S mutant, provided by Dr Craig Clements, Monash University, Melbourne, Australia) was added. The mixed cell populations were subsequently cultured for 4 days in 96-well round bottomed plates (TPP, Trasadingen, Switzerland) at 37°C and T cell proliferation was measured using [^{3}H]-thymidine as described above.

6.2.3 Enrichment of $CD4^+$ T cells

NWT cells ($2x10^8$ total cells) were subjected to CD4 negative selection with the Miltenyi $CD4^+CD25^+$ Regulatory T cell Isolation Kit (Miltenyi Biotec, Germany) using autoMACS cell separator, as per the manufacturer's instructions. Total $CD4^+$ T cell yields were ranging between 40-50% with greater then 95% purity. Enriched $CD4^+$ T cells were counted, washed twice in PBS at 800g for 10 min and resuspended in complete media at concentration of $4x10^6$ cells/ml.

6.2.4 Co-culture of transfected DC and $CD4^+$ T cells

Transfected DC were washed twice in PBS and centrifuged at 800g for 10 min to remove LipofectAMINE™ (Invitrogen, USA) and free virus. DC were resuspended in complete media at a concentration of $4x10^5$ cells/ml. DC were irradiated with a dose of 30 Gy prior to co-culture. DC ($4x10^5$ cells) were mixed with $4x10^6$ $CD4^+$ T cells in each well, in 24-well flat-bottom plate (Greiner Bio-One, Germany) and incubated under 5% CO_2 at 37^oC for 5 days. Two wells of $CD4^+$ T cells alone ($4x10^6$ $CD4^+$ T cells in each well) were also cultured in parallel and these were used as responder autologous cells in T_{APC} assay (see below).

6.2.5 Flowcytometry for detecting trogocytosis

Following the DC/$CD4^+$ T cell co-culture, non adherent T cells were harvested by gentle pipetting. Cells were washed twice in FACS wash (PBS, 2% Sodium Azide, 5% heat inactivated FCS) and centrifuged at 800g for 10 min. Non-specific Fc binding was blocked by incubating cells in 10% Heat Inactivated Rabbit Serum for 20 min at 4°C. The following primary mAb were added for 30 min at 4°C: anti-CD40 (IgG2a, Serotec, UK), anti-CD80 (IgG1, Immunotech, France), anti-CD86 (IgG1, Serotec, UK), anti-HLA-G (IgG2a, Exbio, Czech Republic) and anti-MHC II (IgG1, University of Melbourne, Australia). Background fluorescence was determined by labelling cells with isotype matched control mAb, ID4.5 (IgG2a, Dr Prue Hart, Flinders University, Australia) and X63 (IgG1, ATCC, USA). Following incubation with primary mAb, cells were washed again as above. Secondary anti-mouse mAb (conjugated to FITC) was added to the cells for 30 min 4°C. Cells were washed and co-labelled with PE conjugated anti-CD4 (IgG1, BD Bioscience, USA) or PE conjugated anti-CD8 (IgG1, Serotec, UK) for 30 min at 4°C. Cells were then fixed using FACS Lysing Solution (BD Bioscience, USA) acquired by FACSCanto and analysed using

FACSDiva software (BD Bioscience, USA). The gate was drawn based on forward and side scatter properties in order to exclude DC from analysis.

6.2.6 ILT2-Fc binding

Following the DC/$CD4^+$ T cell co-culture, non adherent T cells were harvested by gentle pipetting. Cells were washed twice in FACS wash (PBS, 2% Sodium Azide, 5% heat inactivated FCS) and centrifuged at 800g for 10 min. Non-specific Fc binding was blocked by incubating cells in 10% Heat Inactivated Rabbit Serum for 20 min at 4°C. The following blocking mAb were added for 30 min at 4°C: anti-HLA-G (Clone 87G, IgG2a, Exbio, Czech Republic) and anti-MHC I (Clone W6/32, IgG2b, Laboratory derived supernatant). Control for blocking was performed by pre-labelling cells instead with isotype matched control mAb: ID4.5 (IgG2a, Dr Prue Hart, Flinders University, Australia) and IgG2b (Serotec, UK). Following incubation with blocking mAb, cells were washed again as above. Anti-human ILT2-Fc (5 μg/ml) was added to the cells for 30 min 4°C. Cells were washed and ILT2-Fc binding was detected using PE conjugated anti-human F(ab')2 (Immunex, France). Cells were then fixed using FACS Lysing Solution (BD Bioscience, USA) acquired by FACSCanto and analysed using FACSDiva software (BD Bioscience, USA).

6.2.7 Trogocytosis time course

Cultures of transfected DC / $CD4^+$ T were left untreated or supplemented with 10 nM RAPA or 100 nM Cyclosporin A((Neoral®, Sandoz Pharmaceuticals, Austria) either at the time of initiation of co-culture or at 72h of culture. By adding the above agents at 72h post culture we aimed to analyse if the agents could directly inhibit trogocytosis process in already activated T cells, rather then indirectly by interfering with T cell activation.

Samples were taken at 24, 72, and 120 h after the beginning of the co-culture and labelled with anti-HLA-G (87G) and either anti-CD4 (BD Bioscience, USA) or anti-CD8 (Serotec, UK) mAb. Data was acquired by FACSCanto and analysed using FACSDiva software (BD Bioscience, USA). The gate was drawn based on forward and side scatter properties in order to exclude DC from analysis.

6.2.8 Immunomagnetic isolation of $CD3^+$ T cells

Following the DC/$CD4^+$ T cell co-culture, non adherent T cells were harvested by gentle pipetting, washed twice in Running Buffer (2 mM EDTA and 0.5% heat inactivated-FCS in PBS) and centrifuged at 800g for 10 min. $1x10^7$ non-adherent cells were resuspended in 80 μl of Running Buffer. 20 μl of CD3 microbeads were added per $1x10^7$ cells and the mixture was incubated for 15 min at 4°C. The cells were then washed with 2 ml of Running Buffer, centrifuged at 300g for 10 min and resuspended in 500 μl of Running Buffer. Cells were selected using the "depletes" setting on the autoMACS cell separator (Miltenyi Biotec, Germany), positive fraction was collected, washed twice in PBS and resuspend in complete RPMI media to a concentration of $2.5x10^5$ cells/ml. Purity of the cells was > 95%.

6.2.9 T cell proliferation assay

A hundred microlitres of $CD3^+$ cell suspension ($2.5x10^5$ cells/ml) was plated per well in 96-well round bottom plate. To each well, an additional 100 μl of either complete RPMI media or anti-HLA-G (clone 87G, final concentration of 5 μg/ml in 200 μl) or conditioned supernatant of anti-MHC I (clone W6/32) mAb was added to make up 200 μl final volume. Single cells were then incubated at 37°C, 5% CO_2 for 3 days. At day 2 of the culture, cells were pulsed with 1 μCi of [^{3}H]-thymidine (Amersham, UK) for 18 h. Cells were harvested with Tomtec Cell Harvester (Turku, Finland) onto Wallac gridded filter mats (Wallac,

USA). Filter mats were treated with β-scintillant and cellular tritium incorporation measured using a Wallac MicroBeta® Scintillation Counter (Wallac, USA).

6.2.10 T_{APC} assay

Purified $CD3^+$ T cells from DC/$CD4^+$ T cell co-cultures were irradiated with a dose of 30 Gy and used as a stimulator T_{APC} cells. Depending on the requirements, the T_{APC} assay was performed with either $2.5x10^4$ or with $1x10^5$ T_{APC} per well. Autologous responder $CD4^+$ T cells were resuspended in complete media and added to a final ratio of 1:10 (T_{APC} : $CD4^+$ T cells). Cells were incubated for 3 days at 37°C and 5% CO_2. At day 2 of the culture, cells were pulsed with 1 μCi of [^{3}H]-thymidine (Amersham, UK) for 18h. Cells were harvested with Tomtec Cell Harvester (Turku, Finland) onto Wallac gridded filter mats (Wallac, USA). Filter mats were treated with β-scintillant and cellular tritium incorporation measured using a Wallac MicroBeta® Scintillation Counter (Wallac, USA).

6.2.11 Statistical analysis

An independent-samples *t-test* was performed, using SPSS Software V12.0, in order to compare the MLR results for different treatment groups. The data was considered to be statistically significant at $P \leq 0.05$.

6.3 Results

6.3.1 DC transfectants express structurally functional membrane bound HLA-G

Since human monocyte derived DC normally do not express HLA-G1 molecules, Adenoviral vectors (AdV) were generated to induce expression of HLA-G1 in these cells. Following DC transfection with AdV containing HLA-G1 (AdV-HLA-G1), AdV-HLA-G5 and AdV-VB (vector blank control) the mRNA for HLA-G was transcribed only in

AdV-HLA-G1 and AdV-HLA-G5 transfectants (**Figure 6.1A**). HLA-G mRNA was successfully translated to protein in 91% DC (**Figure 6.1B**). HLA-G1 was structurally functional since 75% of the HLA-G1^{+} DC bound the ILT2-Fc ligand in the presence of isotype mAb (**Figure 6.1C**). Specificity of ILT2-Fc binding to HLA-G1 was demonstrated by the absence of ILT2-Fc binding to the AdV-VB and AdV-HLA-G5 control cells as well as the observation that ILT2-Fc binding was reduced (from 75% to 40%) in the presence of HLA-G blocking mAb W6/32. ILT2-Fc binding was not blocked with anti-HLA-G mAb clone 87G. This suggested that the previously reported blocking property of 87G in functional assays may not be achieved by blocking HLA-G/ILT2 binding but instead by blocking signalling through the ILT2. Despite structurally functional HLA-G1 expression, AdV-HLA-G1 transfected DC were unable to inhibit T cell proliferation during co-culture (**Figure 6.1D**). The addition of purified HLA-G (C42S) or wild type was also unable to inhibit T cell proliferation during mDC:T cell nor during RAPA-DC co-culture (**Figure 6.1E**). However, in **Figure 6.1E**, HLA-G (C42S) was shown to inhibit T cell proliferation during monocyte:T cell MLR by 50% (P =0.05).

6.3.2 Allogeneic T cells acquire HLA-G1 from transfected DC via trogocytosis and suppress proliferation of bystander autologous T cells

In order to determine if DC were able to transfer HLA-G1 to T cells and modulate T cells responses, a co-culture of transfected DC and allogeneic T cells was set up. Following the co-culture, allogeneic T cells (20% of each CD4^{+} and CD8^{+}) acquired HLA-G1 molecules only from AdV-HLA-G1 DC but not from AdV-HLA-G5 or AdV-VB (**Figure 6.2A**). HLA-G1 was short-lived on T cells with the expression of HLA-G1 decreasing to the baseline levels 24 h post trogocytosis (**Figure 6.2C**). In our experiments, trogocytosis occurred as early as 24 h post culture and peaked at day 5 (**Figure 6.2B**). Based on the timecourse experiments, T cells from day 5 of the culture were purified using CD3

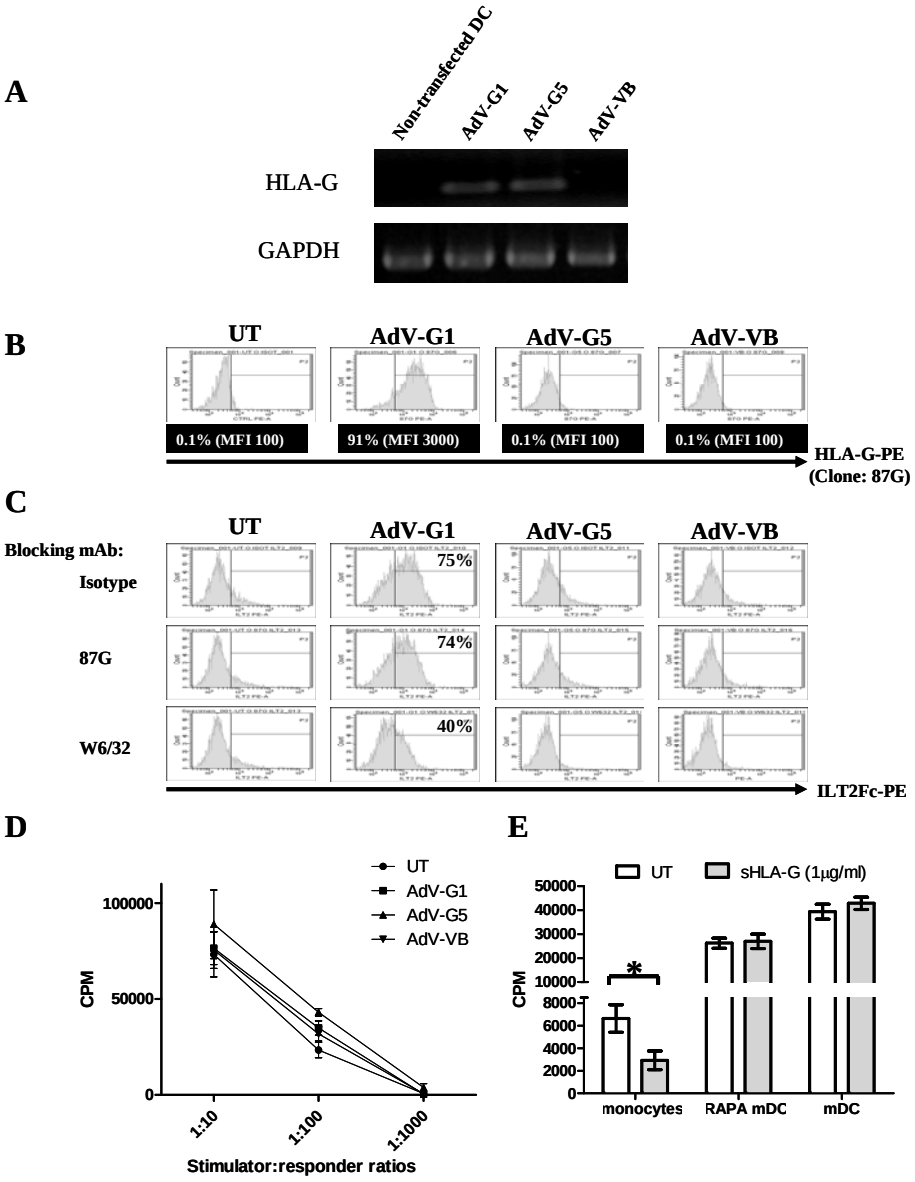

Figure 6.1. Transfection of DC with AdV-HLA-G induces high expression of HLA-G surface protein capable of binding its ligand, ILT2. Human DC were transfected with AdV-G1, AdV-G5 and AdV-VB or left untreated for 48h. (A) RNA was extracted from the transfected cells, reverse transcribed and subjected to the PCR analysis using specific HLA-G primers. (B) Transfected DC were analysed for their HLA-G expression (C) HLA-G transfectants were tested for their ability to bind ILT2-Fc. The specificity of the ILT2/HLA-G interactions was assessed in the presence of anti-HLA-G (87G), anti-MHC-I (W6/32) or isotype control mAb's. (D) Transfectants were co-cultured with the allogeneic T cells for 5 days. At day 5 the T cell proliferation was measured and recorded as CPM (+/- SD). (E) Monocytes, RAPA-DC or mDC were cultured with allogeneic T cells in 1:10 (stimulator : T cell ratio) in the presence or absence of sHLA-G, for 5 days. At day 5, T cell proliferation was measured and represented as CPM (+/- SD). The data are representative of 3 different experiment, (*p = 0.05).

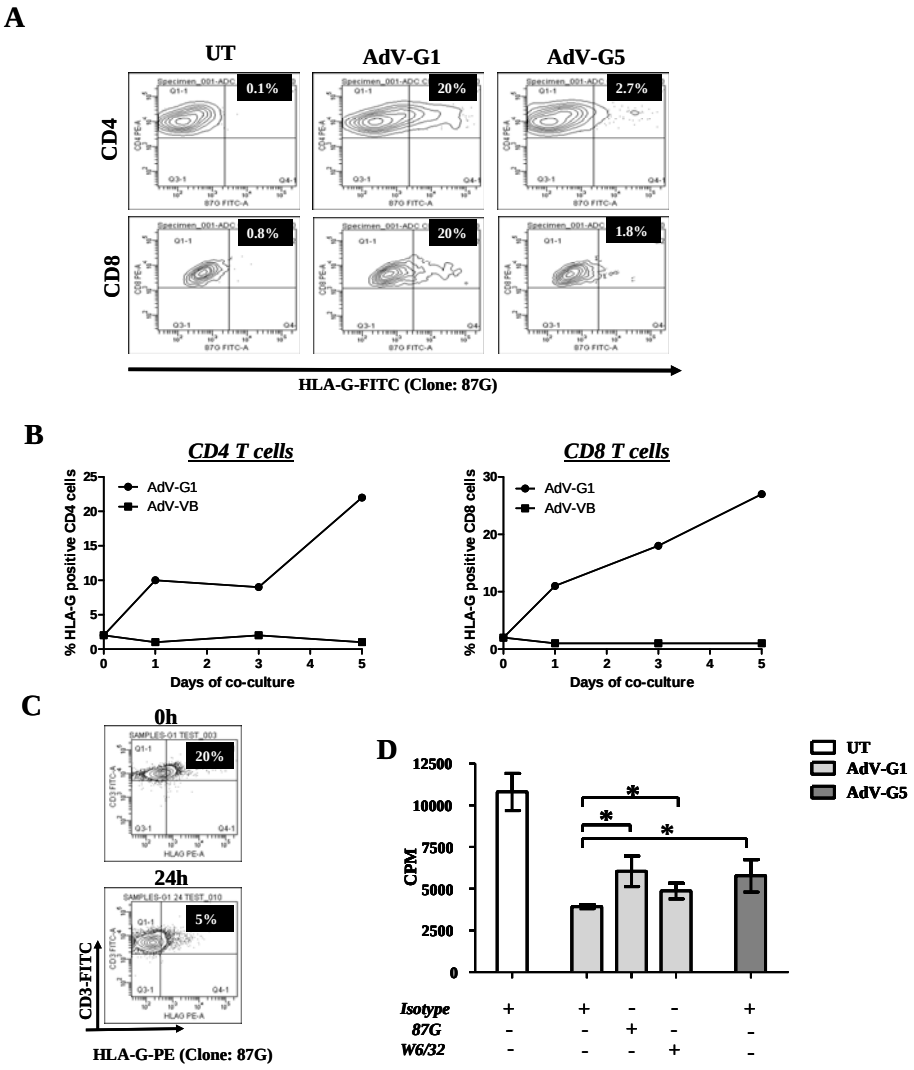

Figure 6.2. Allogeneic T cells transiently acquire HLA-G1 molecule from genetically modified DC during alloimmune activation. Untransfected or transfected DC were co-cultured with allogeneic T cells in 1:10 (DC:T cell) ratio for 5 days. (A) At day 5 cells were collected and labelled with: anti-CD4 ($CD4^+$ T cells) or anti-CD8 ($CD8^+$ T cells) and co-labelled with anti-HLA-G mAb. The percentage of positive cells expressing specific markers are shown in the contour plot. (B) Transfected DC were co-cultured with allogeneic $CD4^+$ T cell in 1:10 (DC:T cell) ratio for up to 5 days. Cells were collected at t = 0, 1, 3 and 5 and labelled with: anti-CD4 or anti-CD8 and co-labelled with anti-HLA-G mAb. The percentage of either CD4 or CD8 positive cells expressing HLA-G1 are shown. (B) At day 5 cells were positively selected using anti-CD3 microbeads. Cells were then either immediately stained with anti-CD3 and anti-HLA-G (0h) or cells were left in culture for 24h at 37°C and then stained as above (24h). (D) T cells were positively selected using anti-CD3 microbeads at day 5 of the co-culture with DC. $CD3^+$ cells were then plated at $2.5x10^4$ cells/well in presence or absence if either isotype control, 87G or W6/32 mAb, and incubated for 3 days. The T cell proliferation was quantified by measuring [^{3}H]-thymidine uptake and results are represented as +/- SD (CPM), (*$p \leq 0.05$) The data are representative of 3 independent experiments.

microbeads and used in a functional assay. The purity of the cells was greater than 95% (**Appendix 6.1**). Proliferation results demonstrated that there was a reduction in proliferation in the group containing HLA-G1 acquired T cells when compared to the T cells from untreated (60% inhibition, P =0.05) or AdV-HLA-G5 (30% inhibition, P =0.05) DC cultures (**Figure 6.2D**). This inhibition was HLA-G specific as the addition of HLA-G specific mAb (87G) and W6/32 (to a lower extent) reversed T cell proliferation by 30% and 5% respectively (**Figure 6.2D**).

6.3.3 T cell proliferation and CD80/86 signalling are important for trogocytosis

In order to investigate the mechanism of HLA-G1 trogocytosis between AdV-HLA-G1 transfected DC and $CD4^+$ and $CD8^+$ T cells, immunosuppressive agents CsA (100 nM) and RAPA (10 nM) as well as CTLA4-Ig and ILT2-Ig were added to the DC:T cell cultures at the beginning of culture (the latter is only relevant to CsA and RAPA). In some experiments CsA and RAPA were also added at day 3 for 48h. The results in **Figure 6.3A** demonstrated that baseline proliferation of T cells occurred as early as day 1 and peaked at day 5 of the culture mimicking the timecourse of HLA-G1 trogocytosis observed in **Figure 6.2B**. However, it can be noted that at 72h, expression of HLA-G on CD4 and CD8 cells seemed to decrease but this could be due to day to day variations in mAb staining. The addition of CsA or RAPA either at the beginning or during DC culture resulted in 50% and 30% inhibition in T cell proliferation (relative to the controls), respectively (P =0.04). Both CsA and RAPA inhibited trogocytosis of HLA-G by 50-60% in $CD4^+$ T cells and 20-60% in $CD8^+$ T cells (**Figures 6.3B** and **6.3C**). The most consistent/profound inhibition was at day 5 irrespective of time at which the agents were added, a feature probably associated with the sensitivity of the assay. Another parameter which was involved in trogocytosis was CD80/86 interaction during culture. Addition of

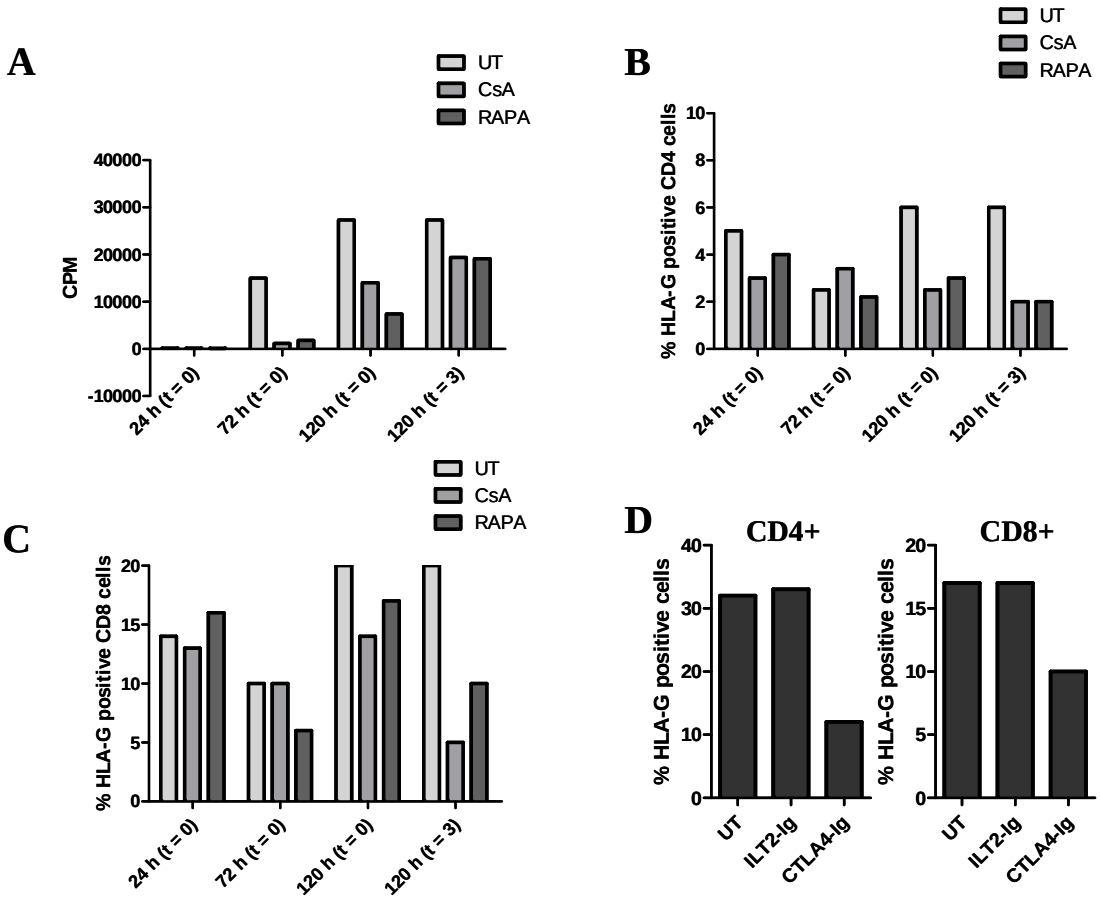

Figure 6.3. Immunosuppressive agents and blockade of CD80/86 molecules inhibits HLA-G trogocytosis. Untransfected or HLA-G transfected DC were co-cultured with allogeneic T cells in 1:10 ratio. CsA or RAPA were either added at the beginning of culture (t = 0) or at day 3 of culture (t = 3). At each time point (24h, 72h and 120h) cells were harvested and their (A) proliferation and (B, C) expression of HLA-G on CD4+ and CD8+ cells respectively, was assessed. (D) HLA-G1 transfected DC were co-cultured with the allogeneic T cells in 1:10 (DC:T cell) ratio for 5 days. ILT2-Ig (500 ng/ml) or CTLA4-Ig (500 ng/ml) were added at the beginning of the DC:T cell co-culture. Cells were collected at day 5 and labelled with either anti-CD4 or anti-CD8 and co-labelled with anti-HLA-G mAb. The percentages of HLA-G expressing cells were recorded. The data are representative of 3 independent experiments.

CTLA4-Ig but not ILT2-Ig reduced the number of HLA-G1 expressing $CD4^+$ and $CD8^+$ T cells by 60% and 30%, respectively (**Figure 6.3D**). ILT2-Ig in this experiment served as Ig control, demonstrating that the Ig portion of CTLA4 was not responsible for the observed effects. Furthermore, blocking HLA-G1 interactions during DC:T cell culture, with ILT2-Ig, did not impair trogocytosis (**Figure 6.3D**).

6.3.4 T cells acquire attenuated APC properties from tolerogenic RAPA-DC

In this set of experiments, it was investigated if T cells could acquire costimulatory molecules CD40, CD80, CD86 and MHC II from DC during culture and amplify the immune responses by acting as APC. The results demonstrated that $CD3^+$ T cells did acquire CD40 (46%, MFI = 1880), CD80 (40%, MFI = 1928), CD86 (58%, MFI = 3165) and MHC II (68%, MFI = 9216) molecules from untreated DC (**Figure 6.4A**). Expression of costimulatory molecules was primarily due to trogocytosis and least due to the endogenous production of costimulatory molecules, since PHA-activated T cells expressed significantly lower levels of these molecules when compare to the controls (**Figure 6.4A**). On the other hand, we have demonstrated in **Chapter 3** that Rapamycin treatment of DC generated tolerogenic DC expressing low CD40, CD80, CD86 and MHC II molecules. In this study we therefore aimed to investigate if these tolerogenic DC could transfer their tolerogenic phenotype to T cells. When RAPA-DC were co-cultured with allogeneic $CD4^+$ T cells, T cells acquired lower levels of the costimulatory molecules CD40 (37%, MFI = 1524), CD80 (30%, MFI = 1300), CD86 (48%, MFI = 2566) and MHC II (56%, MFI = 6400) when compared to the untreated DC cultures (**Figure 6.4A**). Functionally, when T_{APC} from untreated DC cultures were used in the stimulation assay, they were able to induce significant proliferation of autologous T cells. In contrast, T_{APC} generated by RAPA-DC UT were inferior stimulators of T cell proliferation (40% of untreated, P =0.03)

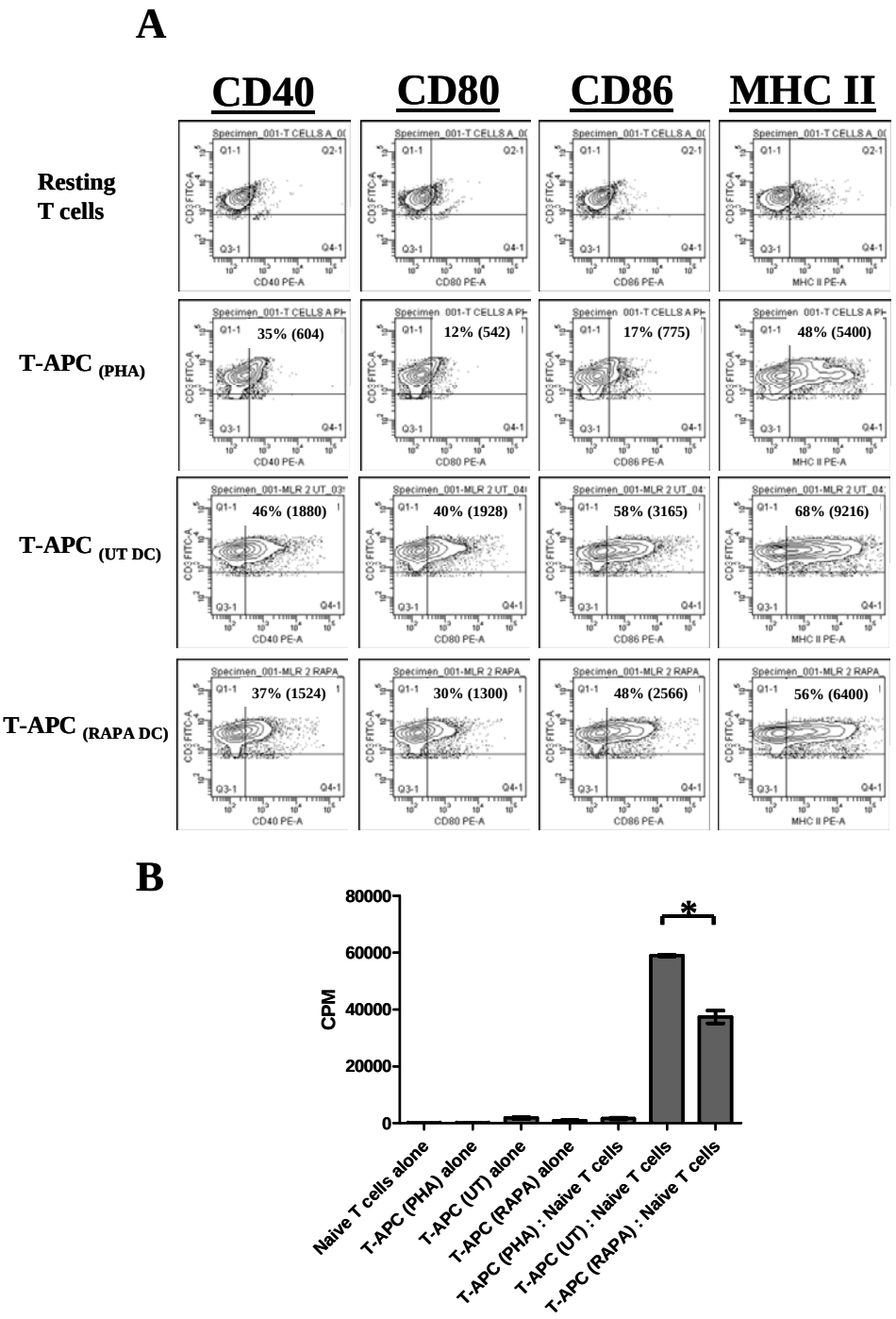

Figure 6.4. Allogeneic T cells acquire lower levels of positive costimulatory molecules from RAPA-DC, and as a consequence have poor allostimulatory capacity. Mature DC grown in the presence or absence of RAPA (10 nM) were cultured with allogeneic T cells for 5 days. At day 5, (A) total cells were collected and labelled with anti-CD3 and co-labelled with anti-CD40, -CD80, -CD86 and -MHC Class I mAb. The data are representative of 3 different experiments, (B) cells were positively selected using CD3 microbeads, irradiated and used as antigen presenting stimulator cells against the resting autologous T cells, (*$p \leq 0.05$). The data are representative of 3 independent experiments.

(**Figure 6.4B**). Although control PHA-activated $CD4^+$, T cells expressed detectable levels of costimulatory molecules however they did not induce autologous $CD4^+$ T cell proliferation, a feature probably attributed to the absence of allogeneic MHC II and a low level of costimulatory molecules (**Figure 6.4B**).

6.3.5 Combination of pharmacological and genetic modification of DC further reduced proliferative and T_{APC} properties of T cells

Since it was observed that both genetic modification of DC with HLA-G as well as RAPA modification could confer tolerogenic properties to DC individually (**Figures 6.3D** and **6.4B**), we aimed to investigate if the combination of the two modifications approached could further enhance the immunomodulatory properties of DC. Here it was shown for the first time that RAPA DC could be transfected with AdV. The induction of HLA-G in RAPA DC with AdV was similar to those of UT shown in **Figure 6.1B**. Despite inhibiting MLR, RAPA-DC in combination with HLA-G1 transfection did not contribute further to T cells hyporesponsiveness relative to the control AdV-VB transfected RAPA-DC (**Figure 6.5B**). However, T cells that were cultured with transfected RAPA-DC acquired low costimulatory molecules but they also acquired moderate HLA-G expression (**Figure 6.5C**). Functionally, these T cells exhibited a slight reduction in proliferative capacity (5% reduction compared to $HLA\text{-}G1^+$ T cells from untreated DC cultures, $P = 0.05$) and a moderate reduction in their APC activity (40% inhibition compared to $HLA\text{-}G1^+$ T cells from untreated DC cultures, $P = 0.04$).

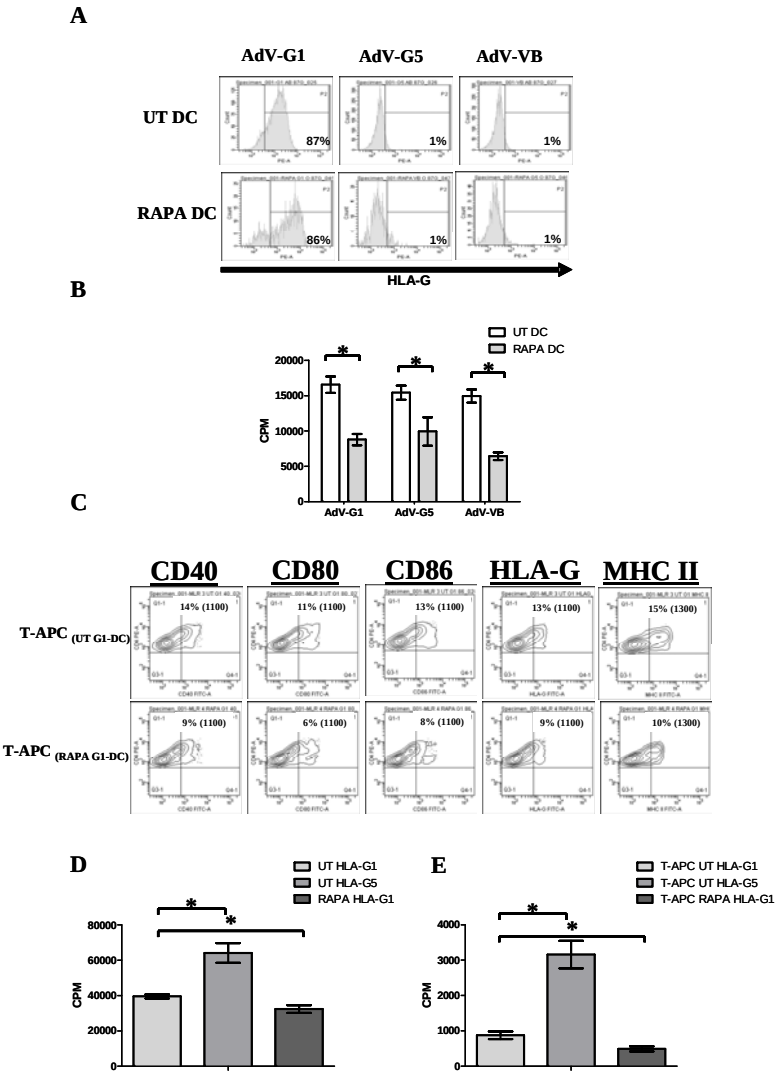

Figure 6.5. Combination of pharmacological and genetic manipulation marginally enhances DC tolerogenic properties. Mature DC grown in the presence or absence of RAPA (10 nM) were also transfected with AdV-G1 and AdV-G5 for 48h. (A) Transfectants were labelled with anti-HLA-G and the percentage HLA-G expressing cells was recorded. (B) Transfected untreated or RAPA-treated DC were cultured with allogeneic T cells for 5 days. At day 5 of co-culture T cell proliferation was measured using [^{3}H]-thymidine incorporation (C) Transfectants were co-cultured with allogeneic T cells as above. At day 5, total cells were labelled with anti-CD4 and co-labelled with anti-CD40, CD80, CD86, HLA-G and MHC II mAb. The percentage of CD4 positive cells expressing HLA-G1 molecule are shown. (D, E) DC were co-cultured with allogeneic CD4$^+$ T cells for 5 days in 1:10 ratio (in 24 well plate). At day 5, CD3 cells were positively selected. Purity of CD3 cells was 97-98%. T-APC were co-cultured either alone (D) or with autologous naïve CD4$^+$ T cells (E) in 1:1 ratio for 3 days and the total number of cells per well was 5x10^4. The data are representative of 3 different experiments. (*$p < 0.05$)

6.4 Discussion

In this study, we describe for the first time that tolerogenic DC can be successfully generated by genetically inducing HLA-G1 expression. HLA-G1 expressing DC indirectly modified function of T cells by transferring their HLA-G1 to the allogeneic T cells during co-culture. In contrast, HLA-G5 was not transferred as it is a soluble molecule and therefore it is not expected to localise within the lipid rafts. Following the DC:T cell co-culture, T cells were enriched to >97% purity and under these circumstances, HLA-G^+ T cells inhibited proliferation of other T cells in the absence of DC (**Figure 6.6**). Inhibition of T cell proliferation mediated by the HLA-$G1^+$ T was HLA-G1 specific since the addition of the anti-HLA-G mAb reversed T cell proliferation. This inhibition possibly occurred through HLA-G/ILT2 signalling, since T cells did not express other HLA-G ligands (namely ILT4 or CD8) (**Appendix 6.2**). Due to the unavailability of unconjugated ILT2 blocking mAb (clone HP-F1), we were unable to specifically demonstrate if ILT2 interaction with HLA-G1 was responsible for the observed inhibition, and therefore the above proposition was entirely based on the fact that the other HLA-G1 receptors were not expressed on T cells in our experimental setting. It is also important to note that purification of T cells was performed using anti-CD3 microbeads, and this approach would not distinguish between HLA-$G1^+$ and HLA-G^- T cells. A similar approach was used by others, as sorting of HLA-$G1^+$ T cells could interfere with HLA-G1 receptor binding (150, 152). Our data suggests that HLA-$G1^+$ T cells were potent in suppressing T cell proliferation even at 1:5 ratio (HLA-$G1^+$ T cells vs. HLA-$G1^-$ T cells). Therefore, the observation that T cells become suppressive after acquisition of immunosuppressive molecules from DC may have importance on the direct pathway of allorecognition, described by Lechler's group. During direct pathway of allorecognition, T cells become activated following their encounter with allogeneic DC in the lymph nodes. Following

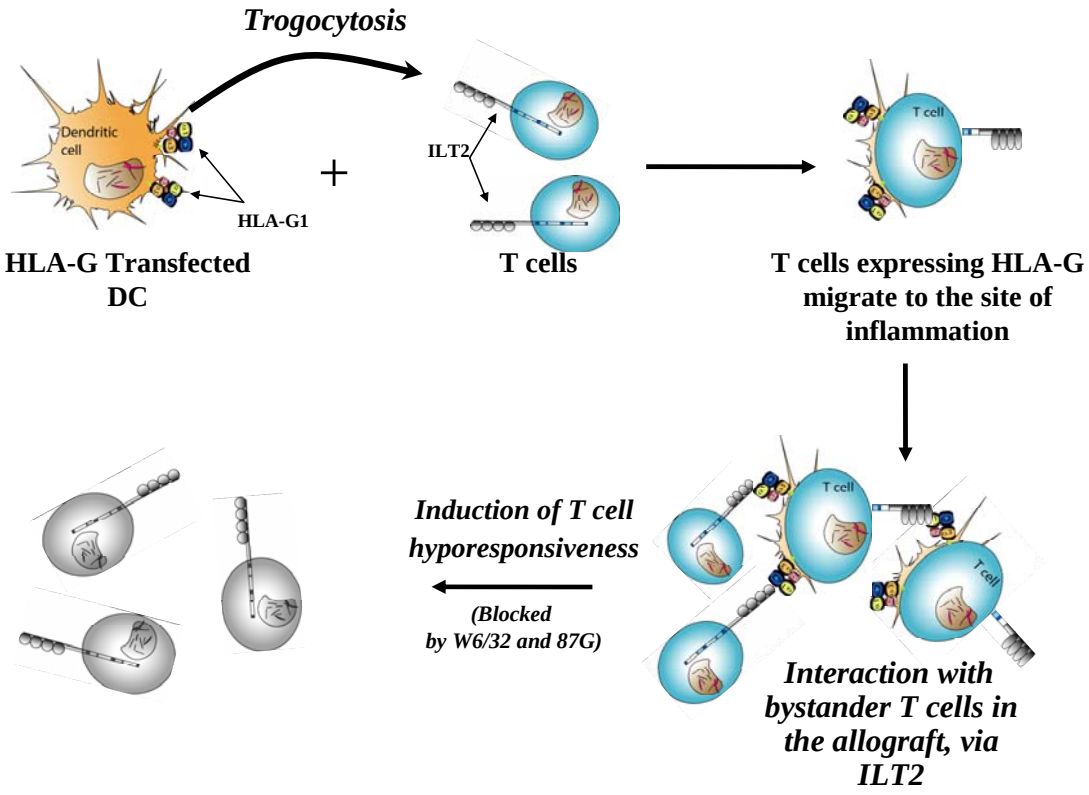

Figure 6.6. Proposal of trogocytosis based suppression of immune response via HLA-G1. Adenoviral delivery of HLA-G1 cDNA into DC has led to the induction of HLA-G1 expression on DC surface. During co-culture these DC interact with allogeneic T cells and transfer their membrane patches of immunological synapse containing HLA-G1 molecules to the allogeneic T cells. These HLA-G1^{+} T cells interact with bystander T cells to induce T cell hyporesponsiveness in HLA-G1 dependent manner.

activation, T cell migrate from the lymph node to the peripheral tissues where they interact with (and potentially suppress via HLA-G) other T cells. Besides HLA-G1, we have also demonstrated that CD40, CD80, CD86 and MHC II molecules were also transferred to allogeneic T cells from DC. Lechler's group in 2005 has previously proposed that this mechanism could serve to amplify the alloimmune responses (144). In agreement with the latter observation, we have also demonstrated that T cells, which acquired positive costimulatory molecules from non-HLA-G1 transfected DC, could act as potent APC.

In **Chapter 3** we demonstrated that RAPA-DC exhibited a low expression of positive costimulatory molecules resulting in the inhibition of T cell proliferation. Therefore, we aimed to investigate if the RAPA-DC were able to confer their tolerogenic phenotype to T cells via trogocytosis. The results showed that RAPA-DC have transferred lower levels of costimulatory molecules to allogeneic T cells, which rendered T cells to be poor APC relative to the control T cells. Thus, here we describe for the first time a novel mechanism by which RAPA-DC could suppress alloimmune response and potentially amplify immunosuppressive responses. We extended the above observation further and for the first time we combined pharmacologic and genetic manipulation of DC using RAPA-DC with AdV-HLA-G1 transfection respectively. Our findings showed that relative to the control cells, T cells which where incubated with RAPA-DC/AdV-HLA-G1 acquired lower levels of costimulatory molecules while at the same time also acquiring HLA-G1. These T cells showed an additional reduction in their APC capacity when compared to T cells from untreated AdV-HLA-G1 transfected DC. However, the percentage reduction is marginal, which casts doubt on biological relevance of these findings. Due to the large cell loss during purification procedures, we were unable to include the RAPA-DC/AdV-HLA-G5 control and therefore we cannot conclude with absolute confidence that the reduction in counts was mainly due to RAPA treatment. However, it can be concluded that in the

presence of RAPA, the effects of HLA-G1$^+$ T cells are enhanced. This still provides strong evidence that both pharmacological and genetic manipulation may provide a novel approach of generating DC with unique and potent tolerogenic properties. However, it is unknown if trogocytosis will happen in transplant patients, since we have demonstrated in this study that trogocytosis was inhibited in the presence of clinically relevant concentrations of CsA and RAPA. We have also demonstrated that even when agents were added post T cell activation (at day 3), trogocytosis was inhibited, suggesting that CsA and RAPA could directly effect trogocytosis rather than effecting trogocytosis through inhibiting T cell activation. Since CsA and RAPA are known to inhibit the calcineurin and mammalian target of Rapamycin (mTOR) signalling pathways, respectively, thus affecting multiple biochemical processes within the cell (243-247), it may be suggested that trogocytosis could involve calcineurin and mTOR pathways. In addition, further evidence by Carosella's group showed that when renal biopsies of patients with non-rejecting allografts were analysed for their expression of HLA-G there was no evidence of CD3$^+$ T cells expressing HLA-G within the renal biopsies (336). However, it cannot be excluded that trogocytosis could occur at other immunological sites such as lymph nodes as previously demonstrated in murine models (440).

Surprisingly, AdV-HLA-G1 transfected DC were unable to inhibit T cell proliferation directly during MLR assay. The adenoviral background may have contributed to this observation since we showed that Adenoviral antigenicity induced a strong alloimmune response. During the autologous MLR assay, where stimulator DC were transfected with AdV-HLA-G1 or AdV-VB, these DC were shown to induce significant proliferation of autologous T cells (**Appendix 6.3**). However there was no difference between AdV-HLA-G1 and AdV-VB transfected DC, suggesting that HLA-G1 was not contributing to the alloimmune response, although previous studies showed an ability of

HLA-G1 to induce a $CD8^+$ T cell immune responses *in vitro* (441). Therefore, in our experimental settings it appeared that HLA-G1 may be able to exert its effects only in situations where there is a low level of costimulation such as in T:T cell interactions. We then wanted to investigate if HLA-G alone (in the absence of virus) could inhibit T cell proliferation by adding it directly to DC:T cell culture. Our finding was in agreement with the report by Amniot's group, who demonstrated that the addition of HLA-G1 (1μg/ml) was unable to inhibit T cell proliferation in DC:T cells MLR. However, when monocytes were used as the stimulators in the MLR, T cells proliferation was significantly inhibited in the presence of soluble HLA-G. This observation appeared to be associated with the costimulatory strength of the stimulator cells. Besides costimulatory strength, we have previously shown in **Chapter 3** that monocytes exhibited the highest surface expression of ILT4 in contrast to iDC and mDC. ILT4 expression was shown, by Horeszukos's group, to be a key requirement for DC to respond to HLA-G tetramers (166, 214, 215). HLA-G dimers and multimers exhibit stronger affinity to ILT4 binding then to HLA-G monomers. In Horeszukos's studies above, the authors have generated an ideal environment for DC to respond to HLA-G by culturing DC under the non-classical condition using GM-CSF and TGF-β (215). This culture condition was shown to profoundly induce ILT4 expression on DC when compared to the classically generated DC which did not express detectable levels of ILT4. Resulting from ILT4 engagement by HLA-G tetramers, the authors demonstrated that HLA-G inhibited maturation in these alternatively generated DC (214). Although the studies above provide knowledge about the requirements of DC to respond to HLA-G, they may not reflect the true biological situation. The reasons for the latter are: that DC were not classically generated and HLA-G tetramers are artificially made structures and thus do not occur *in vivo*. Therefore, we propose that the more biologically relevant role of HLA-G mediated effects during the alloimmune response may primarily be on monocytes and T

cells under low inflammatory conditions. Since transplant patients are given immunosuppressive agents, these low immune environments may exist and thus the HLA-G effect may be evident. Indeed it was demonstrated that elevated HLA-G serum levels were associated with better allograft outcomes in cardiac and liver-kidney transplant patients (205, 224). Furthermore it was demonstrated that immunosuppressive agents induced HLA-G serum levels in cardiac patients with better allograft survival (205, 337). In addition, Suciu-Foca's group has demonstrated that regulatory T cells in patients with long term heart allograft survival upregulated ILT3 and ILT4 expression on the cadaveric donor monocytes isolated from the cryopreserved tissue samples; no such observations were made in patients who have experienced episodes of acute rejection (164, 167). Therefore, based on our observations and observation by others it can be proposed that the immunosuppressive agents could induce serum HLA-G, which then could interact with monocytes that have high ILT4 expression, which was induced by T_{REG} cells. This interplay between immunosuppressive agents, ILT4, and HLA-G may facilitate better transplant outcomes by acting on monocytes and T cells (442, 443).

In conclusion, the present study has demonstrated for the first time that genetic modification of DC to express HLA-G could be an attractive approach for cell-based therapy. However, further *in vivo* studies using these DC are necessary to investigate if trogocytosis mediated suppression could occur in an animal model of transplantation. Furthermore, it is also necessary to investigate if HLA-G trogocytosis can occur in transplant patients, since we have demonstrated that immunosuppressive agents could interfere with this process. In order to investigate the role of HLA-G trogocytosis on alloimmune suppression and to investigate which immunosuppressive agents can interfere with trogocytosis process in large animal model of transplantation, we aimed to investigate if sheep contained a HLA-G equivalent molecule. The preliminary data showed that

anti-human HLA-G mAb (87G) cross-reacted with approximately 20% of cells from total sheep PBMC (**Appendix 6.4**). These positive cells resided in the monocyte/lymphocyte region (**Appendix 6.5**) on the forwards and side scatter and were only present in 3 out of 5 animals tested (**Appendix 6.4**). This data is consistent with the observation from **Chapter 3** showing that monocytes but not DC expressed HLA-G. The variability in the expression between different sheep was similar to the studies showing differential expression of HLA-G between the individuals (203). However, we did not analyse functional aspects of these 87G-positive cells but we did show that like in humans the addition of soluble HLA-G or transfection with AdV-G1 did not inhibit T cell proliferation during DC-MLR (**Appendix 6.5**). The aim of these experiments was to investigate if human HLA-G molecule could cross-react with sheep cells. This would have provided more biologically significant results rather then extrapolating findings from sheep HLA-G homologue. Nevertheless, we could not confirm that human HLA-G molecule did not cross-react with sheep, since there is a possibility that the HLA-G ligands on DC and PBMC were not adequately expressed, as seen in human DC. Extrapolating from our findings in **Chapter 3**, ILT4 appeared to be the crucial receptor responsible for HLA-G mediated suppressive effects but unfortunately, anti-human ILT4 did not cross-react with any ovine PBMC (data not shown). This finding could explain why we did not see any inhibition of sheep PBMC MLR.

Finally, RAPA-DC have been previously shown to have strong tolerogenic properties in the murine animal model and here we describe a novel mechanism by which human RAPA-DC could downregulate immune responses. The approach of combining genetic and pharmacological modification of DC could provide a novel alternative in order to diversify and amplify tolerogenic properties of DC and potentially generate potent tolerogenic DC.

CHAPTER 7
CONCLUDING REMARKS

7.1 Concluding Remarks and Future Directions

Although immunosuppressive agents such as Cyclosporine A and Rapamycin have greatly improved allograft survival, these agents are largely non-selective and have detrimental side-effects, such as nephrotoxicity and induction of cancers. It is therefore imperative to find a therapy which is more immunospecific, tolerance inducing and with minimal side-effects. Immunosuppressive agents have not been directly associated with the induction of tolerance; however tolerance is possible as observed in the small number of transplant patients reviewed in **Chapter 1**. A major feature of those patients was establishment of donor microchimerism and in one patient in particular persistence of donor DC was established. Therefore, this highlighted the potential importance of DC in the induction of tolerance. On the contrary, it is well known that DC are involved in the initiation of the alloimmune responses by priming and activating alloreactive T cells. Conversely, observations in human studies demonstrated that DC (in particular iDC) could also have immunosuppressive properties. Using a murine model of islet transplantation, the importance of iDC in the prolongation of allograft survival was first noted (129). Nevertheless, these allografts were eventually rejected, a feature attributed to the maturation of injected iDC *in vivo*. This led to the concept of manipulating DC in order to generate maturation-resistant DC, capable of prolonging allograft survival with the final aim of inducing tolerance. Several approaches of manipulating DC have been employed to date and these include pharmacological, biologic and genetic manipulation. The expected benefit of manipulated DC is the assumed ability of these cells to migrate to secondary lymphoid tissues to convey tolerogenic signals to the allospecific T cells. Although these approaches have had success in generating tolerogenic DC *in vitro*, animal studies in particular using large animal models are not readily forthcoming.

In the current study, pharmacological and genetic manipulation approaches were used in order to induce *in vitro* tolerogenic human DC. The data reported in **Chapter 3** highlighted the ability of the immunosuppressive agent RAPA to generate human DC with *in vitro* tolerogenic properties. To date there were only two reports studying the ability of RAPA to generate tolerogenic human DC. However, our observations supported findings by Piemonti's group who also showed that RAPA downregulated maturation of DC (252), but not that of Woltman's group who demonstrated that RAPA was not able to modify DC (340). One possible reason is that Woltman's group used CD40L to mature DC, which maybe more potent maturation stimuli then TNF-a, thus cancelling effects of RAPA. Importantly, we have demonstrated for the first time that the addition of RAPA to mature DC induced tolerogenic DC. These RAPA-DC were able to induce substantial allogeneic T cell hyporesponsiveness *in vitro*. However the data observed allows the proposal that administration of RAPA to transplant patients would interfere with DC maturation and also directly affect mature DC function *in vivo*. The observation that RAPA reduced the expression of the immunosuppressive molecules ILT2, ILT3 and ILT4 on DC was unexpected. Thus, a follow-up of these *in vitro* observations in clinical samples of DC may throw "new light" on the *in vivo* observations of RAPA.

Moreover the observation that RAPA induced IDO expression in DC highlights this unrecognised role of the mTOR pathway. It is therefore tempting to speculate that the reported improvement in renal graft function in RAPA-treated patients following cyclosporine withdrawal may be associated with high serum IDO (444).

In order to test the *in vitro* observations made in **Chapter 3** above *in vivo*, ovine DC were treated with RAPA and analysed for their ability to prolong allograft survival in NOD/SCID model of vascularised ovine skin transplantation. The DC were obtained by the cannulation of the pseudo-afferent lymphatics of sheep. Phenotypically, ovine DC

resembled mature human DC such as high MHC II expression, dendrite formation and the potent allostimulatory capacity of allogeneic PBMC. Similar to human observations (**Chapter 3**), ovine RAPA-DC also induced T cell hyporesponsiveness *in vitro.* Further analysis revealed that the mechanism of tolerogenic ovine RAPA-DC was not due to downregulation of positive costimulatory molecules, or DC killing due to drug toxicity. According to the human studies in **Chapter 3**, the induction of IDO by RAPA in DC may be a plausible mechanism to explain these observation. Therefore, further studies are warranted to investigate the role of IDO in the induction of T cell hyporesponsiveness by RAPA-DC for both sheep and human cells.

Preliminary data in the NOD/SCID model indicated that RAPA-DC may be able to inhibit alloimmune responses in skin by limiting $CD4^+$ and $CD8^+$ T cell infiltration; however this was only observed in 60% of the animals. However it is acknowledged that larger numbers of animals within the treatment groups in this study will be confirmatory of the observed responses. It is important to note that stimulator and donor pairs were selected for transplantation experiments based on their strong alloreactivity, which may have represented major HLA haplotype mismatch in comparison to human transplants where patients are closely matched. Therefore, it is possible that in closely matched pairs the effect of RAPA-DC would be more profound. Importantly, RNA expression analysis from one pair of animals demonstrated that RAPA-DC induced FoxP3 expression, which may associate RAPA-DC with the induction of tolerance, however this needs to be substantiated in the future. Although the long term effects on graft outcome could not be tested in the NOD/SCID model the *in vivo* immunomodulatory effects of RAPA-DC were verified with the potential that these cells are likely to inhibit the direct pathway of allorecognition, an important mechanism in acute allograft rejection. The ability of RAPA-DC to induce tolerance in the preclinical ovine model of kidney allotransplantation will be investigated

provided that we can firmly conclude that RAPA-DC can inhibit T cell hyporesponsiveness in NOD/SCID model of onvine skin transplantation.

In the second part of this thesis it was investigated if genetic modification of human DC to express HLA-G1 or HLA-G5 molecules conferred tolerogenic properties to DC. The rationale for using HLA-G to genetically modify DC was based on the studies showing that high serum HLA-G associated with better allograft survival in liver/kidney transplant patients and that HLA-G was found in renal biopsies from patients without any episodes of acute rejection (**1.7.4**). In order to induce HLA-G expression in DC an adenoviral construct incorporating either HLA-G1 or HLA-G5 was generated and characterised (**Chapter 5B**). Adenoviral vectors successfully induced both mRNA and HLA-G protein expression in more then 80% of DC. HLA-G was structurally functional as it was able to bind its ligand ILT2-Fc. Functional aspect of HLA-G-expressing DC was analysed in **Chapter 6**, where it was shown that during DC-T cell co-culture allogeneic T cells acquired HLA-G from the transfected DC via trogocytosis. The resulting HLA-G^+ T cell population was capable of inhibiting autologous T cell proliferation when compared to the control HLA-G^- T cells. This observation may have clinical importance in the patients where HLA-G was shown to be associated with allograft acceptance and may provide a mechanism for HLA-G immuno-modulation in these individuals. Therefore it maybe necessary to investigate if DC and T cells from the patients with better allograft survival express surface HLA-G relative to the DC and T cells from normal individuals and patients with allograft rejection. Furthermore, it will be important to investigate if the recipient's T cells express HLA-G with donor polymorphism and vice versa. This would prove the existence of HLA-G trogocytosis in humans and its association with better allograft outcomes. Preceding the patient studies, it is necessary to investigate the efficacy of HLA-G^+ T cells in attenuating immune responses *in vivo*. For example NOD/SCID model described in **Chapter 5** could

be used provided that sheep contain HLA-G-like molecule. From our observations we were unable to clearly show if the human HLA-G was cross-reactive with sheep but we did observe the cell subset of sheep PBMC, which was recognised with an anti-human HLA-G mAb (87G). The latter may indicate the presence of the HLA-G molecule in sheep but further studies are needed in order to assess whether these 87G positive ovine cells could bind human receptors and induce functional signalling. Alternatively, it may be possible to use humanised NOD/SCID mice, where human skin would be transplanted and mice co-injected with human HLA-G transfected DC and allogeneic PBMC, as previously reported by our laboratory (236). The experiment would involve either injection of HLA-G-transfected DC or HLA-G^+ T cells in the transplanted NOD/SCID mice. For the *in vivo* experiments, it may be possible to enhance the potency of HLA-G^+ T cells by only selecting specific HLA-G expressing T cells. This may be achieved by developing/using specific mAb which would not block the function of HLA-G. Furthermore, as the maximal transfection efficiency of human DC was 85%, flow sorting could be conducted in future studies to achieve close to 100% purity, which may improve HLA-G transfer rate to T cells.

Moreover it was demonstrated that HLA-G transfected DC were incapable of inhibiting T cell proliferation during DC-MLR, a finding which was attributed to the absence of ILT4 on DC. As discussed in **Chapter 6**, it would be crucial to induce ILT4 expression in human HLA-G-transfected DC and determine if ILT4 is indeed essential for inhibitory signalling of HLA-G in DC.

It is still debatable if Adenoviral vectors will be used *in vivo* to deliver genes to target cells because of their strong immunogenicity. However, *ex vivo* manipulation of DC is expected to limit the adenoviral antigenicity in the host, but we did demonstrate that in our system transfected DC still induced an immune response. Recent reports suggest that

the “new generation” adenoviral vector may be used in clinical studies in the near future (445). These vectors are devoid of the majority of adenoviral antigens and will be designed against specific receptors on desired target cells thus minimising antigenicity and non-specificity (445). Nevertheless the adenoviral vectors still provide the highest levels of transfection in DC and allow for fundamental proof-of-concept experiments for the development of novel therapies. Therefore future studies should use “new generation” vectors to deliver HLA-G in DC. This could minimise adenoviral antigenicity and enhance HLA-G mediated effects thereby enhancing tolerogenic capacity of DC.

In conclusion, we have demonstrated that RAPA treatment and HLA-G transfection generated human DC with tolerogenic properties *in vitro*. Translational studies using ovine DC and NOD/SCID model highlighted the potential of using RAPA-DC as tolerogenic cell based therapy *in vivo*. RAPA findings could be extended to a large animal model by administering RAPA to sheep at the time of cannulation and collecting the DC. The adoptive transfer of these DC in the NOD/SCID model of vascularised skin transplantation should mirror the consequences of the *in vivo* effects of RAPA administered to sheep on the generation of tolerogenic DC. With respect to HLA-G, further studies are warranted in order to ascertain the HLA-G-mediated tolerogenic effects on allograft rejection via trogocytosis. Additional finding in the current study highlighted that monocytes, but not DC, exclusively responded to HLA-G treatment and inhibited T cell proliferation. It is therefore important to investigate if monocytes are responsible for preventing allograft rejection in the presence of HLA-G, using a humanized NOD/SCID model. Based on the outcome, it may be plausible to develop therapy targeting HLA-G to monocytes using mAb’s.

Overall, this thesis has provided novel findings and a strong basis for future studies highlighting the potential of human DC modification for use as tolerogenic cell therapy. In

addition, this thesis has investigated the approach of combining pharmacological and genetic manipulation of DC in order to generate DC with unique tolerogenic properties.

Materials

Antibodies

Anti-Human antibodies

CD80 (IgG1)	Immunotech, France
CD86 (IgG1)	Serotec, UK
MY-4 FITC-conjugated (IgG2b)	Coulter Corp., USA
CD3-FITC-conjugated (IgG1)	BD Bioscience, USA
CD4-PE conjugated (IgG1)	BD Biosciences, USA
CD8-PE conjugated (IgG1)	Immunotech, France
CD56-PE (IgG2b)	BD Biosciences, USA
CD14 (IgG2b)	Serotec, UK
CD83 (IgG2b)	Serotec, UK
MHC Class I (IgG2b)	Laboratory-derived supernatant
MHC Class II (IgG2a)	Laboratory-derived supernatant
CD40 (IgG2a)	Serotec, UK
ILT2-PE-conjugated (IgG1)	BD Bioscience, USA
ILT3 (IgG1)	R&D Systems, USA
ILT4 (IgG2b)	Santa Cruz Biotech, USA
HLA-G (IgG2a)	Abcam, USA

Anti-ovine antibodies

MHC Class I (SBU I, IgG1)	University of Melbourne*
MHC Class II DQ/DR (SBU II, IgG1)	University of Melbourne*

CD1a (clone 20.27, IgG1)	University of Melbourne*
Anti bovine-CD21 (IgG1) – (ovine cross-reactive)	Serotec, UK
CD25 (IgG1)	Serotec, UK
CD31 (IgG2a)	Serotec, UK
CD4 (clone 44.38, IgG2a)	University of Melbourne*
CD8 (clone 38.65, IgG2a)	University of Melbourne*
CD14 (IgG1)	Serotec, UK

*University of Melbourne, School of Veterinary Science, Australia

Control antibodies

1D4.5 (IgG2a)	Dr P.Hart, Flinders University
X63 (IgG1)	ATCC, USA
Mouse IgG2a	eBioscience, USA
Rat IgG2a	Santa Cruz Biotech, USA
PE conjugated mouse IgG2a	BD Biosciences, USA
FITC conjugated mouse IgG2b	BD Biosciences, USA

Secondary antibodies

FITC conjugated Sheep anti-mouse IgG	Chemicon, Australia
PE conjugated Sheep anti-mouse IgG	Chemicon, Australia

Other antibodies

PE conjugated anti-human F(ab')2	Immunex, France
Biotin conjugated horse anti-mouse IgG	Vector Laboratories, USA
Biotin conjugated rabbit anti-rat IgG	Vector Laboratories, USA

Cell Lines

Bacterial

TG1α *E.coli*	IMVS, Adelaide
BJ5183 *E.coli*	Vogelstein, B.[+]
DH10β *E.coli*	IMVS, Adelaide

Cell culture

Jeg-3 cells	Jones, B.[#]
HEK 293 cells	Reynolds, P.[*]

[+] The Johns Hopkins University, Baltimore, USA

[*] The Royal Adelaide Hospital, Adelaide, South Australia

[#] Mater Medical Research Institute, Brisbane, Australia

Cytokines and recombinant proteins

Recombinant human HLA-G (wt)	Kijer-Nilsen, L.[*]
Recombinant human HLA-G (C42S)	Clements, C.[#]
Recombinant human Interleukin-10 (IL-10)	Bender Medsystems, Austria
Recombinant human Interleukin-4 (IL-4)	Peprotec, USA
Recombinant human Granulocyte-Macrophage Colony Stimulating Factor (GM-CSF)	Schering-Plough, Australia

Recombinant human Tumour Necrosis Factor α (TNFα)	Genzyme Corporation, USA
Recombinant human CTLA4-Ig	R&D Systems

[*] The University of Melbourne, Victoria, Australia

[#] Monash University, Victoria, Australia

Radiochemicals

[^{3}H]-labeled thymidine	Amersham, Australia

Flow Cytometry Reagents

FACS Lysing™ solution	Becton Dickinson, USA
Sodium azide	Ajax Chemicals, Australia
PE conjugated rat anti-human FoxP3 Staining Kit (clone: PCH101)	eBiosciences, USA

Tissue Culture Reagents

BetaPlate scintillation fluid	Wallac, Finland
Foetal Calf Serum (FCS)	CSL, Australia
L-Glutamine	Multicel, Australia
Lymphoprep™	Nycomed, Norway
Histodenz™	Sigma, USA
Dulbecco's Modified Eagle Medium (DMEM)	Gibco BRL, USA
Penicillin/Streptomycin	Cytosystems, Australia
RPMI 1640 media	Invitrogen, USA
Trypsin EDTA	Sigma, USA

Histological Reagents

Avidin/Biotin blocking kit	Vector Laboratories, USA
Harris Hematoxylin Solution	Sigma, USA
Normal horse serum	ICN Biomedicals, Australia
Streptavidin-Alkaline phosphate conjugate	Roche, Germany
SubX^{TM} clearing solution	Surgipath Medical Industries, USA
SubX^{TM} mounting media	Surgipath Medical Industries, USA
Vectastain ABC kit	Vector Laboratories, USA

Molecular Biology Reagents

Agarose (DNA grade)	Progen, Australia
Ampicillin	Roche, Germany
Bgl II	Roche, Germany
Custom oligonucleotides	Sigma-Genosys, USA
Sal I restriction endonuclease	New England Biolabs, USA
EcoR I restriction endonuclease	New England Biolabs, USA
EcoR V restriction endonuclease	Roche, Germany
Kpn I restriction endonuclease	Fermentas, Lithuania
JETSTAR Midi Prep Plasmid kit	Genomed, USA
Kanamycin	Life Technologies, USA
LipofectAMINE 2000^{TM}	Invitrogen, USA
$MgCl_2$ solution (25 mM)	Fisher Biotech, USA
Mineral Oil	Sigma, USA
MMLV Reverse Transcriptase	Life Technologies, USA

dNTPs	Promega, USA
Not I restriction endonuclease	New England Biolabs, USA
Oligo dT	Amersham, Australia
Pac I restriction endonuclease	New England Biolab, USA
Pme I restriction endonuclease	New England Biolab, USA
pUC19/HpaII Molecular Markers	Geneworks, Australia
RNase A	Sigma, USA
RNAsecure reagent	Ambion, USA
RNAsin	Promega, USA
RNA Storage Soln. (1mM Sodium Citrate pH 6.4)	Ambion, USA
SPP1/*EcoR* I Molecular Markers	Geneworks, Australia
T4 Ligase	Promega, USA
Tth 1 Polymerase	Fisher Biotech, USA
Tth 1 PCR buffer	Fisher Biotech, USA
Ultraclean DNA purification kit	Geneworks, Australia

Plasmid vectors

pGEM-T-Easy® Vector Kit	Promega, USA
pAdEasy-1	Vogelstein, B[+]
pShuttle-CMV	Vogelstein, B[+]
pAdTrack-CMV	Vogelstein, B[+]

[+] The Johns Hopkins University, Baltimore, USA

Other Reagents

Bacto-Yeast extract	Oxoid, UK
Dimethyl sulphoxide (DMSO)	Ajax Chemicals, Australia
Diethanolamine	Ajax Chemicals, Australia
Ethylenediamine tetraacetic acid (EDTA)	Sigma, USA
Ethidium bromide	Sigma, USA
GelRed™ Nucleic Acid Gel Stain	Biotium, USA
Phenol	Progen, Australia
Sigma 104 Substrate	Sigma, USA
Trypan Blue	BDH, Australia
Tween-20	Bio-Rad, USA

Solutions and Buffers

Agarose Gel Electrophoresis Buffers and Solutions

50x TAE

Compound	Conc.	Amount
Trizma base	1.6 M	193.8 g
Sodium acetate	800 mM	65.6 g
EDTA	40.27 mM	14.9 g
H_2O		To 100ml
pH to 7.2. Diluted 1/10 in dH_2O for use		

6x Loading Buffer

Compound	Conc.	Amount
50X TAE	1X	50 µl
Glycerol	50%	1.25 ml
Bromophenol Blue	24%	600 µl
H_2O		To 2.5 ml

Ethidium Bromide (1.25 µg/ml)

Compound	Conc.	Amount
Ethidium Bromide (10 mg/ml stock)	1.25 µg/ml	50 µl
H_2O		To 400 ml

GelRed™ Nucleic Acid Gel Stain (1X)

Compound	Conc.	Amount
GelRed™ (10,000 X stock)	1X	5 µl
0.1 M Sodium Chloride		To 50 ml

Agarose Gels

Compound	Conc.	Amount
Agarose (0.8% gel)	0.8%	0.48 g
Agarose (1% gel)	1%	0.6 g
Agarose (2% gel)	2%	1.2g
H_2O		To 60ml

RNA Extraction Buffers and Solutions

TRIZOL® Reagent

Compound	Conc.	Amount
TRIZOL® Reagent	100%	N/A

RNA Secure/Citrate Solution

Compound	Conc.	Amount
RNAsecure	4%	4 µl
RNA citrate storage solution	96%	96 µl

Cloning and Transfection Buffers and Solutions

Luria Broth (LB)

Compound	Conc.	Amount
Bacto-Yeast Extract		2.5 g
Bacto-Tryptone		5 g
Sodium Chloride		5 g
H_2O		To 500 ml
pH adjusted to 7.0 and autoclaved		

LB Agar

Compound	Conc.	Amount
Bacteriological Agar		15 g
LB		To 1 l
Kanamycin (30 mg/ml stock)	30 µg/ml	1 ml
LB was heated until agar was dissolved and cooled to 55°C before kanamycin was added. LB agar was poured into perti dishes and flamed to remove air bubbles.		

1M $CaCl_2$

Compound	Conc.	Amount
$CaCl_2$	1M	7.351 g
H_2O		To 50 ml
Solution autoclaved		

1M $MgCl_2$

Compound	Conc.	Amount
$MgCl_2.6H_2O$	1M	10.165 g
H_2O		To 50 ml
Solution autoclaved		

$CaCl_2/MgCl_2$ Transformation Solution

Compound	Conc.	Amount
1M $CaCl_2$	0.1M	2 ml
1M $MgCl_2.6H_2O$	20 mM	400 μl
H_2O		To 20 ml

Mini-Preparation Solution 1

Compound	Conc.	Amount
D-Glucose	50 mM	0.9 g
Tris-HCl	25 mM	0.934 g
0.5 M EDTA	10 mM	2 ml
H_2O		To 100 ml
pH adjusted to 8.0 and autoclaved		

Mini-Preparation Solution 2

Compound	Conc.	Amount
1 M sodium hydroxide	0.2 M	4 ml
20% SDS	1%	1ml
H_2O		To 20 ml
Solution autoclaved		

Mini-Preparation Solution 3

Compound	Conc.	Amount
Potassium acetate	3 M	29.4 g
Glacial acetic acid		11.5 ml
H_2O		To 100ml
pH adjusted to 4.8 and autoclaved		

Mini-Preparation Storage Solution (TE8/RNase)

Compound	Conc.	Amount
DNase inactivated RNaseA	200 ng	10 μl
TE8		5 ml

SOC Medium

Compound	Conc.	Amount
Bacto-Yeast Extract		5 g
Bacto-Tryptone		20g
NaCl (5M)	10 mM	2 mL
KCl (1M)	2.5 mM	2.5 mL
H_2O		To 1 L
pH adjusted to 7.0 and autoclaved		

Tissue Culture Buffers and Solutions

Phosphate Buffered Saline (PBS)

Compound	Conc.	Amount
Sodium dihydrogen orthophosphate	40.1 mM	6.25 g
Sodium chloride,	1.2 M	70g
Sodium hydrogen orthophosphate	161 mM	22.85 g
H_2O		To 1 L
Solution autoclaved and diluted 1/10 for use.		

RPMI 1640

Compound	Conc.	Amount
RPMI 1640 powdered media		1 sachet
Sodium pyruvate	1 mM	10 ml
Sodium bicarbonate	23.81 mM	2 g
HEPES	9.99 mM	2.38 g
Penicillin/Streptomycin	50 IU/ml	10 ml
Solution acidified to a pH of 7.3 by CO_2 bubbling and filter sterilised.		

S10g Tissue Culture Medium

Compound	Conc.	Amount
Fetal calf serum (FCS)	10%	10 ml
L-Glutamine	1%	1 ml
RPMI		To 100ml

Dulbecco's Modified Eagle Medium (DMEM)

Compound	Conc.	Amount
MEM		1 sachet
Penicillin/streptomycin	(1 U/ml)	5 ml
$NaHCO_3$	26 mM	2.2 g
Solution prepared under endotoxin-free conditions		

Complete DMEM (cDMEM) Culture Medium

Compound	Conc.	Amount
FCS	10%	10 ml
L-Glutamine	1%	1 ml
Non-essential amino acids	1%	1 ml
DMEM		To 100 ml

Citric Saline Solution

Compound	Conc.	Amount
KCl	1.35 M	10.06 g
Sodium citrate	150 μM	4.4 mg
H_2O		To 100 ml
Solution autoclaved		

Electroporation Media

Compound	Conc.	Amount
D-glucose	10 mM	100 μl
DTT	1mM	1 μl
RPMI 1640		To 10 ml

Buffers and Solutions for Adenoviral purification

25 mM HEPES buffer pH 7.4

Compound	Conc.	Amount
HEPES	25 mM	0.6 g
sH_20		To 100 ml
* pH adjusted at 7.4 and autoclaved		

0.3 M NaCl Solution in HEPES pH 7.4

Compound	Conc.	Amount
NaCl	0.3M	1.8 g
HEPES (25 mM)		To 100 ml
* pH Adjusted to 7.4 and autoclaved		

0.6 M NaCl Solution in HEPES pH 7.4

Compound	Conc.	Amount
NaCl	0.6M	3.6 g
HEPES (25 mM)		To 100 ml
* pH Adjusted to 7.4 and autoclaved		

1 M NaCl Solution in HEPES pH 7.4

Compound	Conc.	Amount
NaCl	1M	5.8 g
HEPES (25 mM)		To 100 ml
* pH Adjusted to 7.4 and autoclaved		

1 M NaOH Solution in HEPES pH 7.4

Compound	Conc.	Amount
NaOH (10M)	1M	10 ml
HEPES (25 mM)		To 100 ml
* pH Adjusted to 7.4 and autoclaved		

Flow Cytometry Buffers and Solutions

FACS Washing Buffer

Compound	Conc.	Amount
FCS	2%	5 ml
Sodium azide	0.1%	100 µl
PBS		To 100 ml

FACS Lysing Buffer

Compound	Conc.	Amount
FACS Lysing solution	10%	10 ml
PBS		To 100 ml

ELISA Solutions

Coating buffer

Compound	Conc.	Amount
Na_2CO_3	150 mM	0.159 g
$NaHCO_3$	350 mM	0.293 g
H_2O		To 100 ml
pH adjusted to 9.6.		

PBS-Tween

Compound	Conc.	Amount
NaCl	0.14 M	8 g
KH_2PO_4	1.5 mM	0.2g
$Na_3HPO_4x12H_2O$	18.6 mM	2.9 g
KCl	2.7 mM	0.2 g
Tween-20		1 ml
H_2O		To 1000 ml
pH adjusted to 7.2-7.4.		

Diethanolamine buffer (per 500 ml)

Compound	Conc.	Amount
Diethanolamine	9.7%	48.5 ml
$MgCl_2x6H_2O$	0.5 mM	50 mg
NaN_3	3 mM	0.1 g
H_2O		To 500 ml

Phosphate Substrate

Compound	Conc.	Amount
Sigma 104 substrate		2 tablets
Diethanolamine buffer		10 ml
Sigma 104 substrate tablets dissolved in buffer at 37°C in the dark		

Immunohistology Solutions

Diaminobenzidine substrate solution

Compound	Conc.	Amount
Diaminobenzidine		1 mg
Tris buffer		1 ml
Solution diluted 50% with a 0.02% hydrogen peroxide solution and stored in the dark.		

Eosin

Compound	Conc.	Amount
1% aqueous eosin	10 mg/ml	50 ml
1% phloxine	10 mg/ml in H_2O	5 ml
Glacial acetic acid		2 ml
EtOH	95%	390 ml

Hydrogen peroxide solution

Compound	Conc.	Amount
Hydrogen peroxide	0.02%	2 µl
H_2O		To 10 ml